MARMARA UNIVERSITY
INSTITUTE FOR GRADUATE STUDIES IN PURE AND APPLIED SCIENCES

INVESTIGATION OF APORPHINE ALKALOIDS FOR THEIR ANTIMICROBIAL ACTIVITIES

FATMA GİZEM AVCI

Ph.D. THESIS

Department of Bioengineering

Thesis Supervisor

Prof. Dr. Berna SARIYAR AKBULUT

ISTANBUL, 2018

MARMARA UNIVERSITY
INSTITUTE FOR GRADUATE STUDIES IN PURE AND APPLIED SCIENCES

INVESTIGATION OF APORPHINE ALKALOIDS FOR THEIR ANTIMICROBIAL ACTIVITIES

FATMA GİZEM AVCI

Ph.D. THESIS

Department of Bioengineering

Thesis Supervisor

Prof. Dr. Berna SARIYAR AKBULUT

ISTANBUL, 2018

MARMARA UNIVERSITY
INSTITUTE FOR GRADUATE STUDIES IN PURE AND APPLIED SCIENCES

Fatma Gizem AVCI, a Doctor of Philosophy student of Marmara University Institute for Graduate Studies in Pure and Applied Sciences, defended her thesis entitled "Investigation of Aporphine Alkaloids for Their Antimicrobial Activities", on December 28, 2018 and has been found to be satisfactory by the jury members.

Jury Members

Prof. Dr. Berna SARIYAR AKBULUT (Advisor)
Marmara University .....(SIGN).....

Prof. Dr. Dilek KAZAN (Jury Member)
Marmara University .....(SIGN).....

Assoc. Prof. Dr. Gizem DİNLER DOĞANAY (Jury Member)
Istanbul Technical University .....(SIGN).....

Prof. Dr. Murat KASAP (Jury Member)
Kocaeli University .....(SIGN).....

Assist. Prof. Dr. Kaan YILANCIOĞLU (Jury Member)
Üsküdar University .....(SIGN).....

APPROVAL

Marmara University Institute for Graduate Studies in Pure and Applied Sciences Executive Committee approves that Fatma Gizem AVCI be granted the degree of Doctor of Philosophy in Department of Bioengineering, Bioengineering Program on 02.01.2019..... (Resolution no: 2019/01-02).

Director of the Institute
Prof. Dr. Bülent EKİCİ

ACKNOWLEDGEMENTS

I would like to express my deepest gratitude to my supervisor Prof. Dr. Berna SARIYAR AKBULUT for her all endless support, encouragement, valuable advice, and understanding. Throughout the years, we have shared many experiences that have expanded my knowledge. It was a great opportunity to work with her.

I would like to thank Prof. Dr. Dilek KAZAN and Assoc. Prof. Dr. Gizem DİNLER DOĞANAY for their valuable advice and contributions during this thesis.

I am really thankful to Assoc. Prof. Dr. Nihat Alpagu SAYAR, Assoc. Prof. Dr. Kazım Yalçın ARĞA, Prof. Dr. Bülent MERTOĞLU, Prof. Dr. Ahu ALTINKUT UNCUOĞLU, and Prof. Dr. Murat KASAP for their support. And also I would like to thank the jury members for their attention.

I would like to thank Prof. Dr. Ahmet Alp SAYAR for making this work possible in the Department of Bioengineering. I am also very grateful to Marmara University Bioengineering Department faculty members for their support and understanding during this period.

The funding provided by TÜBİTAK-MAG project 113M052 is gratefully acknowledged.

I would like to express my special thanks to my dear friends Fatma Ece ALTINIŞIK KAYA, Orkun PİNAR, Ceyda KULA, Ceyhun BEREKETOĞLU, Kübra KARAOSMANOGLU YÖNETEN, and Beste TURANLI for their endless and priceless support.

Last but not least, I would like to express my deepest love and appreciation to my precious family for their everlasting support, endless patience, understanding, and deep love throughout my life. I would not have finished this thesis without their encouragement.

December, 2018 **Fatma Gizem AVCI**

TABLE OF CONTENTS

ACKNOWLEDGEMENTS i

TABLE OF CONTENTS ii

ÖZET v

ABSTRACT vi

CLAIM FOR ORIGINALITY vii

SYMBOLS viii

ABBREVIATIONS ix

LIST OF FIGURES xi

LIST OF TABLES xii

1. INTRODUCTION 1

1.1. Antibiotic Resistance 1

1.2. Plants: Sources of new antibiotics 3

1.2.1. Alkaloids 4

1.3. Omic technologies for the evaluation of antimicrobial MOA 5

1.3.1. Proteomics 9

1.3.2. Transcriptomics 11

1.4. *Bacillus subtilis* 13

2. MATERIALS AND METHODS 14

2.1. Materials 14

2.1.1. Bacterial strain and growth medium 14

2.1.2. Alkaloids 14

2.1.3. Laboratory equipment, materials, and buffers/solutions 14

2.2. Methods 19

2.2.1. Activation of microorganisms and preparation of bacterial glycerol stocks . 19

2.2.2. Growth of the microorganism 19

2.2.3. Endospore staining 19
2.2.4. Cell viability measurement 20
2.2.5. Analysis with scanning electron microscopy (SEM) 20
2.2.6. Protein extraction 20
2.2.7. Protein clean-up 21
2.2.8. Two-dimensional gel electrophoresis (2-DE) 21
2.2.9. Visualization of protein spots 22
2.2.10. Determination of the differentially expressed proteins on 2-DE gels 23
2.2.11. Identification of proteins via mass spectrometric analysis 23
2.2.12. Total RNA isolation 23
2.2.13. RNA-Seq experimental procedure 24
2.2.14. Raw data processing and determination of differentially expressed genes 25
2.2.15. Principal component analysis 25
2.2.16. Quantitative real-time PCR (qPCR) 26
3. RESULTS AND DISCUSSION 28
3.1. Results 28
3.1.1. Determination of alkaloid working concentration 28
3.1.2. Effects of alkaloids on cell viability 30
3.1.3. *In vitro* effects of alkaloids on *B. subtilis* 168 cells 31
3.1.4. Protein profiles of *B. subtilis* 168 in response to alkaloids 32
3.1.5. Transcriptomic analysis of alkaloid treated *B. subtilis* 168 cells using RNA-Seq 42
3.1.6. Statistical analysis of RNA-Seq data 44
3.1.7. Validation of gene expressions by qPCR 46
3.2. Discussion 48
3.2.1. Drug efflux proteins 49

3.2.2. Electron transport and ATP synthesis 50
3.2.3. Purine and pyrimidine metabolism 51
3.2.4. Oxidative stress 52
3.2.5. Other pathways 53
4. CONCLUSION 55
REFERENCES 56
APPENDIX A. (-)-Roemerine alkaloid. 70
APPENDIX B. BSA calibration curve. 71
APPENDIX C. Table of identified proteins. 72
APPENDIX D. The 2-DE gel images of alkaloid treated cells. 76
APPENDIX E. Differentially expressed genes. 78
CURRICULUM VITAE……

ÖZET

APORFİN ALKALOİTLERİN ANTİMİKROBİYAL AKTİVİTELERİNİN ARAŞTIRILMASI

Mevcut antibiyotiklere direnç gösteren bakteri sayısındaki artışla birlikte farklı etki mekanizmalarına sahip yeni antimikrobiyallerin keşfine ihtiyaç duyulmuştur. Bu bağlamda bitkilerden elde edilen maddeler antimikrobiyal aktiviteleri ve farklı hedeflere bağlanma özellikleri ile dikkat çekmektedirler. Bu çalışmada, benzer kimyasal yapılara sahip boldine, bulbocapnine ve (-)-roemerine aporfin alkaloitlerinin mikrobiyal canlılık, proteom ve transkriptom üstündeki etkileri araştırılmıştır. *Bacillus subtilis* 168 model organizma olarak seçilmiştir. Farklı konsantrasyonlardaki alkaloitlerin mikrobiyal canlılık üzerindeki etkileri büyüme eğrileri ile gözlemlenmiştir. *Bacillus subtilis* 168'in endospor oluşturan bir bakteri olduğu göz önünde bulundurularak alkaloit çalışma konsantrasyonu 75 $\mu g \cdot \mu L^{-1}$ olarak belirlenmiştir. Canlı hücre sayıları koloni oluşturan birim metodu ile ölçülmüştür. Alkaloitlerin hücre bütününe olan etkileri taramalı elektron mikroskobu ile görüntülenmiştir. Proteom ve transkriptom düzeyinde etki mekanizmalarının değerlendirilmesi için bir saat boyunca alkaloitlere maruz bırakılan hücreler kullanılmıştır. Ekspresyon seviyeleri farklı olan proteinler iki boyutlu jel elektroforezini takiben kütle spektroskopisi ile tanımlanmıştır. Transkriptom düzeyindeki değişiklikleri belirlemek için RNA sekanslama teknolojisi kullanılmıştır. Ekspresyon seviyesi değişen genler SubtiWiki veritabanındaki kategorilere göre sınıflandırılmıştır. RNA sekanslama sonuçları qPCR ile doğrulanmıştır. Seçilen alkaloitler arasında sadece roemerine hücre ölümüne neden olmuştur. Boldine ve bulbocapnine hücre yüzeyinde bazı değişiklikler yaratmalarına rağmen roemerine kadar etkili olmamıştır. Proteom ve transkriptom sonuçları değerlendirildiğinde, sadece roemerine antimikrobiyal aktivite göstermiştir. Roemerine'in hücre içerisinde birikmesi demir alımı gibi çeşitli yolakların tekrar düzenlenmesiyle sonuçlanan oksidatif strese ve reaktif oksijen türlerinin oluşmasına neden olmuştur.

Anahtar kelimeler: Aporfin alkaloit, *Bacillus subtilis* 168, roemerine, boldine, bulbocapnine, antimikrobiyal, proteom, transkriptom.

Aralık, 2018 **Fatma Gizem AVCI**

ABSTRACT

INVESTIGATION OF APORPHINE ALKALOIDS FOR THEIR ANTIMICROBIAL ACTIVITIES

Increase in the number of resistant bacteria against existent antibiotics has necessitated the discovery of new antimicrobials with novel action mechanisms. In this respect, plant-derived substances are in focus due to their distinct antimicrobial activities and multi-target properties. In this study, effects of three structurally similar aporphine alkaloids, boldine, bulbocapnine, and (-)-roemerine, on microbial viability, proteome, and transcriptome were investigated. *Bacillus subtilis* 168 was selected as the model organism. Alkaloid effect on the microbial viability was followed by monitoring growth with different alkaloid concentrations. Alkaloid working concentration was set to 75 $\mu g \cdot \mu L^{-1}$ since higher concentration triggered endospore formation. Viable cell numbers were determined by measuring colony forming units. Effects of the alkaloids on whole-cells were visualized using a scanning electron microscope. Alkaloid effects on the proteome and transcriptome were investigated on one-hour alkaloid treated cells. Differentially expressed proteins were identified using two-dimensional gel electrophoresis followed by mass spectrometry. RNA-Sequencing technology was applied to get the changes at the transcriptomic level. Differentially expressed genes were classified according to the categories of SubtiWiki database. RNA-Sequencing results were validated by qPCR. Results have shown that among the selected alkaloids only roemerine ceased growth and caused bacterial death. Although boldine and bulbocapnine had some effects on cell surfaces, they were not as effective as roemerine. When proteome and transcriptome results were evaluated together, only roemerine showed antimicrobial activity. Roemerine accumulation resulted in oxidative stress and building up of reactive oxygen species, which eventually deregulated various pathways such as iron uptake.

Keywords: Aporphine alkaloids, *Bacillus subtilis* 168, roemerine, boldine, bulbocapnine, antimicrobial, proteome, transcriptome.

December, 2018 **Fatma Gizem AVCI**

CLAIM FOR ORIGINALITY

INVESTIGATION OF APORPHINE ALKALOIDS FOR THEIR ANTIMICROBIAL ACTIVITIES

Rapid antibiotic resistance development against current antimicrobials leads to a loss in drug efficacy thus; treatment of bacterial infections with existing antimicrobials has become a bottleneck. Due to the limited availability of novel antibiotics with different targets, there is an urgent need for new antimicrobial classes. Plant-derived molecules, especially alkaloids, may serve as alternatives to available drugs with their diverse structures and biological activities. However, lack of information on their mechanism of action limits their use. Boldine, bulbocapnine, and (-)-roemerine are among the aporphine alkaloids that possess different activities despite their similar chemical structures. This dissertation investigates the antimicrobial mechanisms of these three aporphine type alkaloids in *Bacillus subtilis* 168. *B. subtilis* is one of the best-studied microorganisms with its annotated whole genome sequence and is a model for low G+C gram-positives, which include deadly pathogens such as *Bacillus anthracis*. A multi-omic approach, namely RNA sequencing based transcriptional profiling together with global differential protein expression analysis, was used for the first time to assess the effects of these alkaloids on this microorganism. Among the tested alkaloids, only roemerine possessed antimicrobial activity. The findings will enlighten the mechanism of action of these alkaloids especially roemerine, which could be regarded as a new drug lead in antimicrobial drug development.

December, 2018 Prof. Dr. Berna SARIYAR AKBULUT Fatma Gizem AVCI

SYMBOLS

bp **:** Base pair

cm **:** Centimeter

h **:** Hour

kV **:** Kilovolt

M **:** Molar

mA **:** Miliamper

mg **:** Miligram

mL **:** Mililiter

mm **:** Milimeter

mM **:** Milimolar

m/s **:** Meter per second

ng **:** Nanogram

nm **:** Nanometer

nM **:** Nanomolar

rpm **:** Rate per minute

V **:** Volt

µg **:** Microgram

µL **:** Microliter

µm **:** Micrometer

ABBREVIATIONS

2-DE	**:** Two-dimensional gel electrophoresis
ABC	**:** ATP binding cassette
APS	**:** Ammonium persulfate
BGI	**:** Beijing Genomics Institute
CBB	**:** Coomassie brilliant blue
CHAPS	**:** 3-[(3-cholamidopropyl)dimethylammonio]-2-hydroxy-1-propanesulfonate
CFU	**:** Colony forming units
DMSO	**:** Dimethyl sulfoxide
DTT	**:** Dithiothreitol
GEO	**:** Gene expression omnibus
IPG	**:** Immobilized pH gradient
MALDI-TOF-MS	**:** Matrix-assisted laser desorption ionization time of flight mass spectrometry
MATE	**:** Multidrug and toxin extrusion
MDR	**:** Multidrug resistance
MFS	**:** Major facilitator superfamily
MIC	**:** Minimum inhibitory concentration
MOA	**:** Mechanism of action
MS	**:** Mass spectrometry
NB	**:** Nutrient broth
NGS	**:** Next generation sequencing
PCA	**:** Principal component analysis
pI	**:** Isoelectric point
PMF	**:** Proton motive force
RND	**:** Resistance nodulation division
ROS	**:** Reactive oxygen species
qPCR	**:** Quantitative real-time polymerase chain reaction
QuasR	**:** Quantify and annotate short reads
RNA-Seq	**:** RNA sequencing

SAR **:** Structure-activity relation

SDS **:** Sodium dodecyl sulfate

SDS-PAGE **:** Sodium dodecyl sulfate polyacrylamide gel electrophoresis

SEM **:** Scanning electron microscopy

SMR **:** Small multidrug resistance

TBP **:** Tributylphosphine

TEMED **:** Tetramethylethylenediamine

UNG **:** Uracil-n-glycosylase

LIST OF FIGURES

Figure 1.1 Major antibiotics and their targets (Singh and Barrett, 2006). 2
Figure 1.2 Resistance mechanisms to antibiotics (Abreu et al., 2012). 3
Figure 1.3 Aporphine alkaloids. 5
Figure 1.4 Overview of 2-DE (Raatschen and Bandow, 2012). 11
Figure 1.5 Experimental pipeline of the prokaryotic strand-specific transcriptome. 13
Figure 3.1 Endospore formation upon exposure to 75 $\mu g \cdot mL^{-1}$ and 100 $\mu g \cdot mL^{-1}$ roemerine for 1, 4, and 8 hours. 28
Figure 3.2 Effect of different concentrations of roemerine on *B. subtilis* 168 growth.. 29
Figure 3.3 Effect of different concentrations of boldine on *B. subtilis* 168 growth. 29
Figure 3.4 Effect of different concentrations of bulbocapnine on *B. subtilis* 168 growth. 30
Figure 3.5 The CFU mL^{-1} of cells treated with DMSO and 75 $\mu g \cdot mL^{-1}$ of alkaloids. Alkaloids and DMSO were added at the 3rd hour. 31
Figure 3.6 One-hour alkaloid treated and control cells images obtained from SEM: a) Control, b) Roemerine, c) Boldine, d) Bulbocapnine. 32
Figure 3.7 The 2-DE gel images of proteins from control (left) and roemerine treated (right) cells. 34
Figure 3.8 The 2-DE gel images of proteins from control (left) and boldine treated (right) cells. 38
Figure 3.9 The 2-DE gel images of proteins from control (left) and bulbocapnine treated (right) cells. 40
Figure 3.10 Differentially expressed genes categorized based on the groupings in SubtiWiki database. 44
Figure 3.11 PCA plot of samples treated with different alkaloids. 45
Figure 3.12 Loadings plot from PCA. 45
Figure 3.13 Heatmap constructed using the Mahalanobis distances from PCA. The colour scale indicates the read numbers of the genes for each condition. 47

LIST OF TABLES

Table 1.1 Plant-derived compounds with MOA evaluated by omic technologies. 7
Table 1.2 Technical advantages and restrictions of transcriptome and proteome expression profiling (Freiberg et al., 2004). 9
Table 2.1 List of laboratory equipment and suppliers. 14
Table 2.2 List of materials and suppliers. 16
Table 2.3 Buffers and solutions used in 2-DE. 18
Table 2.4 Buffers and solutions used in CBB-G250 staining. 18
Table 2.5 Primers designed for analysis with qPCR in this work. 27
Table 3.1 Summary of the identified proteins under one-hour roemerine treatment..... 35
Table 3.2 Summary of identified proteins under one-hour boldine treatment..... 39
Table 3.3 Summary of identified proteins under one-hour bulbocapnine treatment. 41
Table 3.4 Summary of control and alkaloid treated *B. subtilis* 168 cDNA samples. 42
Table 3.5 Number of differentially expressed genes following one-hour alkaloid treatment. 42
Table 3.6 Classification of the genes according to SubtiWiki database. 43
Table 3.7 Expression levels of selected genes. 46

1. INTRODUCTION

Over the past decades, the number of antibiotic resistant-bacteria has increased considerably. This resistance resulted in decreased drug efficacy, prolonged illness, and high medical cost (Piddock, 2006; Tanwar et al., 2014). Therefore, the discovery of new antimicrobials with a novel mechanism of action (MOA) is necessary to overcome the crisis in antibiotic resistance.

Plant-derived natural products have been used as therapeutics since ancient times (Pratiwi et al., 2015). Plants are rich sources for thousands of compounds such as phenolics and polyphenols, quinones, flavones, flavonoids and flavonols, tannins, coumarins, terpenoids and essential oils, alkaloids, lectins, and polypeptides (Gaur et al., 2018; Wink and Schimmer, 2009). Alkaloids are among the most active secondary metabolites with their multi-target properties (Wink, 2015). Although progress in their identification and isolation, MOA for most of them has not been clearly elucidated which is an essential step in determining the drug potencies of these natural products (Swiney and Anthony, 2011). Conventional approaches such as biochemical and genetic methods are commonly used to identify possible drug targets. However, these techniques are usually time-consuming and require huge quantities of the compounds under study (dos Santos et al., 2016). Omic technologies provide crucial and robust data for the analysis of MOA and have a greater potential in the discovery of targets when compared to conventional methods (Roemer and Boone, 2013; Tang, 2015).

In this thesis study, the effects of three structurally similar aporphine alkaloids, boldine, bulbocapnine, and (-)-roemerine, on the microbial viability, proteome, and transcriptome of *Bacillus subtilis* 168 (DSM 402) were evaluated. *B. subtilis* was chosen since its complete annotated whole genome sequence is available and it is a model for low-G+C gram-positives (Harwood and R, 2007; Kobayashi et al., 2003). The results provided significant clues about the MOA of these alkaloids.

1.1. Antibiotic Resistance

The introduction of antibiotics into clinical medicine is one of the milestones in the treatment of infectious diseases to reduce morbidity and mortality (Andersson and Hughes, 2010). Antibiotics may target different mechanisms such as DNA replication,

RNA transcription, protein synthesis, and cell wall synthesis to inhibit bacterial functions (Figure 1.1) (Clatworthy et al., 2007). In recent years, the extensive use of antibiotics led to a selective pressure on bacteria and eventually to the development of multidrug resistance strains (Bell et al., 2014; Kumar and Schweizer, 2005).

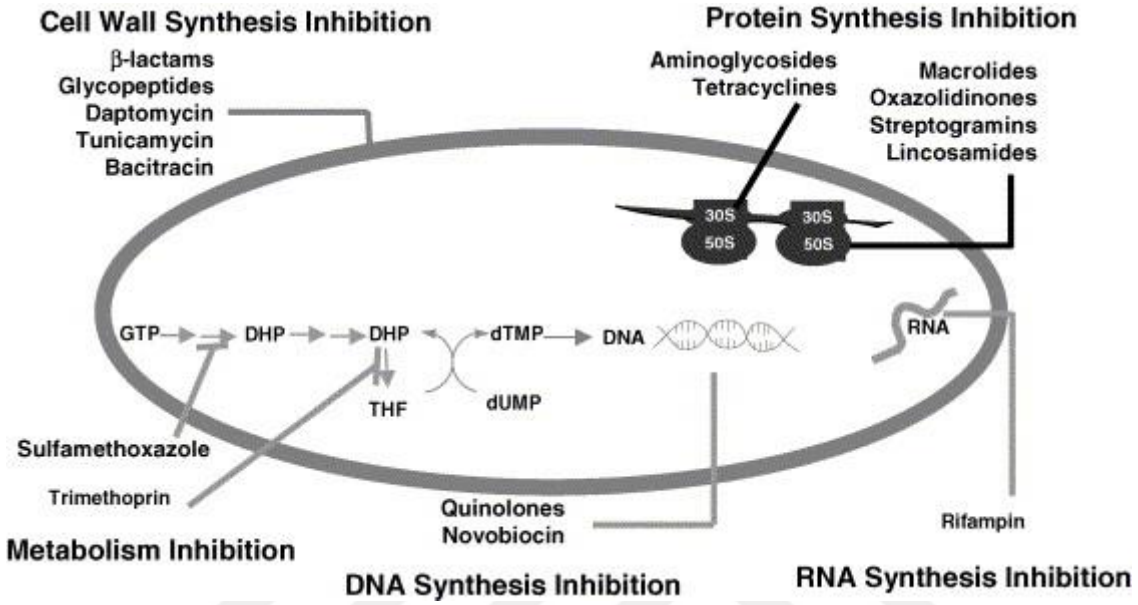

Figure 1.1 Major antibiotics and their targets (Singh and Barrett, 2006).

Although bacteria can have intrinsic resistance mechanisms against antibiotics, they can also acquire resistance by genomic mutations or transfer of genetic elements encoding resistance. Antibiotic resistance can also be mediated through different mechanisms. Major antibiotic resistance mechanisms can be classified into three main groups: 1) minimization of the intracellular concentration of the antibiotic by decreased penetration or increased efflux, 2) alteration of the target site by genetic mutation or post-translational modification, and 3) inactivation of the antibiotic by enzymatic degradation or modification (Figure 1.2).

Minimization of the intracellular concentration of the antibiotic: Decreased penetration of the antibiotics is related to reduced permeability of the outer membrane. Uptake of the antibiotics is limited by down-regulation of porins or by substitution of porins with more selective channels. Efflux of the antibiotics out of the cells by the pumps can keep the intracellular concentrations at low levels. Overexpression of the efflux pumps,

especially multidrug resistance pumps with a wide range of substrates, contributes to high levels of resistance.

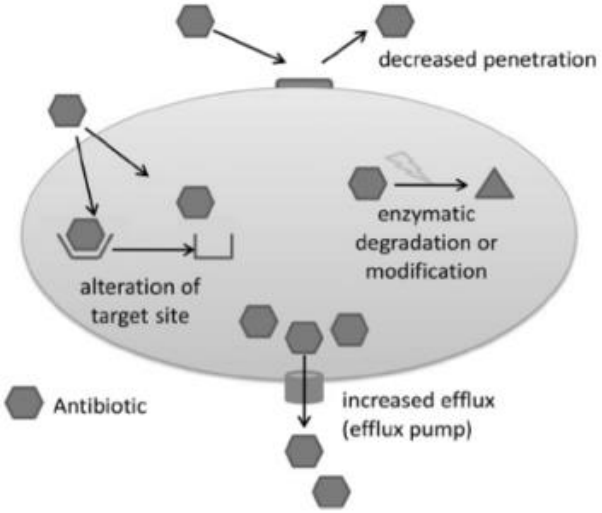

Figure 1.2 Resistance mechanisms to antibiotics (Abreu et al., 2012).

Alteration of the target site: Prevention of efficient antibiotic binding to its target site can be achieved by single point mutations affecting the target structure or by modification of the target site such as through addition of a chemical group.

Inactivation of the antibiotics: Hydrolysis of the antibiotics by enzymes is one of the major resistance mechanisms in bacteria. Antibiotics can also be inactivated by the addition of chemical groups to the antibiotics using bacterial enzymes which in turn prevents binding of the antibiotic to its target site (Abreu et al., 2012; Blair et al., 2015; O'Connell et al., 2013; Putman et al., 2000; Shin et al., 2018).

1.2. Plants: Sources of new antibiotics

A large spectrum of plant-derived compounds that include thousands of secondary metabolites such as tannins, coumarins, terpenoids, alkaloids, and polypeptides have therapeutic values and are used for medicinal purposes (Cowan, 1999; Gaur et al., 2018; Savoia, 2012; Wink and Schimmer, 2009). In recent years, some of these natural products have regained attention because of their distinct antimicrobial mechanisms and multi-target properties (Brötz-Oesterhelt and Brunner, 2008; Prakash et al., 2018; Singh and Barrett, 2006). Alkaloids are one of the earliest isolated pure compound groups

with different biological activities, among which is found antimicrobial activity (Ncube et al., 2008).

1.2.1. Alkaloids

Alkaloids are heterocyclic nitrogenous compounds that are derived from amino acids such as arginine, lysine, tyrosine, tryptophan, and phenylalanine (Gokgoz and Akbulut, 2015; Perumal Samy and Gopalakrishnakone, 2010). They are a group of abundantly available natural small molecules with diverse structures and important pharmacological activities and have been used as therapeutical agents by the humankind (Bhadra and Kumar, 2011). Proton-accepting nitrogen atom and proton-donating amine hydrogen atom(s) in alkaloid structures enable the formation of hydrogen bonds with different targets including proteins, receptors, and enzymes which make alkaloids perfect bioactive molecules (Kittakoop et al., 2013). Alkaloids are divided into different subgroups based on their ring structure. Isoquinoline alkaloids are one of the most extensive alkaloids with remarkable therapeutic potential (Bhadra and Kumar, 2011; Wink, 2015).

The aporphine alkaloids are a diverse family of isoquinoline alkaloids with hundreds of members, which have been isolated from more than 20 families and 100 genera of plants. They share a characteristic tetracyclic motif with different levels of oxidation on both aromatic rings. A range of interesting biological activities has been documented, including serotonergic, antiplatelet, anticancer, antioxidant, antimalarial, antimicrobial, and vasorelaxing activity (Chen et al., 2013; Lafrance et al., 2007). In this thesis, alkaloids of the aporphine group, roemerine, bulbocapnine, and boldine were chosen as antimicrobial drug candidates (Figure 1.3).

Roemerine is an aporphine type alkaloid, which shows significant antibacterial (against *Bacillus cereus*, *Escherichia coli*) and antifungal (against *Candida* strains) activities (Wink and Schimmer, 2009). Bulbocapnine is found in *Corydalis* plants and has antiperoxidative and dopamine D1 receptor antagonistic effects (Shin et al., 1998; Wink and Schimmer, 2009). Another aporphine alkaloid, boldine, affects cells by intercalating with DNA and inhibiting DNA polymerase and reverse transcriptase. The pharmacological activities of boldine, such as cytoprotective, anti-tumour promoting, anti-inflammatory, antipyretic and antiplatelet, have been associated with its ability to

scavenge highly reactive free radicals (O'Brien et al., 2006; Wink and Schimmer, 2009).

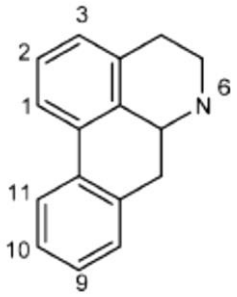

Name	1	2	3	6	9	10	11
Boldine	OCH_3	OH	H	CH_3	OH	OCH_3	H
Roemerine	–O–CH_2–O–		H	CH_3	H	H	H
Bulbocapnine	–O–CH_2–O–		H	CH_3	H	OCH_3	OH

Figure 1.3 Aporphine alkaloids.

These three aporphine-type alkaloids share similar functional groups and the role of these functional groups could be explained by structure-activity relationship (SAR). SAR studies on alkaloids have shown that functional groups on the different backbone carbon atoms of different alkaloid classes may have different contributions to the antibacterial activities (Cushnie et al., 2014; Udvardy et al., 2014). In the case of aporphinoids, Udvardy et al. (2014) have reported that the most frequent substitution pattern is the C1, C2, C9, and C10 tetra-substituted structures with the most common substituents as hydroxyl, methoxy, and methylenedioxy. Furthermore, N-methyl derivatives were found to enhance antibacterial activity. As seen in Figure 1.3, both roemerine and bulbocapnine possess a methylenedioxy group bonded to C1 and C2, whereas boldine has a tetra-substituted structure with methoxy and hydroxyl groups on the preferred carbon atoms for antibacterial activity.

1.3. Omic technologies for the evaluation of antimicrobial MOA

Discovery of new antimicrobial agents has become popular in recent years due to the increase in drug resistance and in the number of ineffective antibiotics. In this respect, natural plant products have been regarded as important alternative sources of new

antimicrobials. Their structural diversity enables them to have a multi-target property. Although fine analytical tools for identification and isolation of antimicrobial phytochemicals proceeds, there still is a huge gap in the characterization of their MOA, which is essential to permit their use as lead molecules in drug-development programs (Arias and Murray, 2015; Radulović et al., 2013; Swiney and Anthony, 2011).

Genome-based expression profiling may be used in antimicrobial drug discovery for different purposes: a) target identification including functionality studies of genes of unknown function, b) MOA studies, and c) development of novel types of whole-cell assays for drug screening. The genome-wide expression of genes consists of two levels: the mRNA level (transcriptome) and protein level (proteome) (Freiberg et al., 2004).

Omic technologies (genomics, transcriptomics, proteomics, and metabolomics) have provided important insights into processes related to antimicrobial drug discovery. They have advantages such as giving deeper and robust data. Their greater potential to reveal new therapeutic targets than conventional assays also make them very attractive (Roemer and Boone, 2013; Tang, 2015). Combination of different omic approaches has enabled the identification of possible drug targets (Table 1.1). In this respect, integration of transcriptomics and proteomics is one the most commonly used strategy. Transcriptomics enables the measurement of mRNA expression levels while proteomics helps to quantify and to identify the proteins expressed by the microorganisms under different conditions. In this thesis, transcriptome and proteome methodologies were simultaneously used to study the MOA of plant-derived antimicrobial candidates.

Table 1.1 Plant-derived compounds with MOA evaluated by omic technologies.

Antimicrobial agent	Pathogen	Methodology	Main target(s)/pathway(s)	Reference
Green tea polyphenols	*Escherichia coli*	Two-dimensional gel electrophoresis (2-DE)	Phospholipid metabolism, carbon and energy metabolism, amino acid biosynthesis	(Cho et al., 2007)
Cryptotanshinone	*Staphylococcus aureus*	Microarray	Oxygen radical generation	(Feng et al., 2009)
Thymol	*Salmonella enterica* serovar Thompson	2-DE	Bacterial envelope and citrate metabolic pathway	(Di Pasqua et al., 2010)
Berberine chloride	*Shigella flexneri*	Microarray	Carbohydrate metabolism, energy production and conversion, amino acid metabolism	(Fu et al., 2010)
Rhodomyrtone	*Streptococcus pyogenes*	2-DE	Virulence genes, glyceraldehyde-3-phosphate dehydrogenase, cAMP factor, streptococcal pyrogenic exotoxin C	(Limsuwan et al., 2011)
Rhodomyrtone	*Staphylococcus aureus*	Microarray	Cell wall biosynthesis, cell division, protein degradation, stress response, virulence factors, energy production, macromolecule biosynthesis	(Sianglum et al., 2012)
Shikonin-containing plant extract	*Staphylococcus aureus*	2-DE	Helicase (RuvB) and bacterial cell wall biosynthesis	(Lin et al., 2012)

Table 1.1 Continued.

Antimicrobial agent	Pathogen	Methodology	Main target(s)/pathway	Reference
Berberine chloride	*Escherichia coli*	Microarray and 2-DE	Cell division, motility, and transport processes	(Karaosmanoglu et al., 2013)
Lupulone	*Mycobacterium tuberculosis*	Microarray	Surface-exposed lipid, cytochrome P450 enzymes, PE/PPE multigene families, ABC transporters, and protein synthesis	(Wei et al., 2014)
Resveratrol	*Staphylococcus aureus*	RNA-Seq based	Inhibition of quorum sensing, synthesis of surface protein, and capsular polysaccharides	(Qin et al., 2014)
Ursolic acid	*Staphylococcus aureus*	RNA-Seq based	Inhibition of metabolism of some amino acids and the expression of adhesins	(Qin et al., 2014)
Plumbagin	*Bacillus subtilis*	2-DE and iTRAQ	Citric acid cycle and heme biosynthesis	(Reddy et al., 2015)
Roemerine	*Escherichia coli*	2-DE	Inhibition of membrane permeability and sugar transporter proteins involved in carbohydrate metabolism	(Gokgoz and Akbulut, 2015)
Roemerine	*Escherichia coli*	Microarray	Inhibition of motility and nutrient uptake	(Ayyildiz et al., 2017)
Berberine chloride	*Escherichia coli*	2-DE	Amino acid synthesis, elongation factors, and outer membrane proteins	(Budeyri Gokgoz et al., 2017)

The advantages/restrictions of transcriptomic and proteomic approaches are summarized in Table 1.2.

Table 1.2 Technical advantages and restrictions of transcriptome and proteome expression profiling (Freiberg et al., 2004).

	Transcriptome	**Proteome**
Information content	Information on mRNA but not on protein level mRNA expression profiling on a whole genome basis possible.	Information on protein amount, synthesis rates, protein modification and degradation. Up to now only a subset of the proteome visualized by proteomics.
Technical demands	The position of genes fixed and known. Virtually all genes covered by a single chip for parallel analysis.	Gel to gel variation of protein position, protein identification required, multiple proteins per spot and spots per protein possible. Only protein subsets detected on a single gel, basic proteins and membrane proteins require special separation conditions.
Costs per sample	Hardware costs higher than in case of 2-DE.	Hardware costs lower, however preparation of gels for various sub-proteomes more labor-intensive.

1.3.1. Proteomics

Proteome is defined as all the proteins expressed by the genome of an organism. Proteomics is the study of protein structure, function or their interactions (Haynes et al., 1998; James, 1997).

Bacteria survive by altering their metabolism rate, growth, and reproduction as a response to changes in their environment (Gidalevitz et al., 2011). Their proteome is quickly adjusted in response to environmental changes such as antibiotic or drug exposure. Proteomics

provides a good starting point for comparative analyses that lead to the discovery of new antimicrobials and then to the elucidation of their MOA (Bandow and Hecker, 2007; Wenzel and Bandow, 2011). Proteomic analyses have been a part of physiological and functional investigations of *B. subtilis* since the early 1980s and have contributed to the understanding of the sequential expression of proteins under different conditions (Richter and Hecker, 1986).

The gel-based approach is a valuable tool to detect and visualize most of the proteins that belong to the metabolic pathways and other cellular components (Aebersold and Mann, 2003). Klose and O'Farrell invented the highly sensitive 2-DE approach which opened up a new promising field that we know today as proteomics (Klose, 1975; O'Farrell, 1975). 2-DE is a common technique used for separating complex protein mixtures and measuring changes in protein expression levels by comparing spot intensities (Jobim et al., 2004). In the 2-DE, proteins are separated by the differences in isoelectric points (pI) in the first dimension and by the differences in molecular weights in the second dimension (Figure 1.4) (Cho, 2007). Visualization of protein spots on 2-DE gels can be achieved using different staining protocols such as Coomassie Brilliant Blue (CBB) G-250 staining (Neuhoff et al., 1988) or silver staining (Chevallet et al., 2006).

2-DE using immobilized pH gradient (IPG) strips coupled with protein identification by mass spectrometry (MS), mainly matrix-assisted laser desorption ionization time of flight mass spectrometry (MALDI-TOF-MS), is a common method for proteome studies (Görg et al., 2004; Völker and Hecker, 2005). MALDI-TOF can identify proteins by peptide-mass fingerprints. In this method, endoprotease (e.g. trypsin) mediated protein digestion generates peptides. The masses of the peptides are then measured by a MALDI-TOF mass spectrometer. Proteins are then identified by matching the empirical list of peptide masses with the theoretical list of peptide masses of different proteins stored in a database such as MASCOT (Koenig et al., 2008; Perkins et al., 1999; Thiede et al., 2005). The proteins identified by MS can further be analyzed using bioinformatic tools to get information on their functions and metabolic pathways.

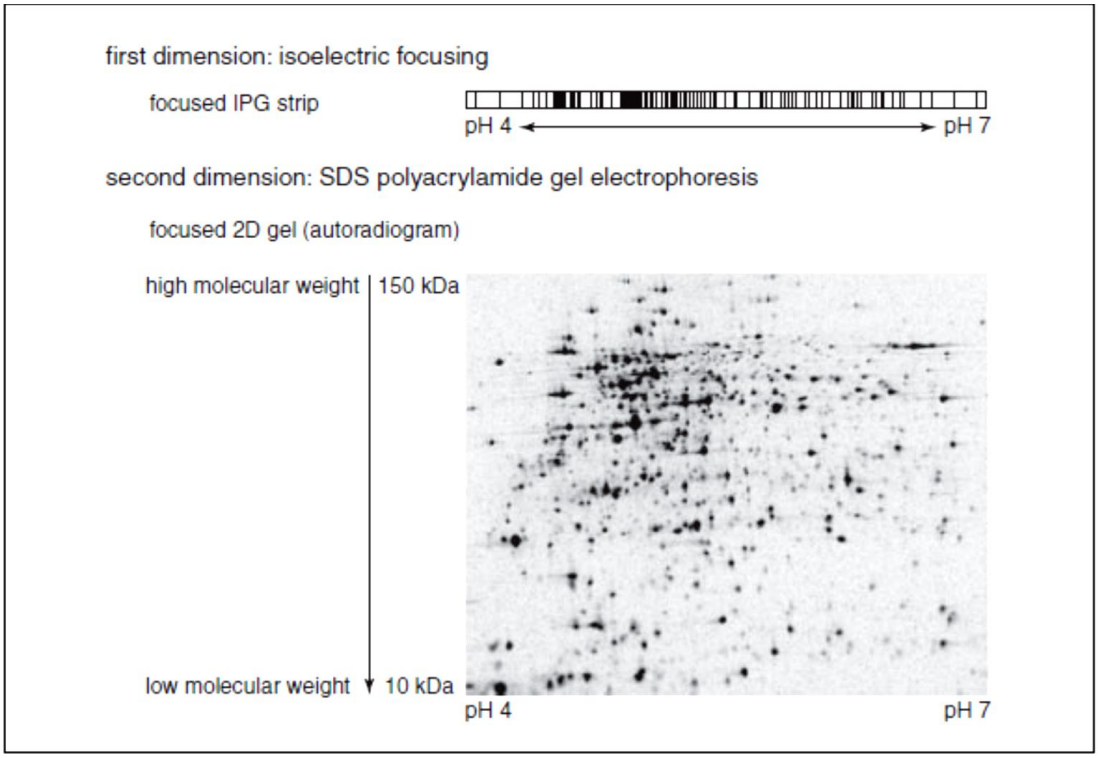

Figure 1.4 Overview of 2-DE (Raatschen and Bandow, 2012).

1.3.2. Transcriptomics

The term ‘transcriptome’ describes the entire set of transcripts in a cell at a specific growth state or physical condition and transcriptomics is a technique used to investigate the changes in RNA expression under these specific conditions (Piétu et al., 1999; Wang et al., 2009).

Gene expression levels change in response to different stimuli such as antimicrobial treatment. Transcriptome analysis aids in the identification and characterization of regulatory networks responsive to these stimuli and provides clues about their mechanisms (Brazas and Hancock, 2005; Freiberg and Brotz-Oesterhelt, 2005). Expression levels of mRNAs could be measured using different techniques including quantitative real-time polymerase chain reaction (qPCR), northern blot, microarray, and next-generation sequencing (NGS) technologies such as RNA sequencing (RNA-Seq).

There has been an enormous progress in the development of methods for quantification of gene expression levels in the past decade (Wang et al., 2009). Among the transcriptome profiling methods, microarray and RNA-Seq are widely used with the

capability of examining the full repertoire of transcripts of an organism (Filiatrault, 2011).

Since 1990s, microarrays have been preferred for large-scale gene expression studies since they have the ability to identify gene expression levels among the different test groups (Marioni et al., 2008). In this technology, extracted transcripts from different conditions are converted to cDNA and then labeled with distinct fluorescent dyes enzymatically in two-color microarrays. These labeled samples are hybridized to the immobilized complementary probe strands in an array representing the genes. The relative abundance of each transcript in the two different conditions can be determined by measuring the light intensity of the distinct fluorescent dyes. Affymetrix and Agilent are two common platforms in this technology (Schena et al., 1995; Tan et al., 2003; Xiang and Chen, 2000).

RNA-Seq has become popular with the introduction of high throughput sequencing technologies to transcriptomics studies. RNA-Seq provides information about the quantity and quality of the transcripts under different conditions (Van Vliet, 2010; Wang et al., 2009; Zhen and Jianhong, 2015). The general steps of prokaryotic strand-specific RNA-Seq are given in Figure 1.5. Roche 454, Illumina, Helicos, and SOLID are some platforms used for RNA-Seq.

Microarray is limited to the transcripts bound to the array slides and needs the genome and transcriptome data for the model organism (Howard et al., 2013). Unlike microarray, RNA-Seq technology does not rely on the prerequisite knowledge of the reference transcriptome (Raz et al., 2011). Furthermore, RNA-Seq data has a very low background signal, a higher dynamic range of expression levels, and higher levels of reproducibility, and also relatively small amounts of total RNA are required for quantification, when compared to microarray (Van Vliet, 2010; Wang et al., 2009). RNA-Seq can use data from the same experiment to characterize exon junctions and to detect non-coding RNA, single nucleotide polymorphisms, and fusion genes (Arnvig et al., 2011; Maher et al., 2009). Microarrays can also detect single nucleotide polymorphisms, map exon junctions, and fusion genes but only with arrays specifically designed for those purposes. Finally, unlike RNA-Seq, microarray chips need to be up-

dated to contain the most up to date sequence information (Croucher and Thomson, 2010; Howard et al., 2013; Perkins et al., 2009).

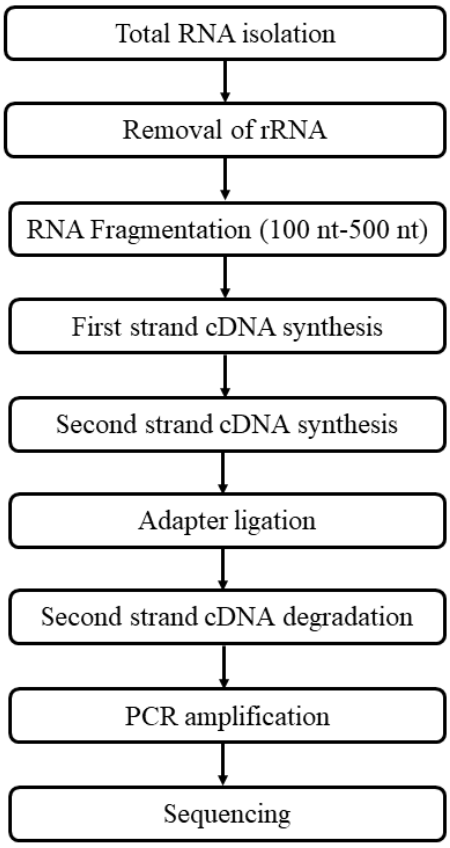

Figure 1.5 Experimental pipeline of the prokaryotic strand-specific transcriptome.

1.4. *Bacillus subtilis*

The genus *Bacillus* is a diverse collection of facultatively anaerobic or aerobic, rod-shaped, endospore-forming bacteria that are widely distributed in nature (Goto et al., 2000). *B. subtilis* 168 was chosen in this thesis because it is one of the best-studied bacteria and is a model for low-G+C gram-positive bacteria, which include both deadly pathogens, such as *B. anthracis*, and bacteria widely used in food and industry, such as lactococci and bacilli (Kobayashi et al., 2003; Kunst et al., 1997). The availability of the complete genome sequence of *B. subtilis* provides the basis to analyze the gene expression profiles under different conditions (Harwood, 2007).

2. MATERIALS AND METHODS

2.1. Materials

2.1.1. Bacterial strain and growth medium

Bacillus subtilis 168 (DSM 402) was used as the model organism in this thesis study. Cells were incubated in nutrient broth (NB, Merck, Germany). NB agar medium was prepared by adding 1.5% (w/v) agar to NB medium.

2.1.2. Alkaloids

Pure (-)-roemerine alkaloid from *Papaver rhoeas* K. was a kind gift of Prof. Günay Sarıyar (Istanbul University). The purity of this alkaloid is given in Appendix A. Boldine and (+)-bulbocapnine hydrochloride were purchased from Sigma-Aldrich (USA) and Fluka (USA), respectively.

2.1.3. Laboratory equipment, materials, and buffers/solutions

Laboratory equipment used and their suppliers are listed in Table 2.1.

Table 2.1 List of laboratory equipment and suppliers.

Equipment	Supplier
Balance	Mettler Toledo AB204-S, USA Denver Instrument, USA
Magnetic stirrers	Velp Scientifica, Italy Heidolph MR3001, Germany
Vortex	Labnet, USA
Autoclave	Nuve (OT 032), Turkey
Class II Biohazard Safety Cabinet	ESCO, USA
Shaking incubator	N-Biotek(NB-205LF), Korea
Deepfreezer (-20°C)	Liebherr, England
Deepfreezer (-80°C)	Thermo Scientific, USA
FastPrep-24	MP Biomedicals, USA
Centrifuge	Sigma 2-16 KL, Germany
Qubit® 2.0 Fluorometer	Invitrogen, USA

Table 2.1 Continued.

Equipment	Supplier
Thermal cycler	GenePro, China
LightCycler 1.5 Real-Time PCR Instrument	Roche, Germany
Mini-Protean 3 electrophoresis system	Bio-Rad, USA
Protean IEF Cell (1-DE system)	Bio-Rad, USA
Protean II XL Cell (2-DE system)	Bio-Rad, USA
Power supply	Apelex PS1006 P, France
Gel imaging system	Bio-Rad (ChemiDoc MP), USA
Drying oven	Nuve (FN400, FN500), Turkey
Ice machine	Arttex Bar Line, Italy
Water purification systems	Elga PURELAB, UK
Spectrophotometer	Bio-Rad (SmartSpec Plus), USA
Refrigerators	Arcelik, Turkey
Ultrasonic bath	Bandelin (Sonorex), Germany
pH meter	Hanna Instruments, Slovenia
Sonicator	Bandelin (Sonoplus), Germany
Waterbath	Memmert, Germany
Microscope	Nikon Eclipse E600, Japan

List of materials and their suppliers are given in Table 2.2.

Table 2.2 List of materials and suppliers.

Materials	**Supplier**
Acetic acid	Sigma-Aldrich
Acrylamide	Sigma-Aldrich
Agarose	Sigma-Aldrich
Ammonium per sulfate (APS)	Sigma-Aldrich
Ammonium sulfate	Merck
Ampholyte (pH 3-10)	Fluka
Bradford Reagent	Bio-Rad
Bromophenol blue	Sigma-Aldrich
CBB-G250	Sigma-Aldrich
3-[(3-cholamidopropyl)dimethylammonio]-2-hydroxy-1-propanesulfonate (CHAPS)	Fisher Scientific
Dithiothreitol (DTT)	Gold Biotechnology
Dimethyl sulfoxide (DMSO)	Duchefa
Ethanol (absolute)	Sigma-Aldrich
FastProtein™ Blue Matrix	MP Biomedicals
Formaldehyde (37%)	Merck
Glutaraldehyde (25%)	Sigma-Aldrich
Glycerol (extrapure)	OmniLife
Glycine	Merck
Hydrochloric acid (HCL) (37%)	Sigma-Aldrich
Iodoacetamide	Sigma-Aldrich
Isopropanol	Merck
LightCycler®FastStart DNA Master^{PLUS} SYBR Green I	Roche
LightCycler Capillaries	Roche
Methanol	Sigma-Aldrich
Mineral Oil	Bio-Rad
N,N-methylen bis-acrylamide	Sigma-Aldrich
Nuclease-free water	Sigma-Aldrich
Nuclease mix	GE, UK
Phosphoric acid (85%)	Sigma-Aldrich
Protease Inhibitor Mix	GE, UK

Table 2.2 Continued.

Materials	**Supplier**
Purelink Genomic DNA Kit	Invitrogen
Protein Lobind microcentrifuge tubes	Eppendorf
Quantitect Reverse Transcription Kit	Qiagen
ReadyStrip IPG strips (pH 4-7, 17 cm)	Bio-Rad
ReadyPrep 2-DE cleanup kit	Bio-Rad
RNase/DNase-free 0.2 mL, 0.5 mL, 1.5 mL thin-wall, clear eppendorf tubes	Axygen
RNase/DNase-free pipette tips 0.1-10 μL, 1-200 μL, 1-1000 μL	Axygen
RNase-free DNase Set	Qiagen
RNAprotect Bacteria Reagent	Qiagen
RNaseZap	Ambion
RNeasy Mini Kit	Qiagen
Sodium dodecyl sulfate (SDS)	Sigma-Aldrich
Silver nitrate	Sigma-Aldrich
Sodium carbonate	OmniLife
Sodiumthiosulfate·$5H_2O$	Merck
Tributylphosphine (TBP)	Sigma-Aldrich
Tetramethylethylenediamine (TEMED)	Merck
Thiourea	Acros Organics
Tris-Base	Sigma-Aldrich
Tris-HCl	Sigma-Aldrich
Urea (Ultra pure)	Merck

The components of buffers/solutions used in 2-DE are listed in Table 2.3.

Table 2.3 Buffers and solutions used in 2-DE.

Buffer /Solution	Components
Optimized Extraction/Rehydration Buffer	8 M Urea, 2 M Thiourea, 4% (w/v) CHAPS, 50 mM DTT, trace amount of bromophenol blue
Equilibration Buffer I	6 M Urea, 2% (w/v) SDS, 0.375 M Tris-HCl (pH 8.8), 20% (v/v) Glycerol, 2% (w/v) DTT
Equilibration Buffer II	6 M Urea, 2% (w/v) SDS, 0.375 M Tris-HCl (pH 8.8), 20% (v/v) Glycerol, 2.5% (w/v) Iodoacetamide
SDS-PAGE Gel Solution	375 mM Tris-HCl (pH 8.8), 0.1% (w/v) SDS, 15% (w/v) Acrylamide, 0.2% (w/v) Bis-acrylamide, 0.03% (v/v) TEMED
APS Solution	1.28% (w/v) APS
Overlay Agarose	0.5% Agarose in 25 mM Tris, 192 mM Glycine, 0.1% (w/v) SDS, trace of bromophenol blue
2-DE Running Buffer	205 mM Glycine, 25 mM Tris, 0.1% (w/v) SDS
2-DE Tank Buffer	231 mM Glycine, 28 mM Tris, 0.113% (w/v) SDS

The list of solutions used in CBB-G250 staining and their components are given in Table 2.4.

Table 2.4 Buffers and solutions used in CBB-G250 staining.

Buffer /Solution	Components
CBB G-250 Fix solution	50% (v/v) Ethanol (96%), 2% (v/v) Phosphoric acid (85%)
CBB G-250 Washing solution	34% (v/v) Methanol, 17% (w/v) Ammonium sulfate, 2% (v/v) Phosphoric acid (85%)
CBB G-250 Staining solution	34% (v/v) Methanol, 17% (w/v) Ammonium sulfate, 2% (v/v) Phosphoric acid (85%), 0.066% (w/v) CBB G-250

2.2. Methods

2.2.1. Activation of microorganisms and preparation of bacterial glycerol stocks

The freeze-dried *B. subtilis* 168 culture was activated according to the supplier's (DSMZ) instructions. 0.5 mL NB was added to the dried pellet, which was kept in a vial under sterile conditions. The content was mixed gently and the mixture was transferred to a test tube with about 5 mL NB. 100 µL of the suspension was streaked onto an agar plate. Agar plates were incubated overnight at 37°C and liquid cultures were incubated at 37°C and 180 rpm for a desired period.

For the glycerol stocks, a single colony from an agar plate was taken with a sterile toothpick and was used to inoculate 5 mL NB in a test tube. The test tube was incubated at 37°C and 180 rpm. At the end of the exponential phase, 250 µL culture was mixed with sterilized 50% (v/v) glycerol with a ratio of 1:1 (v/v) and stored at -80°C until further use.

2.2.2. Growth of the microorganism

B. subtilis 168 cells were grown in erlenmeyer flasks with NB in an orbital shaker at 37°C and 180 rpm. The flask volume to medium volume ratio was kept at 5:1 (v/v) for proper aeration. Overnight cultures were used to inoculate fresh NB in 1:100 ratio and the flasks were incubated until the optical density at 600 nm (OD_{600}) reached 0.55±0.05. Cells were treated with the alkaloids at different concentrations. Alkaloids were dissolved in DMSO and an equal volume of DMSO was added to the control cells. In order to evaluate the effect of DMSO, bacterial growth was followed also in the absence of DMSO. Cell growth was monitored at OD_{600}.

2.2.3. Endospore staining

A modified Schaeffer-Fulton endospore staining procedure was used for staining endospores (Schaeffer and Fulton, 1990). Bacteria to be tested for endospore formation were placed on a slide and heat fixed. Malachite green (5%) was applied to the slides for 5 minutes, which penetrated through the wall of the endospores and stained them green. The slides were washed with water and stained for 3 minutes with safranine. The slides were washed again and blotted dry and then viewed under a light microscope.

2.2.4. Cell viability measurement

Colony forming units (CFU) were determined for the measurement of the number of viable cells treated with alkaloids and DMSO as the control group. Following treatment with DMSO and the alkaloids, samples were plated on NB agar with serial dilutions. Colonies formed on the plates were counted after an overnight incubation at 37°C. The numbers of colonies obtained from triplicate experiments were averaged to get CFU.

2.2.5. Analysis with scanning electron microscopy (SEM)

30 µL of cell suspension (one-hour DMSO, roemerine, boldine, and bulbocapnine treated) was placed onto a 0.22-mm-pore sized membrane filter and allowed for absorption. The cells were fixed for 2 hours by floating the filter on 3% glutaraldehyde. After fixation, the filters were washed three times with water. The filters were then dehydrated in increasing concentrations of ethanol, 30%, 50%, 70%, and 90% (10 minutes each), and finally kept in absolute ethanol for 1 hour. The filters were air-dried overnight in sterile plates and then were coated with platinum sputter coater before imaging. Imaging was performed with Philips XL30 ESEM-FEG/EDAX system under high vacuum mode with 10 kV energy and 3.0 spot size.

2.2.6. Protein extraction

After one-hour treatment with the alkaloids and DMSO, *B. subtilis* 168 cells were harvested by centrifugation at 4000 rpm and 4°C for 15 minutes. Pellets were washed two times with 50 mM Tris buffer (pH 7.8) and centrifuged under the same conditions. Cell pellets were resuspended in different volumes of optimized extraction/rehydration buffer (Table 2.3). Protease Inhibitor Mix (GE, UK) was added to the extraction buffer with 1:100 dilution. Cells were disrupted using FastProtein™ Blue Matrix (MP Biomedicals, USA) for protein extraction. After cell disruption at 4 m/s for 40 seconds using FastPrep-24 Instrument (MP Biomedicals, USA), matrix and cell debris were removed by centrifugation at 10000xg and 4°C for 10 minutes. The supernatant was transferred to a new low protein binding tube and centrifuged again at 20000xg and 4°C for 45 minutes. Protein concentration was measured by the Bradford method (Bradford,

1976). After extraction, same protein samples were treated with a nuclease mix (GE, UK) at room temperature for 45 minutes.

2.2.7. Protein clean-up

Substances like ionic detergents, salts, and lipids were removed and protein samples were concentrated using the ReadyPrep 2-DE cleanup kit (Bio-Rad, USA). 0.5-1 mg protein in a final volume of 100 µL was transferred into a 1.5 mL low protein binding microcentrifuge tube. 300 µL of precipitating agent 1 was added to the protein sample and mixed by vortexing. The mixture was incubated on ice for 15 minutes. 300 µL precipitating agent 2 was added to the tube and mixed by vortexing. The tube was centrifuged at maximum speed for 5 min to form a tight pellet. The supernatant was removed and the tube was centrifuged again for 15-30 seconds to collect any residual liquid at the bottom of the tube. 40 µL of wash reagent 1 was added on top of the pellet. The tube was centrifuged at maximum speed for 5 minutes. The wash reagent was removed with a pipette. 25 µL of proteomic grade water was added on top of the pellet and the tube was mixed by vortexing for 10-20 seconds. 1 mL of pre-chilled wash reagent 2 and 5 µL of wash 2 additive were added and the tube was mixed by vortexing for 1 minute. The tube was incubated at -20°C for 30 minutes and mixed by vortexing for 30 seconds every 10 minutes during the incubation period. After incubation, the tube was centrifuged at top speed for 5 minutes to form a tight pellet. The supernatant was removed and the tube was centrifuged again for 15-30 seconds to remove any residual wash reagent. The pellet was air-dried at room temperature for 3-5 minutes and then it was resuspended by adding an appropriate volume of extraction/rehydration buffer. The tube was mixed by vortexing for at least 30 seconds and incubated at room temperature for 3-5 minutes. The tube was centrifuged at maximum speed for 2-5 minutes at room temperature to clarify the protein sample.

2.2.8. Two-dimensional gel electrophoresis (2-DE)

Two-dimensional separation of proteins was performed by using IPG strips in the first dimension and sodium dodecyl sulfate polyacrylamide gel electrophoresis (SDS-PAGE) in the second dimension.

In the first dimension, proteins were separated according to their pI. Extraction/rehydration buffer, 1% (v/v) ampholyte (pH 3-10), and 1% (v/v) TBP were added to extracted proteins (500-800 μg) in a total volume of 300 μL. Proteins were then pipetted into the rehydration/equilibration tray and 17 cm, pH 4-7 IPG strips (Bio-Rad, USA) were placed on the samples. The IPG strips were covered with 2-3 mL of mineral oil after they completely absorbed protein samples. After the rehydration step, IPG strips were placed on the PROTEAN IEF focusing tray to initiate the first-dimensional separation. 250 V for 20 minutes (linear), 10000 V for 3 hours (linear), and 10000 V for 45000 V-h (rapid) were applied to the strips. As required, wick electrodes were changed during the first-dimensional separation for removal of salts. After isoelectric focusing, IPG strips were immersed in equilibration buffers I and II (Table 2.3) 10 minutes each.

In the second dimension, proteins were separated according to their molecular weights by using SDS-PAGE (Laemmli, 1970). The SDS polyacrylamide gel solutions were prepared by mixing 15% (w/v) acrylamide and 0.2% (w/v) bisacrylamide (Table 2.3). After degassing for 8 minutes, 1.28% (w/v) APS was gently added to the SDS polyacrylamide gel solution and the gel solution was poured into the space between the glass plates. The surface of the gel was covered with isopropanol to obtain a smooth surface and the gel was left at room temperature for polymerization. Isopropanol was removed by washing the gel with HPLC grade water after polymerization. IPG strips were placed on top of SDS polyacrylamide gels by avoiding air bubble formation and then they were fixed by overlaying with agarose solution (Table 2.3). After the agarose solidified, the glass plates were inserted to the electrophoresis tank and the tank was filled with running buffer (Table 2.3). The system was run for 15 minutes at 30 mA in the first step and 215 minutes at 120 mA in the second step for 2 gels.

2.2.9. Visualization of protein spots

CBB-G250 dye method was used to visualize protein spots (Neuhoff et al., 1988). Proteins were first fixed overnight in CBB-G250 fixing solution (Table 2.4) after the second-dimensional separation. Then, the gels were washed for 2 hours in CBB-G250 wash solution. After the removal of wash solution, gels were stained with CBB-G250

staining solution for 2 days. The dye residues were removed by washing the gel with HPLC grade water. The gels were kept in 5% (v/v) acetic acid solution at 4°C.

2.2.10. Determination of the differentially expressed proteins on 2-DE gels

All stained 2-DE gels were scanned using ChemiDoc MP Imaging System (Bio-Rad, USA), Image Lab 5.2.1 software. Differentially expressed protein spots were determined manually and the gel images belonging to treated and control groups were loaded to PDQuest Advance (Bio-Rad, USA) software for the determination of differential protein expression. The software compared the gel images from the control and the alkaloid treated groups and then calculated the fold change for each protein spot. The quantity of each spot was normalized by the local regression model. The statistical significance of image analysis was determined by Student's t-test (statistical level of p-value<0.1 is significant). The proteins with a fold change ≥ 1.5 were accepted as significant (Kocaeli University, DEKART Proteomics Laboratory).

2.2.11. Identification of proteins via mass spectrometric analysis

The selected protein spots were excised from gels using ExQuest Spot-cutter (Bio-Rad, USA) for protein identification. In-gel tryptic digestion of the proteins was carried out using an in-gel digestion kit following the manufacturer's protocol (Pierce, USA). All samples were desalted and concentrated with a 10 µL ZipTipC18 following the recommended protocol (Millipore, USA).

Selected protein spots were identified by using ABSCIEX MALDI-TOF/TOF 5800 system. All peptide mass fingerprints were searched in the MASCOT v.2.5 (Matrix Science) by using SwissProt 57.15 (515203 sequences; 181334896 residues) database. Only significant hits, defined by the MASCOT probability analysis with a p-value< 0.05, were accepted (Kocaeli University, DEKART Proteomics Laboratory).

2.2.12. Total RNA isolation

Total RNA isolation was carried out using the RNeasy Mini Kit (Qiagen, Germany) with one-hour alkaloid treated and control samples. 20 mL RNAprotect Bacteria Reagent (Qiagen, Germany) was added into a falcon tube. 10 mL bacterial culture was

mixed with reagent by vortexing for 5 seconds. The tube was incubated for 5 minutes at room temperature and then centrifuged at 5000xg for 10 minutes. The supernatant was decanted. The pellet was resuspended in 350 µL Buffer RLT and the tube was mixed by vortexing for 5-10 seconds. The suspension was transferred into a tube containing acid washed beads. The cells were disrupted at 6 m/s for 40 seconds using FastPrep-24 Instrument (MP Biomedicals, USA). The beads and the cell lysate were removed by centrifugation at maximum speed for 2 minutes. The supernatant was transferred into a new reaction tube and an equal volume of 70% (v/v) ethanol was added. After mixing, the lysate was loaded to the RNeasy Mini Column placed in a 2 mL collection tube. The tube was centrifuged at 12000 rpm for 15 seconds. Flow-through was discarded. 350 µL Buffer RW1 was loaded onto the RNeasy Mini Column and the tube was centrifuged at 12000 rpm for 15 seconds. Flow-through was discarded. 10 µL DNase I stock solution was added to 70 µL Buffer RDD and mixed gently. 80 µL DNase I incubation mix was added directly onto the RNeasy silica-gel membrane and samples were treated with DNase I at room temperature for 30 minutes. 350 µL Buffer RW1 was added and left on the bench top for 5 minutes. Then, the tube was centrifuged at 12000 rpm for 15 seconds. The collection tube was discarded and the column was placed in a new collection tube. 500 µL Buffer RPE was added and centrifuged at 12000 rpm for 15 seconds. Another 500 µL Buffer RPE was added and centrifuged at 12000 rpm for 2 minutes. After discarding the flow-through, the tube was centrifuged for 1 minute at full-speed. RNeasy column was transferred into a new collection tube for the elution step. 40 µL RNase-free water was added directly onto the RNeasy silica-gel membrane. The tube was centrifuged at 12000 rpm for 1 minute. The eluted sample was aliquoted and kept at -80ºC. The concentration of each RNA sample was measured by Qubit® 2.0 Fluorometer (Invitrogen, USA). The quality of the samples was checked using Agilent 2100 bioanalyzer.

2.2.13. RNA-Seq experimental procedure

The RNA samples of alkaloid treated and control cells were sent to Beijing Genomics Institute (BGI) for RNA-Seq. After removal of rRNA from total RNA samples, fragmentation buffer was added for interrupting mRNA to short fragments. Taking these short fragments as templates, random hexamer-primers were used to synthesize

the first-strand cDNA. The second-strand cDNA was synthesized using a buffer, dATPs, dGTPs, dCTPs, dUTPs, RNase H, and DNA polymerase I after removing dNTPs. Short fragments were purified with QIAQuick PCR Purification Kit (Qiagen, Germany) and resolved with EB buffer for end reparation and adding poly (A). After that, the short fragments were connected with sequencing adapters. Then, the uracil-n-glycosylase (UNG) enzyme was used to degrade the second strand cDNA and the product was purified by MinElute PCR Purification Kit (Qiagen, Germany) before PCR amplification. At last, the library was sequenced using Illumina HiSeqTM4000 technology.

2.2.14. Raw data processing and determination of differentially expressed genes

Sequencing reads (100 bp read length) were aligned to *B. subtilis* 168 genome (RefSeq accession number NC_000964.3) using the quantify and annotate short reads (QuasR) package in R (Langmead et al., 2009). Gene expression levels were quantified by counting the number of reads. Differential expression analyses were performed in R (version 3.3.3) using the package DESeq2 (Love et al., 2014). Differences with an absolute value of $\log_2 \geq 1$ were accepted as significant. Differentially expressed genes were classified according to the SubtiWiki database categories (Michna et al., 2016). The data have been deposited in NCBI's Gene Expression Omnibus (Edgar, 2002) and are accessible through GEO Series accession number GSE104946.

It is important to note that due to the statistical distribution framework applied in the DESeq2 algorithms (negative binomial distribution) some very highly expressed genes (that would be placed as outliers in the positive tail of the distribution) may be recorded with lower differential expression levels than they actually exhibit. These genes were easily identified and manually curated.

2.2.15. Principal component analysis

Principal component analysis (PCA) was used to highlight the differences in the effect of different alkaloids. PCA is an exploratory data analysis technique based on an orthogonal transformation of the read count data for dimensional reduction. The data is analyzed using Matlab's pca function. The first two principal components identified usually account for a significant portion of the differences between samples and

generally, depend on the few most strongly expressed genes (Love et al., 2016). Accordingly, plotting the first two components of each sample provides a visual indication of the similarity/dissimilarity between the samples. Additionally, a plot of the individual genes' effects on the first two principal components helps to identify the genes with the highest influence on the observed behavior.

2.2.16. Quantitative real-time PCR (qPCR)

qPCR was used for the data validation from the RNA-Seq experiment. For this purpose, cDNA was synthesized using Quantitect Reverse Transcription Kit (Qiagen, Germany). RNA samples were thawed on ice whereas gDNA Wipeout Buffer, Quantiscript Reverse Transcriptase, Quantiscript RT Buffer, RT Primer Mix, and RNase-free water were thawed at room temperature. The reaction mix was prepared on ice using 2 µL of 7X gDNA Wipeout buffer, template RNA (up to 1 µg), and RNase-free water in a total volume of 14 µL. The reaction tubes were incubated at 42°C for 2 minutes and then placed on ice. The reverse-transcription master mix was prepared with 1 µL Quantiscript Reverse Transcriptase, 4 µL 5X Quantiscript RT Buffer, and 1 µL RT Primer Mix on ice. 14 µL of genomic DNA elimination reaction which was prepared before, was added to each tube containing the reverse-transcription master mix. Samples were incubated 15 minutes at 42°C for cDNA synthesis and 3 minutes at 95°C to inactivate Quantiscript Reverse Transcriptase. Then, samples were aliquoted and stored at -20°C for further use.

The primers were designed by PrimerPremier 6.0 software (PREMIER Biosoft International, USA) and the annealing temperatures of the designed primers were calculated using Primer Premier 6.0 software and Tm calculator of the pDRAW32 DNA analysis software. Genomic DNA was used as the template to check the primers by PCR and PCR products were run on 2% agarose gel.

16S ribosomal RNA, *rrnA*, was used as the housekeeping gene since its transcription has not changed significantly upon treatment with alkaloids. The qPCR experiments were carried out in a total of 20 µL volume with 3 ng cDNA, 4 µL of 5X SYBR Green I mix (LightCycler FastStart DNA MasterPLUS SYBR Green I, Roche, Germany), and 125 nM of primers. The reactions were performed using LightCycler 1.5 Instrument (Roche, Germany) with the following parameters: 95°C for 10 minutes followed by 40

cycles of 95°C for 10 seconds, annealing at different temperatures (T_a) (given in Table 2.5) for 10 seconds, and 72°C for 45 seconds (extension). The fold change in each gene was calculated according to the $2^{-\Delta\Delta CT}$ method (Livak and Schmittgen, 2001). All analyses were performed with at least two technical replicates.

Table 2.5 Primers designed for analysis with qPCR in this work.

Primer	**Sequence (5'-3')**	**Amplicon length (bp)**	**T_a**
16S *rRNA*-F	TGCGTAGAGATGTGGAGGAA	187	57°C
16S *rRNA*-R	GCGGAGTGCTTAATGCGTTA		
bmr-F	ATTCCAGTAACGCCGACCAT	244	59°C
bmr-R	TGATACCGCCCAGCATACG		
dhbB-F	CGTGGTCTTGATTCGGTAAGGAT	138	59°C
dhbB-R	TTGCTGGCTGCGAGTTGTG		
feuA-F	CACTGATAAAGCCGAACCAACC	136	57°C
feuA-R	CGTGCCTGCTGTGCTGATT		
narH-F	CTGCCAACCATCTGCTCTGA	89	61°C
narH-R	GCCGCTTCCTCCACTTTGT		
aroA-F	GCAACGAGAAACACGCTGGATA	118	60°C
aroA-R	CTGTCGGAAGCAAGAGGTCAC		

3. RESULTS AND DISCUSSION

3.1. Results

3.1.1. Determination of alkaloid working concentration

The effects of boldine, bulbocapnine, and roemerine on the *B. subtilis* 168 growth were investigated by monitoring OD_{600}. The obtained values were plotted as a function of time. The initial upper limit for the concentration of roemerine was selected as 100 $\mu g \cdot mL^{-1}$, based on its minimum inhibitory concentration (MIC). However, following one-hour treatment at this concentration, *B. subtilis* 168 cells formed endospores (Figure 3.1). This concentration was then lowered gradually to 25 $\mu g \cdot mL^{-1}$ to find the concentration, where there was retardation in cell growth without significant spore formation. Eventually, the working concentration of roemerine was selected as 75 $\mu g \cdot mL^{-1}$ (Figure 3.2).

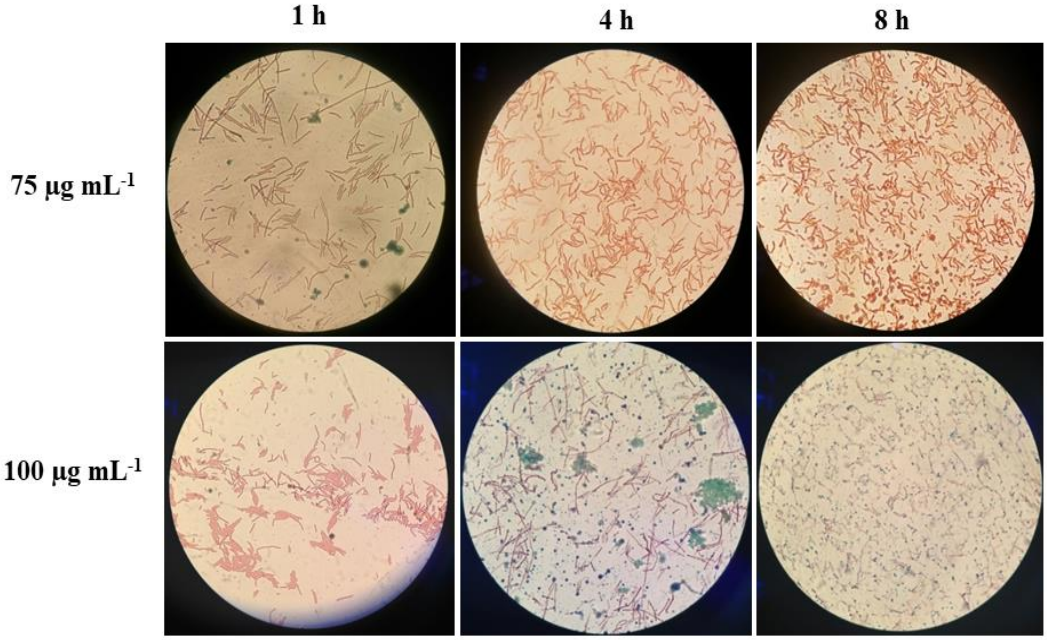

Figure 3.1 Endospore formation upon exposure to 75 $\mu g \cdot mL^{-1}$ and 100 $\mu g \cdot mL^{-1}$ roemerine for 1, 4, and 8 hours.

The upper limit for the concentrations of boldine and bulbocapnine tested were as high as 400 $\mu g \cdot mL^{-1}$ but no effect was observed in *B. subtilis* 168 growth even at these high

values (Figure 3.3 and Figure 3.4). A further increase in the concentration of these alkaloids was impaired by solubility issues.

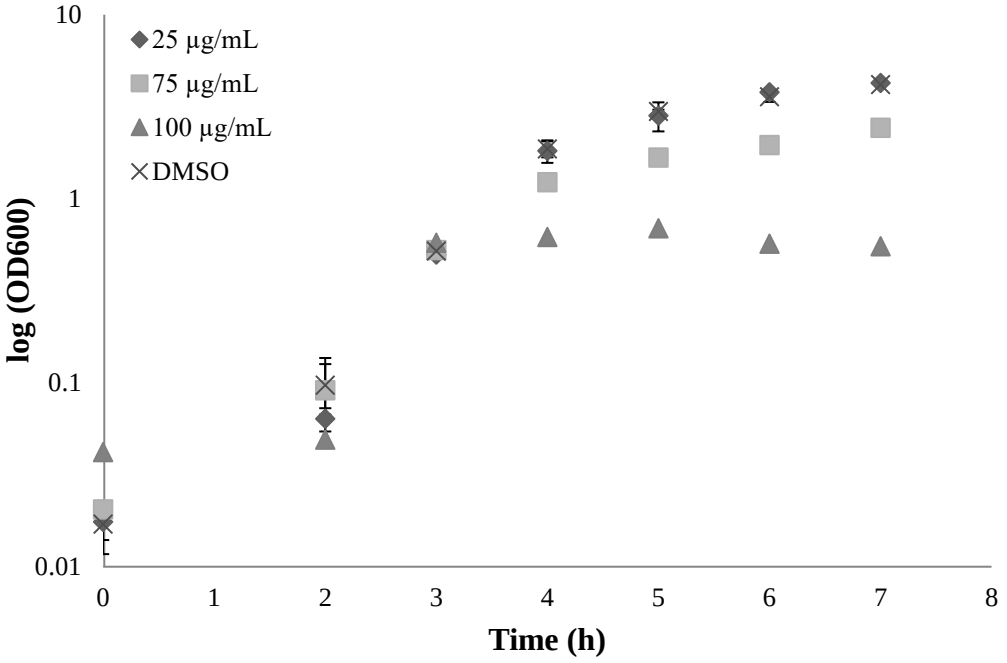

Figure 3.2 Effect of different concentrations of roemerine on *B. subtilis* 168 growth.

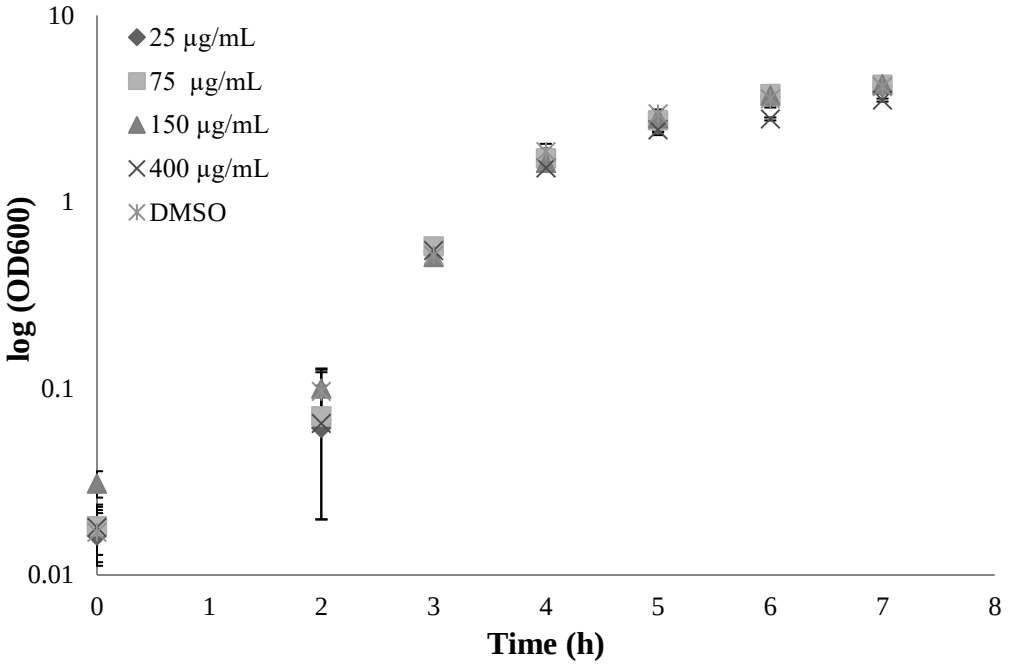

Figure 3.3 Effect of different concentrations of boldine on *B. subtilis* 168 growth.

In the light of these findings, 75 µg·mL^{-1} was set as the working concentration for all alkaloids.

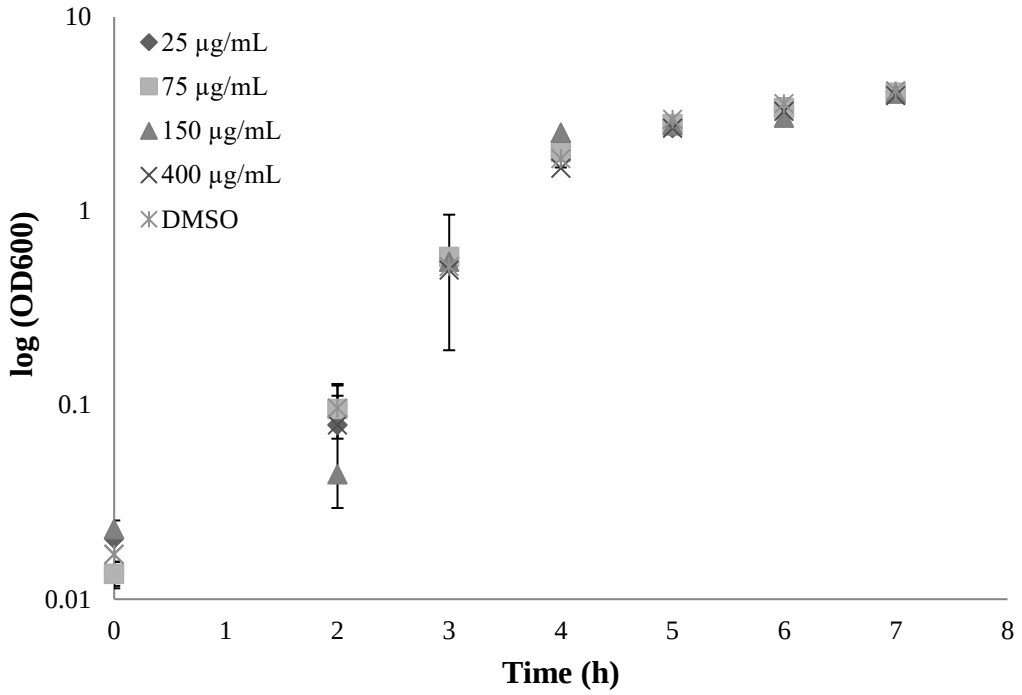

Figure 3.4 Effect of different concentrations of bulbocapnine on *B. subtilis* 168 growth.

3.1.2. Effects of alkaloids on cell viability

The viable cells of the control group and 75 µg·mL^{-1} of alkaloid treated groups were determined by counting CFU. As seen in Figure 3.5, CFU continued to increase after bulbocapnine or boldine treatment, as in the control group. On the other hand, the viable cell number has not increased and further dropped after roemerine treatment. This result indicated that roemerine treatment had an antimicrobial effect on the cells, which caused death. After one-hour treatment, the number of viable cells was sufficient for analysis. Therefore, these cells were used for proteomic and transcriptomic investigations.

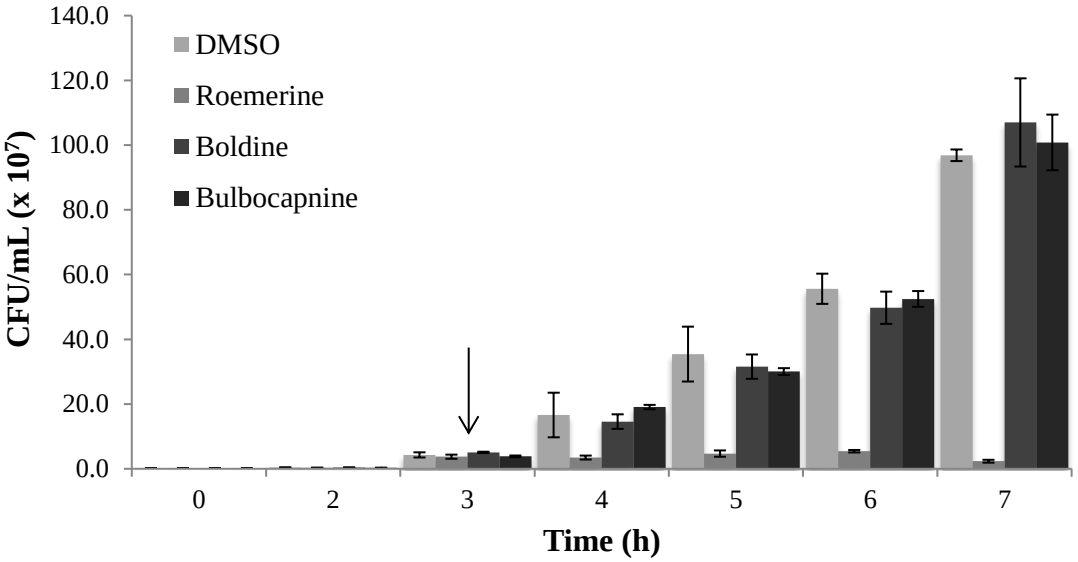

Figure 3.5 The CFU mL^{-1} of cells treated with DMSO and 75 $\mu g \cdot mL^{-1}$ of alkaloids. Alkaloids and DMSO were added at the 3rd hour.

3.1.3. *In vitro* effects of alkaloids on *B. subtilis* 168 cells

The *in vitro* effects of the alkaloids on the cells were visualized by taking images from SEM. Images of control cells have shown that they had shapes and sizes (5.2±0.94 μm) characteristic to *Bacillus* species with smooth cell surfaces (Figure 3.6a). Upon treatment with bulbocapnine or boldine, cells were slightly shorter than control cells (4.5±0.3 μm and 4.3±0.8 μm, respectively). There were rare dimples on the surface of boldine treated cells whereas the surfaces of bulbocapnine treated cells were crumpled and covered with blebs (Figure 3.6c and Figure 3.6d). Roemerine treated cells were comparably shorter in length than the control cells (4.0±0.6 μm). Blebs were all over the surfaces and the shapes of some cells were completely distorted (Figure 3.6b).

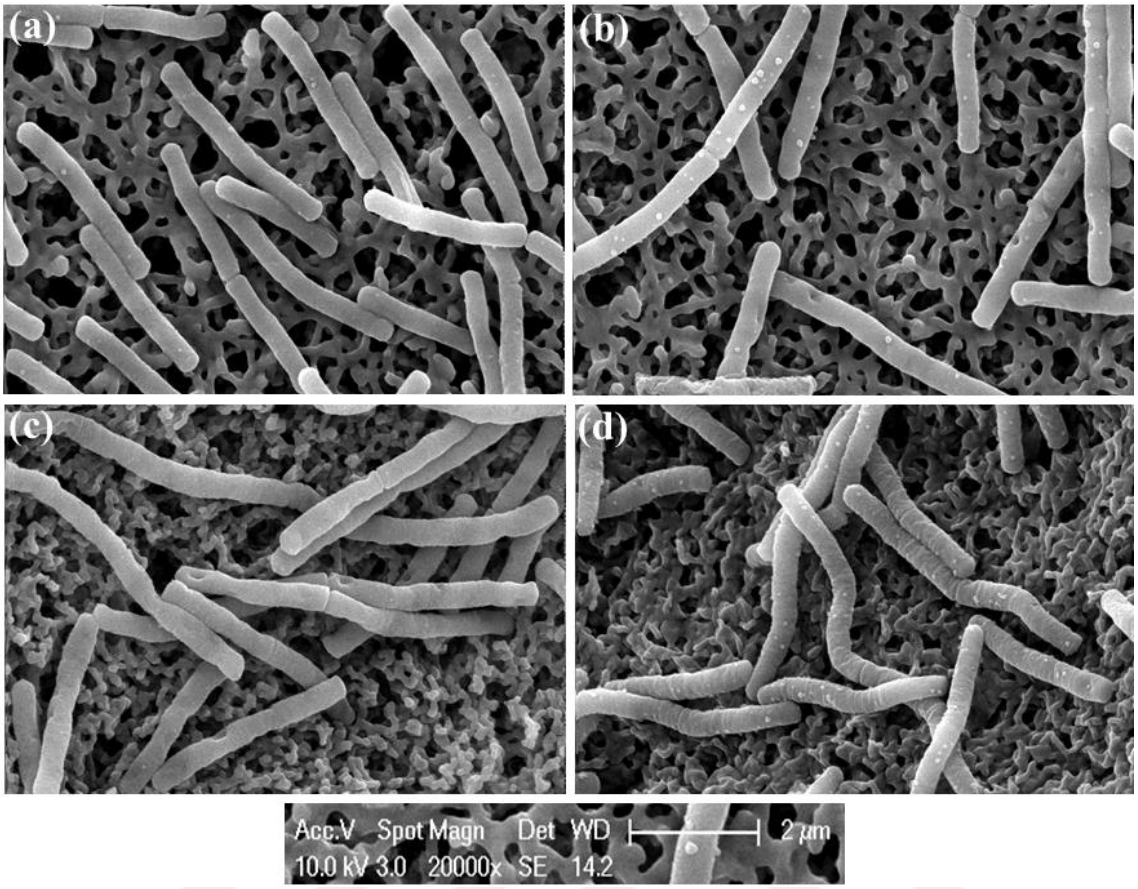

Figure 3.6 One-hour alkaloid treated and control cells images obtained from SEM: a) Control, b) Roemerine, c) Boldine, d) Bulbocapnine.

3.1.4. Protein profiles of *B. subtilis* 168 in response to alkaloids

Protein expression profiles of the control and treated cells were investigated using 2-DE. Differentially expressed proteins were selected manually and excised from the gels by ExQuest Spot-cutter (Bio-Rad, USA) for protein identification. Their fold changes were calculated using PDQuest Advance (Bio-Rad, USA) software and fold changes ≥ 1.5 were accepted as significant. Identified proteins with a fold change of < 1.5 are given in the Appendix C. Protein identification results showed that consecutively positioned protein spots were identical, such as spots R5 to R9 on the roemerine treated gels.

26 protein spots were selected for analysis and identification after comparing roemerine treated gels with DMSO treated control cells (Figure 3.7). This analysis showed that 22 of these spots had significant differential expression (Table 3.1). Among them, 16 spots

were up-regulated while 6 spots were down-regulated upon treatment with roemerine. Since consecutively positioned spots were identified as identical proteins, analysis has returned only 9 different up-regulated and 4 different down-regulated proteins. Of the up-regulated proteins, TpiA, Pta, and IolS are involved in carbon metabolism. Rpl10 is a ribosomal protein. YvyD, YvgN, and YceH are known as general stress proteins whereas LiaH is commonly expressed for resistance against oxidative stress and cell wall antibiotics, and AhpF is commonly expressed for resistance against peroxide stress. The down-regulated protein, GuaB, is known to be involved in purine/pyrimidine biosynthesis, Dps is a general stress protein, and DnaK is a chaperone (The UniProt Consortium, 2017).

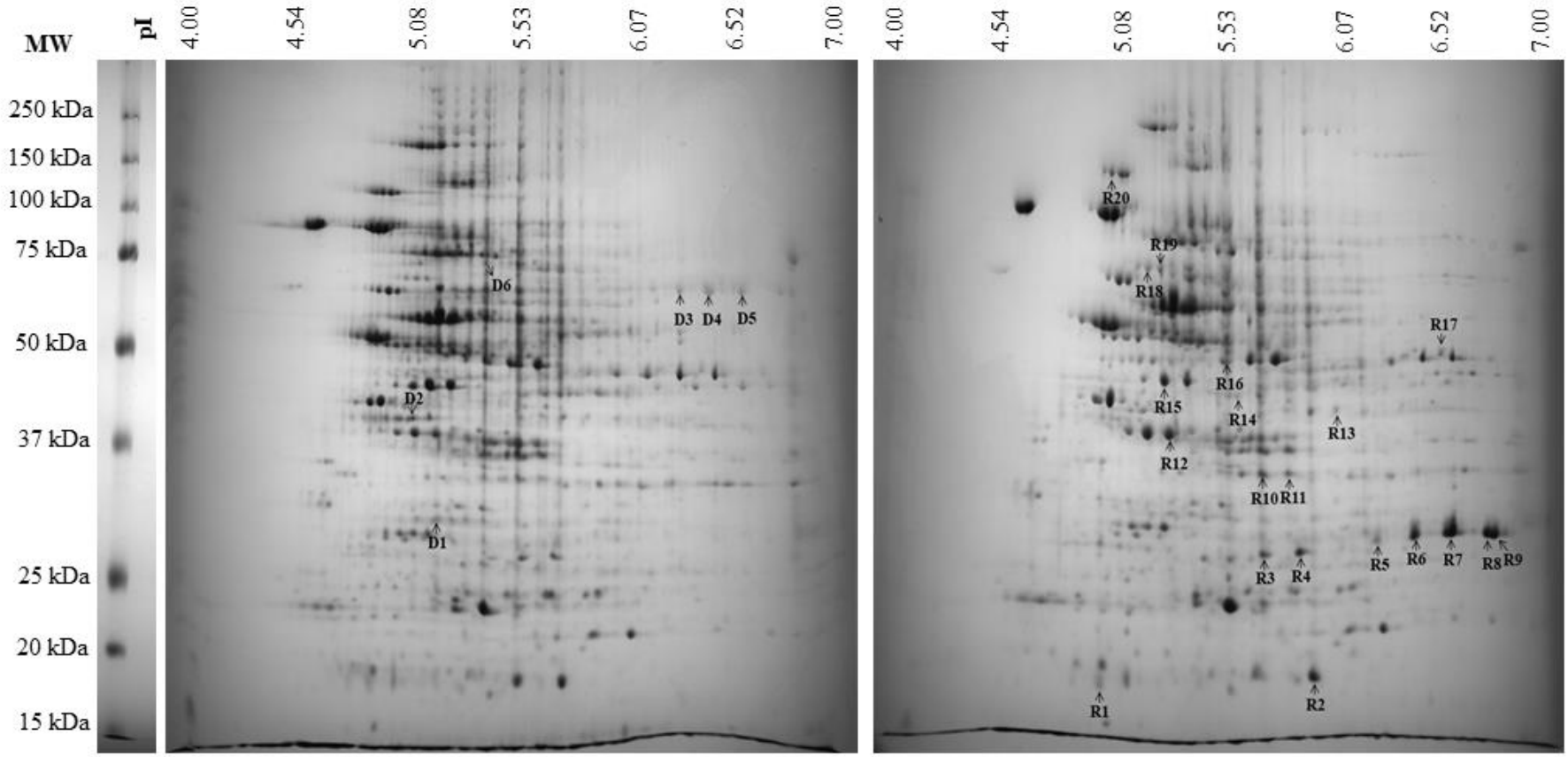

Figure 3.7 The 2-DE gel images of proteins from control (left) and roemerine treated (right) cells.

Table 3.1 Summary of the identified proteins under one-hour roemerine treatment.

Spot ID/SSP No	Gene Name	Protein Name	Best Protein Score	Sequence Coverage (%)	Experimental Protein Mass (kDa)/pI	Fold Change	Regulation	RNA-Seq log2 Fold Change
R7/8204	*liaH*	Protein LiaH	428	62	25.68/6.2	16867.8	Up	2.45
R9/9201	*liaH*	Protein LiaH	595	71	25.68/6.2	16315.3	Up	2.45
R6/8202	*liaH*	Protein LiaH	428	67	25.68/6.2	8367.7	Up	2.45
R8/8206	*liaH*	Protein LiaH	564	65	25.68/6.2	1563.2	Up	2.45
R5/7206	*liaH*	Protein LiaH	393	72	25.68/6.2	3	Up	2.45
R4/6202	*yvyD*	Uncharacterized protein YvyD	229	57	21.97/5.36	4.9	Up	1.12
R3/5202	*yvyD*	Uncharacterized protein YvyD	279	65	21.97/5.36	1.7	Up	1.12
R13/7401	*iolS*	Protein IolS	407	48	35.15/5.5	3.3	Up	1.27
R18/2704	*ahpF*	NADH dehydrogenase	228	35	54.84/4.89	2.7	Up	1.27
R19/2706	*ahpF*	NADH dehydrogenase	245	31	54.84/4.89	1.6	Up	1.27
R10/6301	*yvgN*	Glyoxal reductase	230	43	31.64/5.23	1.9	Up	1.03
R11/5306	*yvgN*	Glyoxal reductase	380	53	31.64/5.23	1.9	Up	1.03
D1/2208	*tpiA*	Triosephosphate isomerase	125	37	27.01/5.00	1.7	Up	-0.46
R2/6003	*rplJ*	50S ribosomal protein L10	456	66	18.07/5.41	1.6	Up	-0.26
D2/2404	*pta*	Phosphate acetyltransferase	402	58	34.77/4.84	1.6	Up	-

Table 3.1 Continued.

Spot ID/SSP No	Gene Name	Protein Name	Best Protein Score	Sequence Coverage (%)	Experimental Protein Mass (kDa)/pI	Fold Change	Regulation	RNA-Seq log2 Fold Change
R17/8604	*yceH*	Uncharacterized protein YceH	389	64	41/65/5.90	1.5	Up	0.55
D3/8703	*guaB*	Inosine-5'-monophosphate dehydrogenase	264	42	52.96/6.18	100	Down	-1.07
D4/8701	*guaB*	Inosine-5'-monophosphate dehydrogenase	150	28	52.96/6.18	2.3	Down	-1.07
D5/8702	*guaB*	Inosine-5'-monophosphate dehydrogenase	205	36	52.96/6.18	2.0	Down	-1.07
D6/4710	*glpK*	Glycerol kinase	127	26	55.05/5.12	100	Down	0.82
R1/1002	*dps*	General stress protein 20U	258	40	16.58/4.64	2.4	Down	-0.09
R20/1803	*dnaK*	Chaperone protein DnaK	423	38	65.96/4.76	2.0	Down	-0.24

The expressions of only 12 of the 22 proteins excised for identification from the gels of boldine treated cells were found to be significant (Figure 3.8). The identification results are summarized in Table 3.2. Eight proteins were up-regulated while three proteins were down-regulated. Among the up-regulated proteins, Rpl 10 is a ribosomal protein, PdhA and GapA are involved in carbon metabolism, EF-Tu is an elongation factor, GatB has a role in protein biosynthesis, YoxD is an oxidoreductase, SigA is one of the proteins responsible for RNA synthesis, and YvgN is a general stress protein. The down-regulated Hag is a flagellin protein, DapH has a function in amino acid biosynthesis, and EF-Ts is an elongation factor which has a function in protein synthesis (The UniProt Consortium, 2017).

From the gels of the bulbocapnine treated cells, 28 spots were excised and identified (Figure 3.9). Among them, only 10 had significantly changed in its expression; 5 were up- and 5 were down-regulated (Table 3.3). CodY is one of the up-regulated proteins and involved in the gene expression regulation. YkwC acts as an oxidoreductase and FabI has a role in fatty acid biosynthesis. Tkt is the transketolase enzyme. Of the down-regulated proteins, PdhA and PdhC are members of carbon metabolism. YjlD is known to be an NADH dehydrogenase in electron transport and ATP synthesis. Protein HprT is involved in the purine salvage and interconversion pathway. LysS is one of the responsible proteins in protein synthesis, modification, and degradation (The UniProt Consortium, 2017).

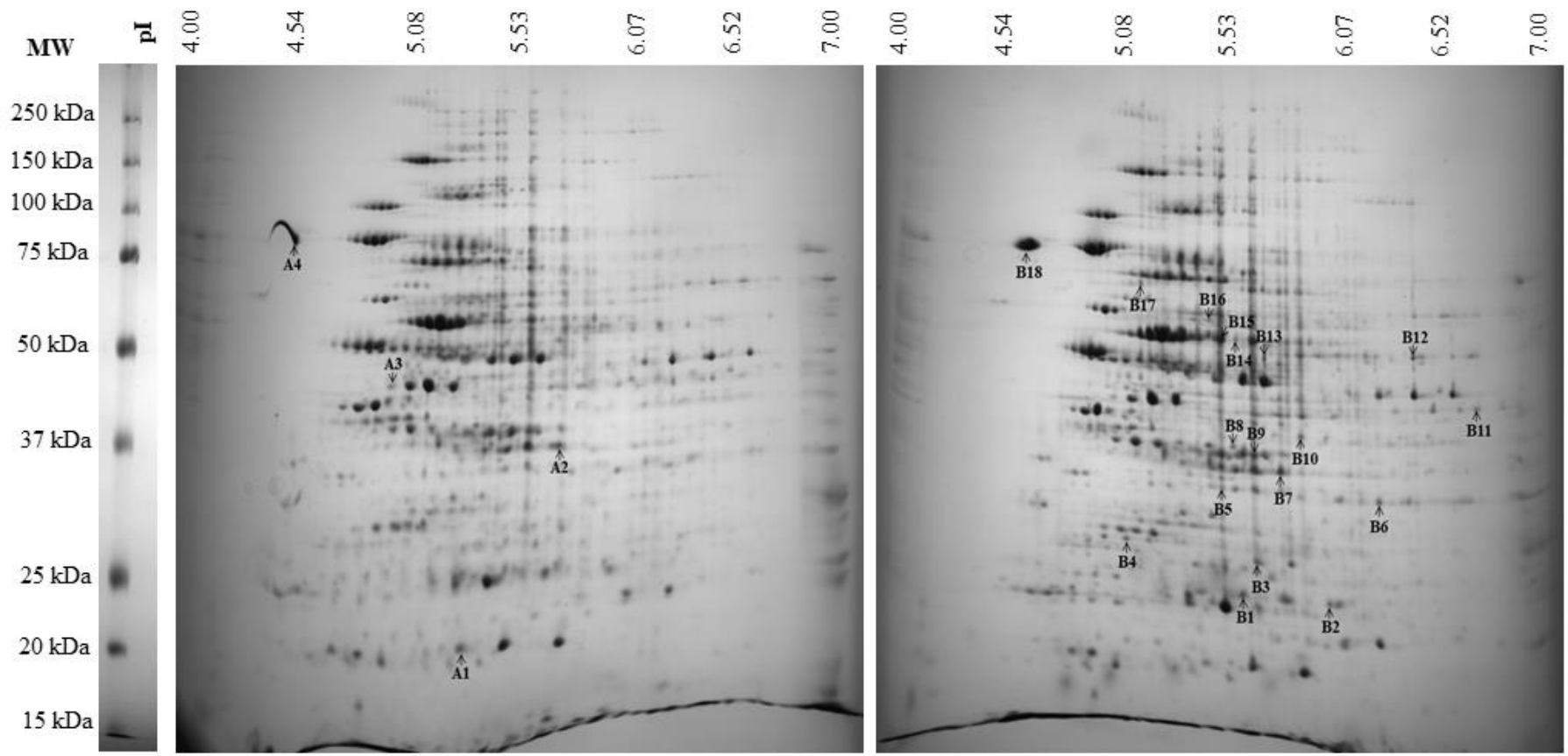

Figure 3.8 The 2-DE gel images of proteins from control (left) and boldine treated (right) cells.

Table 3.2 Summary of identified proteins under one-hour boldine treatment.

Spot ID/SSP No	Gene Name	Protein Name	Best Protein Score	Sequence Coverage (%)	Experimental Protein Mass (kDa)/pI	Fold Change	Regulation	RNA-Seq log2 Fold Change
B2/7102	*yoxD*	Uncharacterized oxidoreductase yoxD	492	61	25.28/5.48	623.9	Up	-
B13/6603	*gapA*	Glyceraldehyde-3-phosphate dehydrogenase 1	111	31	35.81/5.2	601.9	Up	-0.62
B12/9602	*pdhA*	Pyruvate dehydrogenase E1 component subunit alpha	177	37	41.52/5.91	376.2	Up	0.01
B5/4206	*yvgN*	Glyoxal reductase	144	43	31.64/5.23	4.7	Up	-0.48
A1/4001	*rplJ*	50S ribosomal protein L10	366	51	18.07/5.41	4.5	Up	0.09
B17/2704	*sigA*	RNA polymerase sigma factor rpoD	391	44	42.92/4.81	2.0	Up	-0.11
B14/5603	*tufA*	Elongation factor Tu	246	38	43.57/4.92	1.90	Up	-0.09
B15/4607	*tufA*	Elongation factor Tu	438	61	43.57/4.92	1.51	Up	-0.09
B16/4603	*gatB*	Aspartyl/glutamyl-tRNA amidotransferase subunit B	530	52	53.52/5.09	1.7	Up	-0.22
B4/2101	*dapH*	2,3,4,5-tetrahydropyridine-2,6-dicarboxylate N-acetyltransferase	307	42	24.95/4.87	2.6	Down	-0.17
B9/5306	*tsf*	Elongation factor Ts	347	58	32.33/5.17	2.2	Down	0.14
A3/1404	*hag*	Flagellin	287	34	32.61/4.97	1.8	Down	0.37

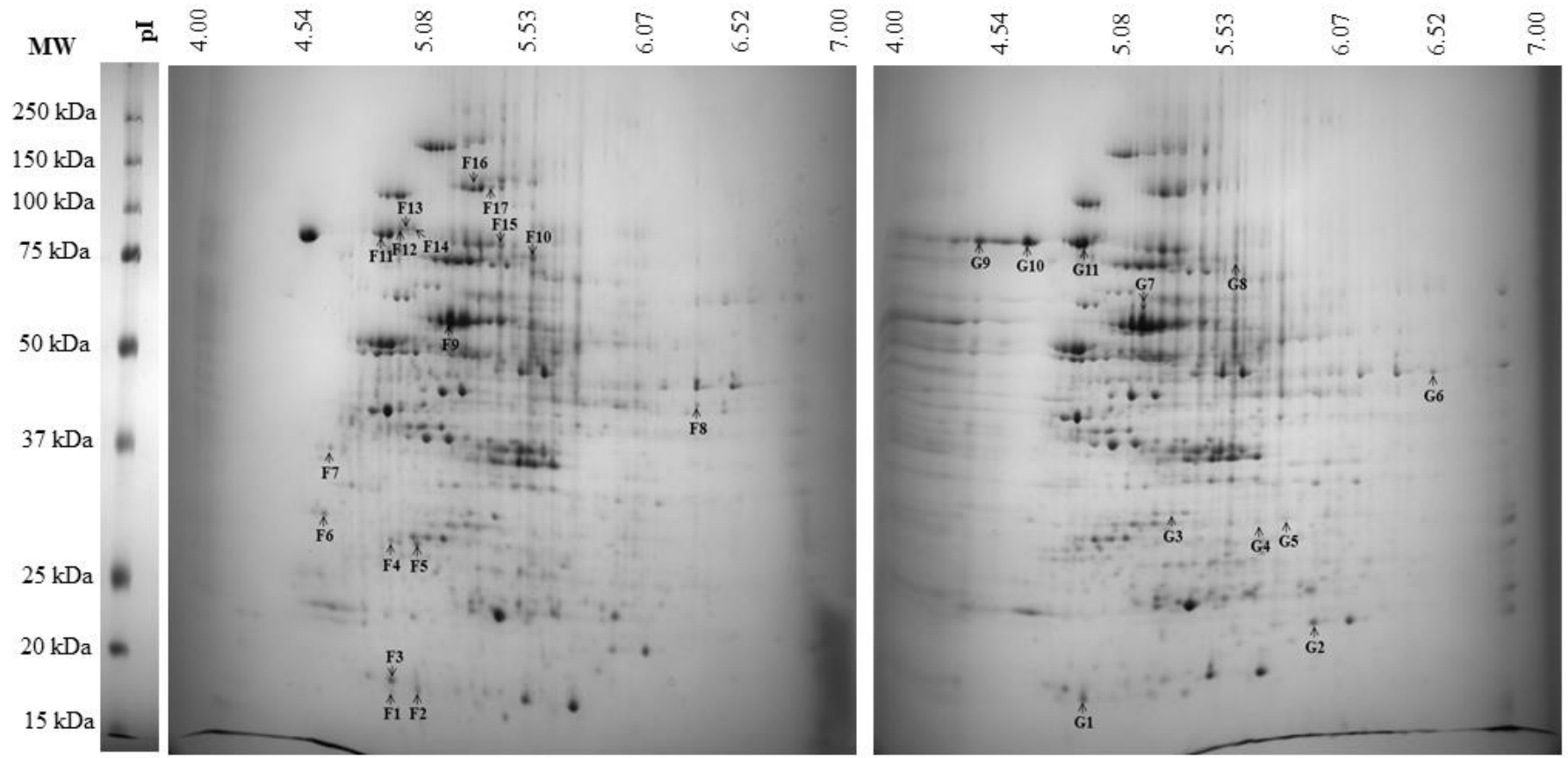

Figure 3.9 The 2-DE gel images of proteins from control (left) and bulbocapnine treated (right) cells.

Table 3.3 Summary of identified proteins under one-hour bulbocapnine treatment.

Spot ID/SSP No	Gene Name	Protein Name	Best Protein Score	Sequence Coverage (%)	Experimental Protein Mass (kDa)/pI	Fold Change	Regulation	RNA-Seq log2 Fold Change
F17/5901	*tkt*	Transketolase	113	29	72.30/4.99	3.88	Up	-0.20
F16/4906	*tkt*	Transketolase	325	40	72.30/4.99	1.52	Up	-0.20
G3/4205	*codY*	GTP-sensing transcriptional pleiotropic repressor CodY	488	54	28.99/4.95	3.2	Up	0.02
G5/7107	*fabI*	Enoyl-[acyl-carrier-protein] reductase [NADH]	183	38	27.86/5.67	2.3	Up	0.04
G4/7106	*ykwC*	Uncharacterized oxidoreductase YkwC	28		30.69/-	1.6	Up	-0.08
F10/6706	*lysS*	Lysyl-tRNA synthetase	230	43	57.50/5.19	52.1	Down	-
F15/5704	*pdhC*	Dihydrolipoyllysine-residue acetyltransferase component of pyruvate dehydrogenase complex	73	24	47.51/5.04	10.3	Down	-0.08
F2/2001	*hprT*	Hypoxanthine-guanine phosphoribosyltransferase	250	71	20.23/4.8	2.9	Down	-0.25
G6/8419	*pdhA*	Pyruvate dehydrogenase E1 component subunit alpha	498	57	41.52/5.91	2.5	Down	-0.01
F8/8414	*yjlD*	NADH dehydrogenase-like protein YjlD	282	24	41.93/6.28	2.34	Down	-0.07

3.1.5. Transcriptomic analysis of alkaloid treated *B. subtilis* 168 cells using RNA-Seq

The effects of 75 $\mu g \cdot mL^{-1}$ of each alkaloid on the *B. subtilis* 168 transcriptome were investigated using RNA-Seq. This analysis that includes read length (bp), clean reads, clean bases, and GC content (%) after data treatment is summarized in Table 3.4. Using the *B. subtilis* 168 genome (RefSeq accession number NC_000964.3) as the reference, all the transcripts were aligned for each condition. Each sample yielded a high number of mapped reads, over 90.0%.

Table 3.4 Summary of control and alkaloid treated *B. subtilis* 168 cDNA samples.

Treatment	Read length (bp)	Clean Reads	Clean bases	GC (%)	Mapped Reads (%)
DMSO	100	11128658	1112865800	44.60	94.4
Roemerine	100	11146966	1114696600	44.87	94.5
Boldine	100	11136066	1113606600	43.95	94.7
Bulbocapnine	100	10976112	1097611200	44.28	94.2

The overall RNA-Seq data from alkaloid treated cells were first comparatively evaluated using DMSO treated cells as the control case. The numbers presented in Table 3.5 show that roemerine treated samples had the highest number of differentially expressed genes.

Table 3.5 Number of differentially expressed genes following one-hour alkaloid treatment.

Treatment	Number of genes	
	Up-regulated	Down-regulated
Roemerine	344	221
Boldine	23	27
Bulbocapnine	14	13

Based on the groupings given in SubtiWiki database, differentially expressed genes were grouped into four main categories; 'Cellular Processes', 'Metabolism', 'Lifestyles', and 'Groups of Genes'. Within each of these, subcategories were selected based on the significantly affected genes/pathways (Table 3.6). The numbers of affected genes in the main categories for each treatment are presented in Figure 3.10. It is important to note that in this figure some of the genes appear in more than one category. In roemerine treated cells, categorization of the gene clusters pointed out that, the most significantly affected genes resided in the 'Metabolism' and 'Groups of Genes' categories. The number of affected genes in the 'Metabolism' category was slightly more than the genes in the 'Groups of Genes' category. These groups of genes were followed by genes in the 'Lifestyles' category. The least number of affected genes was in the 'Cellular Processes' category.

Table 3.6 Classification of the genes according to SubtiWiki database.

Category	Subcategory
Cellular processes	Transporters, Homeostasis
Metabolism	Electron transport and ATP synthesis, Carbon metabolism, Amino acid/ nitrogen metabolism, Lipid metabolism, Nucleotide metabolism, Additional metabolic pathways
Lifestyles	Exponential and early post-exponential lifestyles (Genetic competence), Sporulation, Coping with stress (General stress proteins (controlled by SigB), Heat shock proteins, Coping with hyper-osmotic stress, Resistance against oxidative and electrophile stress, Resistance against toxins/antibiotics, Biosynthesis of antibacterial compounds)
Groups of genes	Essential genes, Membrane proteins

For all categories, the number of affected genes was negligibly small in boldine and bulbocapnine treated cells. There were almost no differentially expressed genes in the 'Lifestyles' category following treatment with these alkaloids. This could also be

expected since there was not much change in the growth of *B. subtilis* 168 cells in the presence of boldine and bulbocapnine.

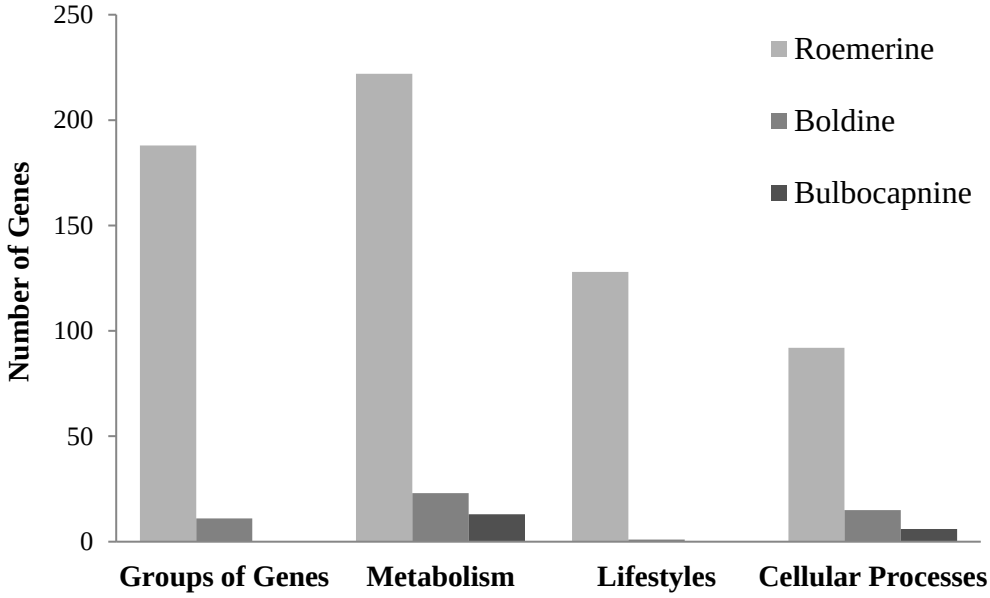

Figure 3.10 Differentially expressed genes categorized based on the groupings in SubtiWiki database.

3.1.6. Statistical analysis of RNA-Seq data

PCA is commonly applied to data matrices of high dimensions to extract information for finding patterns of similarities and differences. The coefficients of this linear combination are called loadings and the actual values of the projection of the samples are called scores (Misra et al., 2002). To compare the effects of the three alkaloids, PCA was applied to the raw reads obtained from RNA-Seq data. The first two principal components of the new projection space captured 97.8% of the information of the data matrix. Thus, they were used to construct the PCA plots (Figure 3.11 and Figure 3.12).

The plot presented in Figure 3.11 showed that the effects of boldine and bulbocapnine on *B. subtilis* 168 were not very different from the effect of DMSO treated control cells; the dots corresponding to boldine, bulbocapnine, and DMSO treated cells resided close to each other. On the other hand, the dot for the roemerine treated *B. subtilis* 168 lied away from these three dots, an important evidence for the different effect of roemerine from boldine and bulbocapnine.

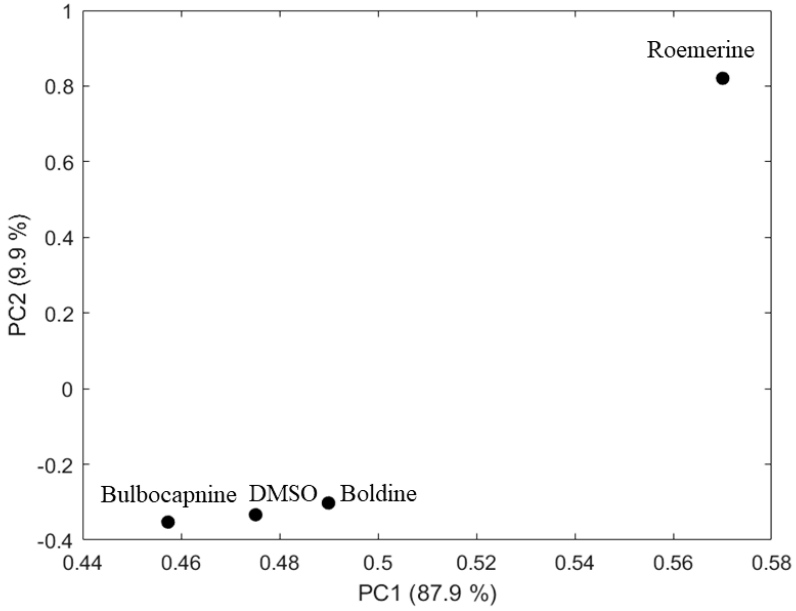

Figure 3.11 PCA plot of samples treated with different alkaloids.

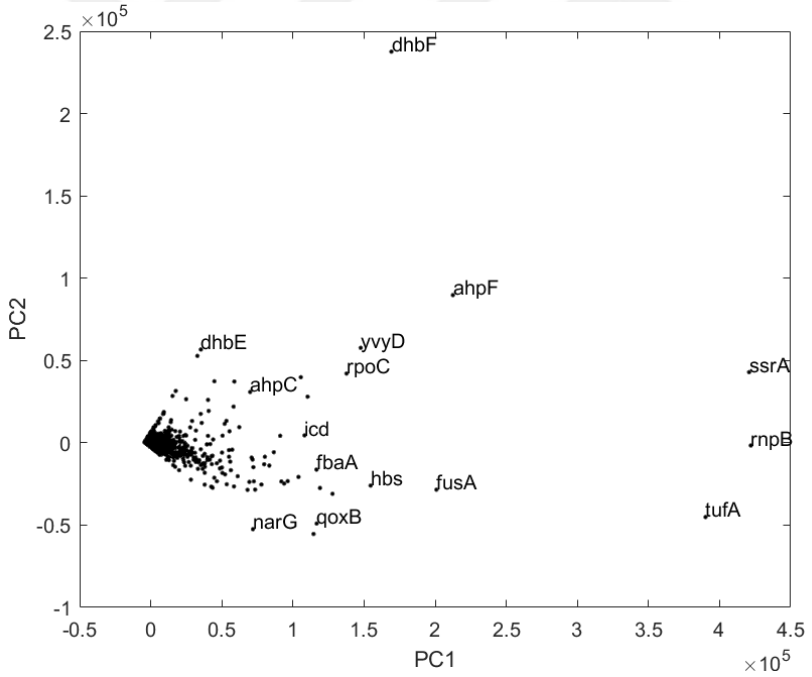

Figure 3.12 Loadings plot from PCA.

Using the calculated Mahalanobis distances, Figure 3.12 was constructed which shows the genes that are responsible for the observed separation in the PCA plot of Figure 3.11. To get a better picture for the genes that lead to the separation obsferved in Figure

3.12 and visualize their regulation patterns, the first 50 genes with the highest calculated Mahalanobis distances were used to draw a heatmap (Figure 3.13).

The heatmap clearly showed that the regulation pattern of the genes in the boldine and bulbocapnine treated *B. subtilis* 168 samples were similar to each other and to the control cells. On the other hand, the regulation pattern of the genes in the roemerine treated *B. subtilis* 168 samples was different from the control cells.

3.1.7. Validation of gene expressions by qPCR

Analysis of the high-throughput transcriptional data from RNA-Seq commonly requires its validation. 16S ribosomal RNA, *rrnA*, was used as the housekeeping gene. Five genes were selected for validation of the RNA-Seq results. The selected genes were all from significantly affected pathways; *dhbB* and *feuA* from Fe uptake and metabolism, *narH* from anaerobic respiration and proton motive force (PMF) generation, *aroA* from aromatic amino acid biosynthesis and *bmr* as a multidrug transporter. The results presented in Table 3.7 show that the regulation pattern of all the selected genes was consistent, though the fold changes varied slightly.

Table 3.7 Expression levels of selected genes.

Regulation pattern / log2 fold change (qPCR / RNA-Seq)			
Gene name	**Boldine**	**Bulbocapnine**	**Roemerine**
dhbB	3.9 / 1.1	2.6 / 0.9	10.2 / >10
bmr	6.1 / 0.8	2.6 / 0.3	7.2 / 1.7
feuA	3.6 / 1.3	2.1 / 0.2	5.9 / 2.4
narH	0.4 / -0.4	-1.5 / -0.2	BDL / > -10
aroA	-0.4 / -1.8	2.5 / 0.4	1.9 / 0.5

*BDL: Below detection limit

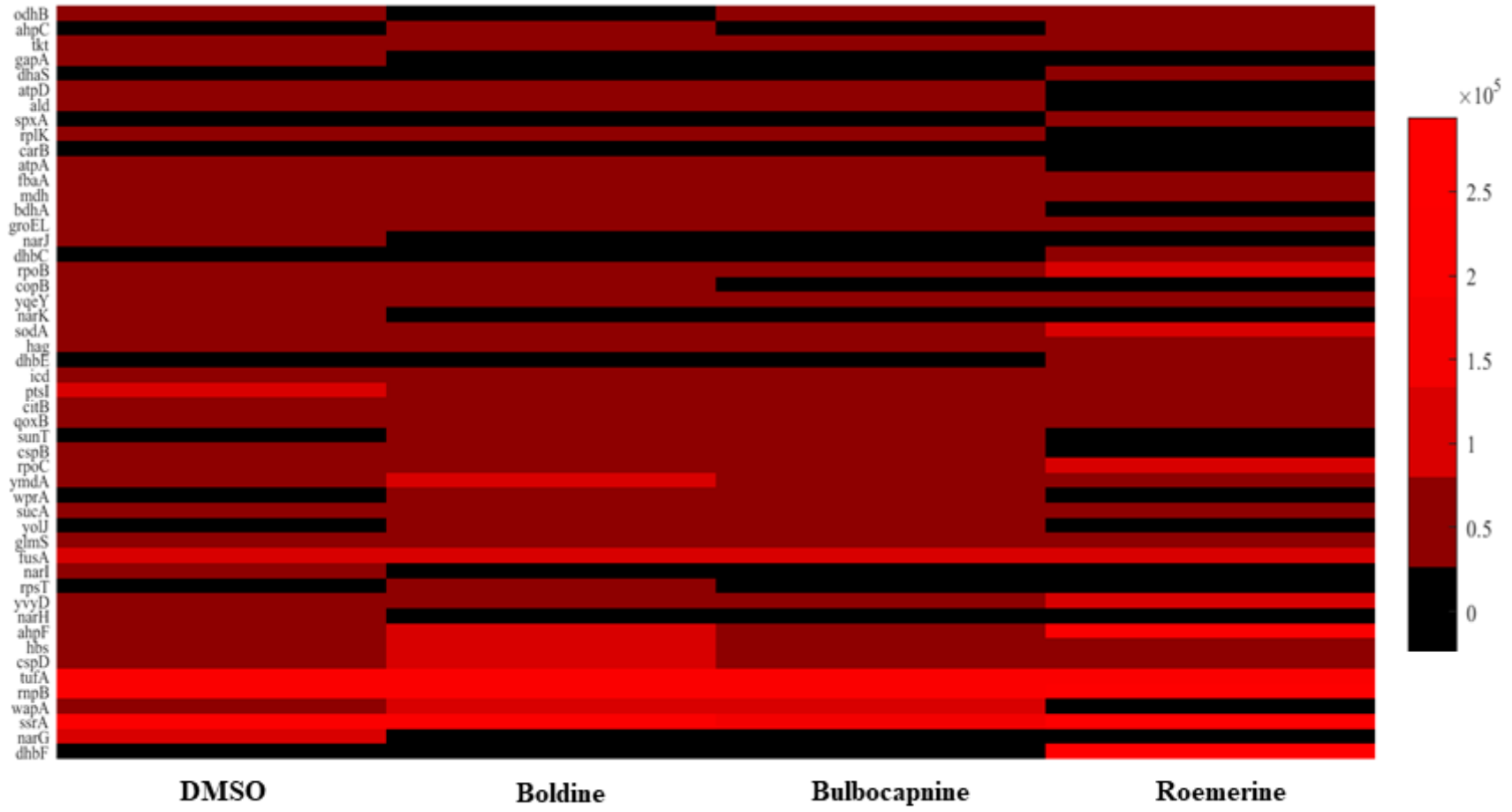

Figure 3.13 Heatmap constructed using the Mahalanobis distances from PCA. The colour scale indicates the read numbers of the genes for each condition.

3.2. Discussion

The elucidation of the MOA of active natural products is an important step in the development of alternative antimicrobial agents against increasing bacterial resistance. Omic technologies provide crucial clues to elucidate the mechanisms and the targets of antimicrobial candidates. Motivated by the evidence that both roemerine and bulbocapnine display antimicrobial activity and the lack of any information on the antimicrobial activity of boldine (Gokgoz and Akbulut, 2015; Orhan et al., 2007), in the present study proteomic and transcriptomic tools were used to get mechanistic details on the antimicrobial effects of three structurally very similar aporphine-type alkaloids on *B. subtilis* 168 cells. Differentially expressed proteins were determined using 2-DE and identified with MS. RNA-Seq analysis was used to understand the effects of the alkaloids on the transcriptome level.

Among the studied alkaloids, only roemerine had significant antimicrobial activity. The growth of *B. subtilis* 168 cells remained unaltered even with high concentrations of boldine or bulbocapnine. The fact that boldine and especially bulbocapnine did not have any antimicrobial activity was rather unexpected because there was a MIC value reported for bulbocapnine (Orhan et al., 2007).

Common functional groups that are responsible for antimicrobial activity are reported to be hydroxyl, methoxy, and methylenedioxy in specified locations in the backbone ring structures (Cushnie et al., 2014; Udvardy et al., 2014). As found in many antimicrobial alkaloids, the methylenedioxy group could be critical for the observed activity of roemerine. Unfortunately, the additional groups on the C10 and C11 of bulbocapnine probably interfered with the electrostatic properties leading to loss of antimicrobial activity. In addition, methoxy and hydroxyl groups on the boldine structure could not contribute to the antimicrobial activity.

In vitro effects of the alkaloids were investigated by taking SEM images from one-hour alkaloid treated cells. The images have shown that there was reorganization in the membrane structure and this response changed with the type of the alkaloid introduced to the growth environment.

Protein patterns of the one-hour alkaloid treated and control cells were comparatively analyzed to understand the MOA of the alkaloids on the proteome level. The results showed that the effects of boldine and bulbocapnine treatments were not as significant as the roemerine treatment. There were only 10 and 8 differentially expressed proteins upon boldine and bulbocapnine treatment, respectively. These proteins belonged to the pathways related to growth such as carbohydrate metabolism, amino acid and protein synthesis or ribosomal proteins. Consequently, it was very difficult to propose a MOA using the changes in the proteome maps alone. Further, RNA-Seq findings confirmed that there were only minor metabolic changes on the cells with boldine and bulbocapnine treatment. The changes recorded with these two alkaloids were not high enough to be considered as significant when compared to the control cells.

Differentially expressed proteins upon treatment with roemerine gave clues about its MOA and the results were consistent with the transcriptomic data obtained from the same cells. Below, proteins and pathways that are believed to be relevant to the antimicrobial activity of the roemerine are considered.

3.2.1. Drug efflux proteins

Multidrug resistance (MDR) pumps are important contributors in all organisms for gaining resistance through efflux of multiple compounds such as antibiotics and anticancer drugs (Nikaido, 2009; Schindler and Kaatz, 2016). This efflux minimizes the intracellular concentration of the antibiotic. In this respect, overexpression of the efflux pumps, especially multidrug resistance pumps, which have a wide range of substrates, contributes to high levels of resistance (Blair et al., 2015). Efflux pumps are classified in five different families, based on their similarities in protein sequences and their affinities for different ligands. These are the ATP binding cassette (ABC) superfamily, the major facilitator superfamily (MFS), the multidrug and toxin extrusion (MATE) family, the resistance nodulation division (RND) superfamily, and the small multidrug resistance (SMR) family. Of these 5 families, only the ABC-type is energized by ATP, the other four families use PMF for efflux (Du et al., 2015).

B. subtilis transporters have been extensively studied because this microorganism possesses a significant genomic abundance of multidrug transporters relative to other gram-positives (Lorca et al., 2007; Neyfakh et al., 1991). BceAB (Ohki et al., 2003),

BmrA (Steinfels et al., 2004), BmrCD (Bernard et al., 2003; Torres et al., 2009) of ABC superfamily; Blt (Ahmed et al., 1995; Baranova et al., 1999), Bmr (Ahmed et al., 1995; Baranova et al., 1999; Woolridge et al., 1997), Bmr3 (Ohki and Murata, 1997; Ohki and Tateno, 2004), LmrB (Murata et al., 2003; Yoshida et al., 2004), and MdtP (Kim et al., 2009) of MFS; YerP (Tsuge et al., 2001) of RND superfamily, and EbrAB (Masaoka et al., 2000) of SMR family are the well-characterized efflux pumps in *B. subtilis*. Among these pumps, Bmr is one of the first-discovered bacterial efflux pumps and Blt is another that is highly homologous to Bmr (52%) (Neyfakh et al., 1991; Schindler and Kaatz, 2016)

The expression levels of the MDR pumps in one-hour bulbocapnine and boldine treated cells did not change significantly according to the RNA-Seq analysis. With the introduction of roemerine into the environment, the expressions of the genes encoding Blt, Bmr, and LmrB were all up-regulated. The common feature of these pumps is that all belong to the MFS superfamily, which utilizes PMF for drug efflux. This could be a result of insufficient ATP levels in the cells. When the expression levels of the pumps of ABC superfamily, which require ATP for their functions, were examined, no significant change was recorded. On the other hand, there is an important clue about the ABC transporter of *B. subtilis*, BmrA. A previous study reported that roemerine enhanced the cytotoxic response mediated by vinblastine with multidrug-resistant KB-V1 cells. In the same study, this finding was linked to the possible interaction of roemerine with P-glycoprotein, an eukaryotic ABC transporter homologous to BmrA (Steinfels et al., 2004; You et al., 1995). In light of this information, it could be hypothsized that roemerine could bind and inhibit BmrA protein in *B. subtilis* 168.

A common feature of the up-regulated MDR pumps that need to be underlined is that none of them are energized by ATP but PMF. The importance of this will become clear in the discussion of the reprogramming of the energy generation pathways.

3.2.2. Electron transport and ATP synthesis

Membrane-localized electron transfer chains are responsible for energy generation in cells. There are four different terminal oxidases namely cytochrome caa_3 (*ctaCDEF*), cytochrome aa_3 (*qox* operon), cytochrome *bd* (*cyd* operon), and ythAB (*yth* operon) in *B. subtilis* that transfer electrons to terminal oxygen for energy production (Hao et al.,

2013; Möbius et al., 2010; Zamboni et al., 2003). Belonging to this system, the expression of genes encoding different terminal oxidases significantly changed after roemerine treatment. All genes in the *cyd* operon were down-regulated. There was only a slight decrease in the expression of the *qox* operon. Cytochrome aa_3 was reported as the most important oxidase in PMF generation during exponential growth phase. This is expected to lead to a failure in the PMF generation (Winstedt and Von Wachenfeldt, 2000).

Nitrate respiration is another system for energy production. However, this system did not contribute to PMF generation. Upon treatment with all studied alkaloids, the *nar* operon (*narGHJI*), which encodes a respiratory nitrate reductase responsible for nitrate respiration (Huang et al., 2015; Nakano et al., 1998), was down-regulated. The extent of this down-regulation was important in roemerine treated cells. The repression of the *nar* complex is also linked to antibiotic resistance. The *narG* gene was reported to be down-regulated in multidrug-resistant *Mycobacterium tuberculosis* (Penuelas-Urquides et al., 2013) and the low concentrations of the *nar* complex were found to enhance the resistance of *Escherichia coli* against aminoglycoside antibiotics (Ma et al., 2013). The change in both types of respiration is an indication for a failure in the generation of PMF.

Substrate transport is not the sole process to which PMF is linked. H^+ that are involved in the building of proton gradient across the membrane are transported across the membrane during respiration to drive ATP synthesis. Thus, ATP synthesis would also be expected to slow down with the shortage in PMF (Proctor and von Humboldt, 1998).

3.2.3. Purine and pyrimidine metabolism

Purine and pyrimidine nucleotides are essential metabolites for the cells because they are major energy carriers (ATP and GTP), subunits of DNA and RNA, and precursors for the synthesis of enzyme cofactors such as NAD and NADP (Moffatt and Ashihara, 2002; Shi et al., 2014). Purines and pyrimidines could be synthesized either by *de novo* synthesis or from salvage reactions. The *de novo* biosynthetic pathway of purines consists of 10 different enzymatic reactions and these enzymes are synthesized from the *pur* operon (*purEKBCSQLFMNHD*) (Shi et al., 2014; Switzer et al., 2002). All the genes in the *pur* operon were down-regulated upon one-hour roemerine treatment. The

down-regulation of the protein GuaB found in *de novo* synthesis of guanine nucleotides was consistent with these findings (Table 3.1).

Pyrimidine nucleotide biosynthesis is regulated by the *pyr* operon (*pyrR-pyrP-pyrB-pyrC-pyrAA-pyrAB-pyrK-pyrD-pyrF-pyrE*). The first gene encodes the bifunctional PyrR protein, which is a uracil phosphoribosyl transferase and involved in the regulation on the *pyr* operon by transcriptional attenuation mechanism. The second gene, *pyrP*, encodes a uracil permease. The remaining genes encode the six enzymes involved in biosynthesis (Quinn et al., 1991; Turner et al., 1998). After one-hour roemerine treatment, all the genes in *pyr* operon except *pyrR* and *pyrAB* were down-regulated. In contrast, a number of genes found in salvage pathways for purine and pyrimidine biosynthesis, *guaC* and *pupG* in roemerine treated cells were up-regulated. Taken together, this could be a sign for minimization in energy consumption since salvage pathways are less energy consuming (Nyhan, 2005).

The down-regulation of the purine and pyrimidine synthesis could also be explained with the growth rates of the cells. Cells with lower growth rates would be expected to display slower DNA replication, therefore their nucleotide requirement would be less (Beckering et al., 2002). There were no significant changes in these pathways with boldine and bulbocapnine treated cells.

3.2.4. Oxidative stress

When bacteria are exposed to adverse conditions, they develop different and complex mechanisms to cope with the harsh circumstances. A consequence of the struggle with stress conditions is the induction of production and accumulation of reactive oxygen species (ROS) and the inhibition of cell growth. ROS generation was linked up with two situations: 1) incomplete reduction of O_2 during respiration, and 2) the presence of bactericidal antibiotics (Kohanski et al., 2007; Zuber, 2009). Since the genes encoding terminal oxidases were down-regulated with roemerine treatment, there was a failure in the reduction process of O_2 which possibly caused ROS production. In addition, ROS could be produced due to the antimicrobial activity of roemerine.

As in line with expectations, to reduce the side effects of ROS produced in response to alkaloid treatment, many genes involved in resistance against or in response to oxidative

and electrophilic stress (*ahpC, ahpD, katA, katE, ohrB*) were up-regulated. However, the number of such genes was significantly higher in roemerine treated cells. In addition, an NADH dehydrogenase AhpF protein was up-regulated upon treatment with roemerine. Moreover, *suf* operon which is responsible for assembly of Fe-S cluster (*sufB, sufC, sufD,* and *sufS*) and urease genes (*ureABC*), which were frequently reported to be induced under oxidative stress (Mostertz et al., 2004), were also significantly up-regulated but only in the roemerine treated cells. Thus, oxidative stress caused by roemerine is undoubtedly higher.

Iron is an important micronutrient for all organisms with many roles in different biological processes including respiration, tricarboxylic acid (TCA) cycle, oxygen transport, DNA biosynthesis (Krewulak and Vogel, 2008). The regulation of its uptake is under the control of Fur regulon in *B. subtilis*. It was reported that Fur regulon undergoes inactivation by reaction with ROS during oxidative stress and this results in deregulation of iron uptake and increased intracellular iron concentration (Varghese et al., 2007). Unfortunately, the accumulated iron ions may react with ROS through Fenton's reaction producing molecules that further damage biological macromolecules (Krewulak and Vogel, 2008; Touati, 2000). Indeed, our RNA-Seq results showed that *fhuBCDG* operon of ferrichrome-Fe^{3+} uptake was up-regulated in roemerine treated cells. In addition, siderophores which are responsible for transporting Fe^{+3} into the cells are normally expressed under iron-limited conditions (Saha et al., 2016) but the genes related with the *B. subtilis* 168 siderophore bacillibactin production (*dhbACEBF* operon) and uptake (*feuABC* and *besA*) were up-regulated after one-hour treatment with any one of the three alkaloids. Again, the level of this up-regulation was extremely high only in roemerine treated cells.

3.2.5. Other pathways

Apart from the pathways mentioned above, there were some highly differentially expressed proteins and genes that are worth to mention. In *B. subtilis* cells, the alternative sigma factor δ^B controls stress response (Petersohn et al., 1999). Since the roemerine presence created a stress environment, the genes controlled by δ^B regulon were up-regulated under roemerine treatment.

Another consequence of the roemerine treatment is the down-regulation of the genes in carbon metabolism. This could be regarded as a direct outcome of the decrease in the growth rates. The only change in the carbon metabolism that is remarkable was the up-regulation of the 10 *iol* genes of the myo-inositol catabolism in roemerine treated cells. The up-regulation of the protein IolS in this pathway supported the RNA-Seq results. The variations in the genes of amino acid and protein synthesis could be difficult to explain since there could be multiple paths affecting them.

LiaH was the most affected protein upon treatment with roemerine. It was reported that the expression of this protein is up-regulated against cell envelope stress such as cell wall antibiotics (Domínguez-Escobar et al., 2014). This result showed that membrane protein(s) could be the target of the roemerine. Many genes of the affected pathways were linked to the cell membrane. Unfortunately, protein maps obtained were only for the soluble proteins. Therefore, expressional differences in membrane proteins were not visualized on these maps. Combined with the images obtained from SEM analysis, this is a strong evidence of the reorganization of the membrane structure and this response changes with the type of the alkaloid introduced to the growth environment.

4. CONCLUSION

The uncertainty in action mechanisms has for long hampered the use of plant-derived substances as lead molecules for drug development. In recent years, omic technologies are extensively used to enlighten the MOA and to identify targets, which makes plant-derived substances promising antimicrobial candidates with their multi-target properties. In the present study, the antimicrobial mechanism of different alkaloids on *B. subtilis* 168 cells was evaluated using proteomic and transcriptomic tools. The results have shown that among the structurally very similar aporphine alkaloids, boldine, bulbocapnine, and roemerine, only the latter possessed significant antimicrobial activity. Functional groups found on the alkaloids have a substantial influence on their antimicrobial activity. In this respect, the methylenedioxy group could be regarded as an important substituent for the activity of roemerine. Cell growth was retarded upon treatment with roemerine and roemerine-treated cells were shorter than the control cells. The obtained transcriptome and proteome profiles suggested that roemerine accumulated in the cells and this accumulation caused building up of ROS, which eventually deregulated various pathways such as iron uptake.

The growth of *B. subtilis* 168 cells did not change even with high concentrations of boldine or bulbocapnine, but transcriptional-wise, similar metabolic pathways were slightly affected. Proteome profiles were also not very different after boldine or bulbocapnine treatments. *In vitro* effects from SEM images showed that the cell sizes were slightly shorter than the control cells and there was reorganization on the cell membrane. The tetra-substituted structure of boldine on C1, C2, C9, and C10 with preferred functional groups was also insufficient to induce an antimicrobial activity.

The antimicrobial activity of roemerine has shown this alkaloid to be a new lead in drug discovery processes. Further studies will be necessary to find the specific targets of roemerine and to evaluate the synergistic effects of roemerine with different substances to reduce its effective concentration.

REFERENCES

Abreu, A.C., McBain, A.J., Simões, M. (2012) Plants as sources of new antimicrobials and resistance-modifying agents. Natural Product Reports, 29, 1007–1021.

Aebersold, R., Mann, M. (2003) Mass spectrometry-based proteomics. Nature, 422, 198–207.

Ahmed, M., Lyass, L., Markham, P.N., Taylor, S.S., Vazquez-Laslop, N., Neyfakh, A.A. (1995) Two highly similar multidrug transporters of Bacillus subtilis whose expression is differentially regulated. Journal of Bacteriology, 177, 3904–3910.

Andersson, D.I., Hughes, D. (2010) Antibiotic resistance and its cost: is it possible to reverse resistance? Nature Reviews Microbiology, 8, 260–271.

Arias, C., Murray, B. (2015) A new antibiotic and the evolution of resistance. The New England Journal of Medicine, 372, 1168–1170.

Arnvig, K.B., Comas, I., Thomson, N.R., Houghton, J., Boshoff, H.I., Croucher, N.J., Rose, G., Perkins, T.T., Parkhill, J., Dougan, G., Young, D.B. (2011) Sequence-based analysis uncovers an abundance of non-coding RNA in the total transcriptome of Mycobacterium tuberculosis. PLoS Pathogens, 7(11), e1002342.

Ayyildiz, D., Arga, K.Y., Avci, F.G., Altinisik, F.E., Gurer, C., Gulsoy Toplan, G., Kazan, D., Wozny, K., Brügger, B., Mertoglu, B., Sariyar Akbulut, B. (2017) Transcriptomic analysis displays the effect of (-)-roemerine on the motility and nutrient uptake in Escherichia coli. Current Genetics, 63, 709–722.

Bandow, J.E., Hecker, M. (2007) Proteomic profiling of cellular stresses in Bacillus subtilis reveals cellular networks and assists in elucidating antibiotic mechanisms of action. Progress in Drug Research, 64, 79–101.

Baranova, N.N., Danchin, A., Neyfakh, A. A. (1999) Mta, a global MerR-type regulator of the Bacillus subtilis multidrug-efflux transporters. Molecular Microbiolgy, 31, 1549–1559.

Beckering, C.L., Steil, L., Weber, M.H.W., Völker, U., Marahiel, M.A., Beckering, C.L., Steil, L., Weber, M.H.W., Vo, U. (2002). Genomewide Transcriptional Analysis of the Cold Shock Response in Bacillus subtilis. Journal of Bacteriology, 184, 6395.

Bell, B.G., Schellevis, F., Stobberingh, E., Goossens, H., Pringle, M. (2014) A systematic review and meta-analysis of the effects of antibiotic consumption on antibiotic resistance. BMC Infectious Diseases, 14, 1–25.

Bernard, R., Joseph, P., Guiseppi, A., Chippaux, M., Denizot, F. (2003) YtsCD and YwoA, two independent systems that confer bacitracin resistance to Bacillus subtilis. FEMS Microbiology Letters, 228, 93–97.

Bhadra, K., Kumar, G.S. (2011) Therapeutic Potential of NucleicAcid-Binding Isoquinoline Alkaloids:Binding Aspects and Implications for Drug Design. Medicinal Research Reviews, 31, 821–862.

Blair, J.M.A., Webber, M.A., Baylay, A.J., Ogbolu, D.O., Piddock, L.J.V. (2015) Molecular mechanisms of antibiotic resistance. Nature Reviews Microbiology, 13, 42–51.

Bradford, M.M. (1976) Determinacion De Proteinas: Metodo De Bradford. Analytical Biochemistry, 72, 248–254.

Brazas, M.D., Hancock, R.E. (2005) Using microarray gene signatures to elucidate mechanisms of antibiotic resistance. Drug Discovery Today, 10, 1245–1252.

Brötz-Oesterhelt, H., Brunner, N.A. (2008) How many modes of action should an antibiotic have? Current Opinion in Pharmacology, 8, 564–573.

Budeyri Gokgoz, N., Avci, F.G., Yoneten, K.K., Alaybeyoglu, B., Ozkirimli, E., Sayar, N.A., Kazan, D., Sariyar Akbulut, B. (2017) Response of *Escherichia coli* to Prolonged Berberine Exposure. Microbial Drug Resistant, 23, 531–544.

Chen, J., Gao, K., Liu, T., Zhao, H., Wang, J., Wu, H., Liu, B., Wang, W. (2013) Aporphine alkaloids: A kind of alkaloids' extract source, chemical constitution and pharmacological actions in different botany. Asian Journal of Chemistry, 25, 10015–10027.

Chevallet, M., Luche, S., Rabilloud, T. (2006) Silver staining of proteins in polyacrylamide gels. Nature Protocols, 1, 1852–1858.

Cho, W.C.S. (2007) Proteomics Technologies and Challenges. Genomics, Proteomics, and Bioinformatics, 5, 77-85.

Cho, Y.S., Schiller, N.L., Kahng, H.Y., Oh, K.H. (2007) Cellular responses and proteomic analysis of Escherichia coli exposed to green tea polyphenols. Current Microbiology, 55, 501–506.

Clatworthy, A.E., Pierson, E., Hung, D.T. (2007) Targeting virulence: a new paradigm for antimicrobial therapy. Nature Chemical Biology, 3, 541–548.

Cowan, M.M. (1999) Plant products as antimicrobial agents. Clinical Microbiology Reviews, 12, 564–82.

Croucher, N.J., Thomson, N.R. (2010) Studying bacterial transcriptomes using RNA-seq. Current Opinion in Microbiology, 13, 619–624.

Cushnie, T.P.T., Cushnie, B., Lamb, A.J. (2014) Alkaloids: An overview of their antibacterial, antibiotic-enhancing and antivirulence activities. International Journal of Antimicrobial Agents, 44, 377–386.

Di Pasqua, R., Mamone, G., Ferranti, P., Ercolini, D., Mauriello, G. (2010) Changes in the proteome of Salmonella enterica serovar Thompson as stress adaptation to sublethal concentrations of thymol. Proteomics, 10, 1040–1049.

Domínguez-Escobar, J., Wolf, D., Fritz, G., Höfler, C., Wedlich-Söldner, R., Mascher, T. (2014) Subcellular localization, interactions and dynamics of the phage-shock protein-like Lia response in Bacillus subtilis. Molecular Microbiology, 92, 716–732.

dos Santos, B.S., da Silva, L.C.N., da Silva, T.D., Rodrigues, J.F.S., Grisotto, M.A.G., Correia, M.T., Napoleão, T.H., da Silva, M.V., Paiva, P.M.G. (2016) Application of omics technologies for evaluation of antibacterial mechanisms of action of plant-derived products. Frontiers in Microbiology, 7, 1–13.

Du, D., van Veen, H.W., Murakami, S., Pos, K.M., Luisi, B.F. (2015) Structure, mechanism and cooperation of bacterial multidrug transporters. Current Opinion in Structural Biology, 33, 76–91.

Edgar, R. (2002) Gene Expression Omnibus: NCBI gene expression and hybridization array data repository. Nucleic Acids Research, 30, 207–210.

Feng, H., Xiang, H., Zhang, J., Liu, G., Guo, N., Wang, X., Wu, X., Deng, X., Yu, L. (2009) Genome-wide transcriptional profiling of the response of Staphylococcus aureus

to cryptotanshinone. Journal of Biomedicine and Biotechnology, 2009:617509.

Filiatrault, M.J. (2011) Progress in prokaryotic transcriptomics. Current Opinion in. Microbiology, 14, 579–586.

Freiberg, C., Brotz-Oesterhelt, H. (2005) Functional genomics in antibacterial drug discovery. Drug Discovery Today, 10, 927–935.

Freiberg, C., Brötz-Oesterhelt, H., Labischinski, H. (2004) The impact of transcriptome and proteome analyses on antibiotic drug discovery. Current Opinion in Microbiology, 7, 451–459.

Fu, H., Liu, L.G., Peng, J.P., Leng, W.C., Yang, J., Jin, Q. (2010) Transcriptional profile of the Shigella flexneri response to an alkaloid: Berberine. FEMS Microbiology Letters, 303, 169–175.

Gaur, G., Raj, U.L., Dang, S., Gupta, S., Gabrani, R. (2018) Plant-Derived Drug Molecules as Antibacterial Agents, In: Functional Food and Human Health. Springer, Singapur, pp. 143–171.

Gidalevitz, T., Prahlad, V., Morimoto, R.I. (2011) The Stress of Protein Misfolding : From Single Cells to Multicellular Organisms.Cold Spring Harbor Perspectives in Biology, 3, a009704.

Gokgoz, N.B., Akbulut, B.S. (2015) Proteomics Evidence for the Activity of the Putative Antibacterial Plant Alkaloid (-)-Roemerine: Mainstreaming Omics-Guided Drug Discovery. OMICS:Journal of Integrative Biology, 19, 478–89.

Görg, A., Weiss, W., Dunn, M.J. (2004) Current two-dimensional electrophoresis technology for proteomics. Proteomics, 4, 3665-3685.

Goto, K., Omura, T., Hara, Y., Sadaie, Y. (2000) Application of the partial 16S rDNA sequence as an index for rapid identification of species in the genus Bacillus. The Journal of General and Applied Microbiology, 46, 1–8.

Guinaudeau, H., Leboeuf, M., Cave, A. (1975) Aporphine Alkaloids. Lloydia, a Quarterly Journal of Biological Science, 38, 275–338.

Hao, T., Han, B., Ma, H., Fu, J., Wang, H., Wang, Z., Tang, B., Chen, T., Zhao, X. (2013) In silico metabolic engineering of Bacillus subtilis for improved production of

riboflavin, Egl-237, (R,R)-2,3-butanediol and isobutanol. Molecular Biosystems, 9, 2034.

Harwood, R.C. (2007) Bacillus subtilis as a Model for Bacterial Systems Biology. Encyclopedia of Life Sciences, e LS.

Haynes, P.A., Gygi, S.P., Figeys, D., Aebersold, R. (1998). Proteome analysis: biological assay or data archive?. Electrophoresis, 19, 1862–1871.

Howard, B.E., Hu, Q., Babaoglu, A.C., Chandra, M., Borghi, M., Tan, X., He, L., Winter-Sederoff, H., Gassmann, W., Veronese, P., Heber, S. (2013) High-Throughput RNA Sequencing of Pseudomonas-Infected Arabidopsis Reveals Hidden Transcriptome Complexity and Novel Splice Variants. PLoS One, 8, e74183.

Huang, Q., Abdalla, A.E., Xie, J. (2015) Phylogenomics of Mycobacterium Nitrate Reductase Operon. Current Microbiology, 71, 121–128.

James, P. (1997) Protein identification in the post-genome era: the rapid rise of proteomics. Quarterly Reviews of Biophysics, 30, 279–331.

Jobim, M.I.M., Oberst, E.R., Salbego, C.G., Souza, D.O., Wald, V.B., Tramontina, F., Mattos, R.C. (2004) Two-dimensional polyacrylamide gel electrophoresis of bovine seminal plasma proteins and their relation with semen freezability. Theriogenology, 61, 255–266.

Karaosmanoglu, K., Sayar, N.A., Aksan Kurnaz, I., Sariyar Akbulut, B. (2013) Assessment of Berberine as a Multi-target Antimicrobial: A Multi-omics Study for Drug Discovery and Repositioning. OMICS: An Integrative Journal of Biology, 18, 42–53.

Kim, J.Y., Inaoka, T., Hirooka, K., Matsuoka, H., Murata, M., Ohki, R., Adachi, Y., Fujita, Y., Ochi, K. (2009) Identification and characterization of a novel multidrug resistance operon, mdtRP (yusOP), of Bacillus subtilis. Journal of Bacteriology, 191, 3273–3281.

Kittakoop, P., Mahidol, C., Ruchirawat, S. (2013) Alkaloids as Important Scaffolds in Therapeutic Drugs for the Treatments of Cancer, Tuberculosis, and Smoking Cessation. Current Topics in Medicinal Chemistry, 14, 239–252.

Klose, J. (1975) Protein mapping by combined isoelectric focusing and electrophoresis of mouse tissues. A novel approach to testing for induced point mutations in mammals. Humangenetik, 26, 231–243.

Kobayashi et al. (2003) Essential Bacillus subtilis genes. Proceedings of the National Academy Sciences of the United States of America, 100, 4678–4683.

Koenig, T., Menze, B.H., Kirchner, M., Monigatti, F., Parker, K.C., Patterson, T., Steen, J.J., Hamprecht, F.A., Steen, H. (2008) Robust prediction of the MASCOT score for an improved quality assessment in mass spectrometric proteomics. Journal of Proteome Research, 7, 3708–3717.

Kohanski, M.A., Dwyer, D.J., Hayete, B., Lawrence, C.A., Collins, J.J. (2007) A Common Mechanism of Cellular Death Induced by Bactericidal Antibiotics. Cell, 130, 797–810.

Krewulak, K.D., Vogel, H.J. (2008) Structural biology of bacterial iron uptake. Biochimica et Biophysica Acta - Biomembranes, 1778, 1781–1804.

Kumar, A., Schweizer, H.P. (2005) Bacterial resistance to antibiotics: Active efflux and reduced uptake. Advanced Drug Delivery Reviews, 57, 1486–1513.

Kunst et al. (1997) The complete genome sequence of the gram-positive bacterium Bacillus subtilis. Nature, 390, 249–256.

Laemmli, U. (1970) Cleavage of structural protins during the assembly of the head of bactephage T4. Journal of Biological Chemistry, 227, 1–6.

Lafrance, M., Blaquiere, N., Fagnou, K. (2007) Aporphine alkaloid synthesis and diversification via direct arylation. European Journal of Organic Chemistry, 2007, 811–825.

Langmead, B., Trapnell, C., Pop, M., Salzberg, S. (2009) Ultrafast and memory-efficient alignment of short DNA sequences to the human genome. Genome Biology, 10, R25.

Li, X.Z., Elkins, C.A., Zgurskaya, H.I. (2016) Efflux-mediated Antimicrobial Resistance in Bacteria: Mechanisms, Regulation and Clinical Implications. Springer.

Limsuwan, S., Hesseling-Meinders, A., Voravuthikunchai, S.P., Van Dijl, J.M., Kayser,

O. (2011) Potential antibiotic and anti-infective effects of rhodomyrtone from Rhodomyrtus tomentosa (Aiton) Hassk. on Streptococcus pyogenes as revealed by proteomics. Phytomedicine, 18, 934–940.

Lin, Y.L., Chen, Y.S., Hsu, Y.M., Yao, C.H., Chang, T.J. (2012) Proteomic Analysis And Antibacterial Effects Of Lithospermi Radix Against Common Bacteria From Human Infected Wounds. Biomedical Engineering:Applications, Basis and Communications, 24, 37–45.

Livak, K.J., Schmittgen, T.D. (2001) Analysis of relative gene expression data using real-time quantitative PCR and. Methods 25, 402–408.

Lorca, G.L., Barabote, R.D., Zlotopolski, V., Tran, C., Winnen, B., Hvorup, N., Stonestrom, A.J., Nguyen, E., Huang, L.W., Kim, D.S., Saier Jr, H.S. (2007) Transport capabilities of eleven gram-positive bacteria: comparative genomic analyses. Biochimica et Biophysica Acta-Biomembranes, 1768, 1342–1366.

Love, M.I., Anders, S., Huber, W. (2014) Differential analysis of count data - the DESeq2 package, Genome Biology, 15, 10-1186.

Love, M.I., Anders, S., Kim, V., Huber, W. (2015) RNA-Seq workflow: gene-level exploratory analysis and differential expression. F1000Research, 4, 1070.

Maher, C.A., Kumar-Sinha, C., Cao, X., Kalyana-Sundaram, S., Han, B., Jing, X., Sam, L., Barrette, T., Palanisamy, N., Chinnaiyan, A.M. (2009) Transcriptome sequencing to detect gene fusions in cancer. Nature, 458, 97–101.

Marioni, J.C., Mason, C.E., Mane, S.M., Stephens, M., Gilad, Y. (2008) Comparison with gene expression arrays RNA-seq : An assessment of technical reproducibility and comparison with gene expression arrays, Genome Research, 18, 1509–1517.

Masaoka, Y., Ueno, Y., Morita, Y., Kuroda, T. (2000) A Two-Component Multidrug Efflux Pump , EbrAB , in Bacillus subtilis. Journal of Bacteriology, 182, 2307–12.

Michna, R.H., Zhu, B., Mäder, U., Stülke, J. (2016) SubtiWiki 2.0--an integrated database for the model organism Bacillus subtilis. Nucleic Acids Research, 44, D654-662.

Misra, J., Schmitt, W., Hwang, D., Hsiao, L., Gullans, S., Stephanopoulos, G.,

Stephanopoulos, G. (2002) Interactive exploration of microarray gene expression patterns in a reduced dimensional space. Genome Research, 12, 1112–1120.

Möbius, K., Arias-Cartin, R., Breckau, D., Hännig, A.L., Riedmann, K., Biedendieck, R., Schröder, S., Becher, D., Magalon, A., Moser, J., Jahn, M., Jahn, D. (2010) Heme biosynthesis is coupled to electron transport chains for energy generation. Proceedings of the National Academy Sciences of the United States of America, 107, 10436–10441.

Moffatt, B.A., Ashihara, H. (2002) Purine and Pyrimidine Nucleotide Synthesis and Metabolism. Arabidopsis Book, 1, e0018.

Mostertz, J., Scharf, C., Hecker, M., Homuth, G. (2004) Transcriptome and proteome analysis of Bacillus subtilis gene expression in response to superoxide and peroxide stress. Microbiology, 150, 497–512.

Murata, M., Ohno, S., Kumano, M., Yamane, K., Ohki, R. (2003) Multidrug resistant phenotype of *Bacillus subtilis* spontaneous mutants isolated in the presence of puromycin and lincomycin. Canadian Journal of Microbiology, 49, 71–77.

Nakano, M.M., Hoffmann, T., Zhu, Y., Jahn, D. (1998) Nitrogen and oxygen regulation of Bacillus subtilis nasDEF encoding NADH-dependent nitrite reductase by TnrA and ResDE. Journal of Bacteriology, 180, 5344–5350.

Ncube, N.S., Afolayan, A.J., Okoh, A.I. (2008) Assessment techniques of antimicrobial properties of natural compounds of plant origin : current methods and future trends. African Journal of Biotechnology, 7, 1797–1806.

Neuhoff, V., Arold, N., Taube, D., Ehrhardt, W. (1988) Improved staining of proteins in polyacrylamide gels including isoelectric focusing gels with clear background at nanogram sensitivity using Coomassie Brilliant Blue G250 and R250. Electrophoresis, 9, 255–262.

Neyfakh, A.A., Bidnenko, V.E., Chen, L.B. (1991) Efflux-mediated multidrug resistance in Bacillus subtilis: similarities and dissimilarities with the mammalian system. Proceedings of the National Academy Sciences of the United States of America, 88, 4781–4785.

Nikaido, H. (2009) Multidrug Resistance in Bacteria. Annual Review of Biochemistry, 78, 119–146.

Nyhan, W.L. (2014) Nucleotide synthesis via salvage pathway. eLS, 1–7.

O'Brien, P., Carrasco-Pozo, C., Speisky, H. (2006) Boldine and its antioxidant or health-promoting properties. Chemico- Biological Interactions, 159, 1–17.

O'Connell, K.M.G., Hodgkinson, J.T., Sore, H.F., Welch, M., Salmond, G.P.C., Spring, D.R. (2013) Combating multidrug-resistant bacteria: Current strategies for the discovery of novel antibacterials. Angewandte Chemie International Edition, 52, 10706–10733.

O'Farrell, P.H. (1975) High resolution two-dimensional electrophoresis of proteins. The Journal of Biological Chemistry, 250, 4007–4021.

Ohki, R., Giyanto, Tateno, K., Masuyama, W., Moriya, S., Kobayashi, K., Ogasawara, N. (2003) The BceRS two-component regulatory system induces expression of the bacitracin transporter, BceAB, in Bacillus subtilis. Molecular Microbiology, 49, 1135–1144.

Ohki, R., Murata, M. (1997) bmr3, a third multidrug transporter gene of Bacillus subtilis. Journal of Bacteriology, 179, 1423–1427.

Ohki, R., Tateno, K. (2004) Increased stability of bmr3 mRNA results in a multidrug-resistant phenotype in Bacillus subtilis. Journal of Bacteriology, 186, 7450–7455.

Orhan, I., Özçelik, B., Karaoğlu, T., Şener, B. (2007) Antiviral and antimicrobial profiles of selected isoquinoline alkaloids from Fumaria and Corydalis species. Zeitschrift fur Naturforschung. C, Journal of Biosciences, 62, 19–26.

Perkins, D.N., Pappin, D.J., Creasy, D.M., Cottrell, J.S. (1999) Probability-based protein identification by searching sequence databases using mass spectrometry data. Electrophoresis, 20, 3551–67.

Perkins, T.T., Kingsley, R.A., Fookes, M.C., Gardner, P.P., James, K.D., Yu, L., Assefa, S.A., He, M., Croucher, N.J., Pickard, D.J., Maskell, D.J., Parkhill, J., Choudhary, J., Thomson, N.R., Dougan, G. (2009) A strand-specific RNA-seq analysis of the transcriptome of the typhoid bacillus Salmonella typhi. PLoS Genetics, 5:e1000569.

Perumal Samy, R., Gopalakrishnakone, P. (2010) Therapeutic potential of plants as anti-microbials for drug discovery. Evidence-Based Complementary and Alternative

Medicine, 7, 283–294.

Petersohn, A., Bernhardt, J., Gerth, U., Höper, D., Koburger, T., Völker, U., Hecker, M., Bernhardt, R.G., Gerth, U.L.F. (1999) Identification of sigma (B)-Dependent Genes in Bacillus subtilis Using a Promoter Consensus-Directed Search and Oligonucleotide Hybridization. Journal of Bacteriology, 181, 5718–5724.

Piddock, L.J.V. (2006) Multidrug-resistance efflux pumps - not just for resistance. Nature Reviews Microbiology, 4, 629–636.

Piétu, G., Mariage-Samson, R., Fayein, N.A., Matingou, C., Eveno, E., Houlgatte, R., Decraene, C., Vandenbrouck, Y., Tahi, F., Devignes, M.D., Wirkner, U., Ansorge, W., Cox, D., Nagase, T., Nomura, N., Auffray, C. (1999) The genexpress IMAGE knowledge base of the human brain transcriptome: A prototype integrated resource for functional and computational genomics. Genome Research, 9, 195–209.

Prakash, B., Kujur, A., Yadav, A. (2018) Drug synthesis from natural products: a historical overview and future perspective, In: Synthesis of Medicinal Agents from Plants, p. 25-46.

Pratiwi, S.U.T., Lagendijk, E.L., Hertiani, T., Weert, S. De, Hondel, C.A.M.J.J. Van Den (2015) Antimicrobial effects of Indonesian Medicinal Plants Extracts on Planktonic and Biofilm Growth of Pseudomonas aeruginosa and Staphylococcus aureus, Journal of Horticulture, 2, 1–14.

Putman, M., van Veen, H.W., Konings, W.N. (2000) Molecular properties of bacterial multidrug transporters. Microbiology and Molecular Biology Reviews, 64, 672–93.

Qin, N., Tan, X., Jiao, Y., Liu, L., Zhao, W., Yang, S., Jia, A. (2014) RNA-Seq-based transcriptome analysis of methicillin-resistant Staphylococcus aureus biofilm inhibition by ursolic acid and resveratrol. Scientific Reports, 4, 5467.

Quinn, C.L., Stephenson, B.T., Switzer, R.L. (1991) Functional organization and nucleotide sequence of the Bacillus subtilis pyrimidine biosynthetic operon. The Journal of Biological Chemistry, 266, 9113–9127.

Raatschen, N., Bandow, J.E. (2012) 2-D gel-based proteomic approaches to antibiotic drug discovery. Current Protocols in Microbiology, 1, 1–16.

Radulović, N.S., Blagojević, P.D., Stojanović-Radić, Z.Z., Stojanović, N.M. (2013) Antimicrobial plant metabolites: structural diversity and mechanism of action. Current Medicinal Chemistry, 20, 932–52.

Raz, T., Kapranov, P., Lipson, D., Letovsky, S., Milos, P.M., Thompson, J.F. (2011) Protocol dependence of sequencing-based gene expression measurements. PLoS One 6:e19287.

Reddy, P.J., Ray, S., Sathe, G.J., Prasad, T.S.K., Rapole, S., Panda, D., Srivastava, S. (2015) Proteomics Analyses of Bacillus subtilis after Treatment with Plumbagin, a Plant-Derived Naphthoquinone. Omics: A Journal of Integrative Biology, 19, 12–23.

Richter, A., Hecker, M. (1986) Heat-shock proteins in Bacillus subtilis: a two-dimensional electrophoresis study. FEMS Microbiology Letters, 36, 69–71.

Roemer, T., Boone, C. (2013) Systems-level antimicrobial drug and drug synergy discovery. Nature Chemical Biology, 9, 222–231.

Saha, M., Sarkar, S., Sarkar, B., Sharma, B.K., Bhattacharjee, S., Tribedi, P. (2016) Microbial siderophores and their potential applications: a review. Environmental Science and Pollution Research, 23, 3984–3999.

Savoia, D. (2012) Plant-derived antimicrobial compounds: alternatives to antibiotics. Future Microbiology, 7, 979–990.

Schaeffer, A.B., Fulton, M.D. (1990) A Simplified Method of Staining Endospores. Science, 77, 194.

Schena, M., Shalon, D., Davis, R.W., Brown, P.O. (1995) Quantitative Monitoring of Gene Expression Patterns with a Complementary DNA Microarray. Science, 270, 467–470.

Schindler, B.D., Kaatz, G.W. (2016) Multidrug efflux pumps of gram-positive bacteria. Drug Resistance Updates, 27, 1–13.

Shi, T., Wang, Y., Wang, Z., Wang, G., Liu, D., Fu, J., Chen, T., Zhao, X. (2014) Deregulation of purine pathway in Bacillus subtilis and its use in riboflavin biosynthesis. Microbial Cell Factories, 13, 101.

Shin, J., Prabhakaran, V.S., Kim, K. (2018) The multi-faceted potential of plant-derived

metabolites as antimicrobial agents against multidrug-resistant pathogens. Microbial Pathogenesis, 116, 209–214.

Shin, J.S., Kim, K.T., Lee Koo, M. (1998) Inhibitory effects of bulbocapnine on dopamine biosynthesis in PC12 cells. Neuroscience Letters, 244, 161–164.

Sianglum, W., Srimanote, P., Taylor, P.W., Rosado, H., Voravuthikunchai, S.P. (2012) Transcriptome Analysis of Responses to Rhodomyrtone in Methicillin-Resistant Staphylococcus aureus. PLoS One, 7:e45744.

Singh, S.B., Barrett, J.F. (2006) Empirical antibacterial drug discovery - Foundation in natural products. Biochemical Pharmacology, 71, 1006–1015.

Steinfels, E., Orelle, C., Fantino, J.R., Dalmas, O., Rigaud, J.L., Denizot, F., Di Pietro, A., Jault, J.M. (2004) Characterization of YvcC (BmrA), a multidrug ABC transporter constitutively expressed in Bacillus subtilis. Biochemistry, 43, 7491–7502.

Swiney, D.C., Anthony, J. (2011) How were new medicines discovered? Nature Reviews Drug Discovery, 10, 507–519.

Switzer, R.L., Zalkin, H., Saxild, H.H. (2002) Purine, pyrimidine, and pyridine nucleotide metabolism. In: Bacillus subtilis and its closest relatives. American Society of Microbiology, p. 255–269.

Tan, P.K., Downey, T.J., Spitznagel, E.L., Xu, P., Fu, D., Dimitrov, D.S., Lempicki, R.A., Raaka, B.M., Cam, M.C. (2003) Evaluation of gene expression measurements from commercial microarray platforms. Nucleic Acids Research, 31, 5676–5684.

Tang, Y.W. (2015) Non-genomic omic techniques, In: Molecular Medical Microbiology (Second Edition), p. 399–406.

Tanwar, J., Das, S., Fatima, Z., Hameed, S. (2014) Multidrug resistance: An emerging crisis. Interdisciplinary Perspectives on Infectious Diseases, 2014, 541340.

The UniProt Consortium (2017) UniProt: the universal protein knowledgebase. Nucleic Acids Research, 45, D158–D169.

Thiede, B., Höhenwarter, W., Krah, A., Mattow, J., Schmid, M., Schmidt, F., Jungblut, P.R. (2005) Peptide mass fingerprinting. Methods 35, 237–247.

Torres, C., Galián, C., Freiberg, C., Fantino, J.R., Jault, J.M. (2009) The YheI/YheH

heterodimer from Bacillus subtilis is a multidrug ABC transporter. Biochimica et Biophysica Acta - Biomembranes, 1788, 615–622.

Touati, D. (2000) Iron and Oxidative Stress in Bacteria. Archives of Biochemistry and Biophysics, 373, 1–6.

Tsuge, K., Ohata, Y., Shoda, M. (2001) Gene yerP, involved in surfactin self-resistance in Bacillus subtilis. Antimicrobial Agents and Chemotherapy. 45, 3566–3573.

Turner, R.J., Bonners, E.R., Grabner, G.K., Switzer, R.L. (1998) Purification and Characterization of Bacillus subtilis PyrR, a Bifunctional pyr mRNA-binding Attenuation Protein/Uracil Phosphoribosyltransferase phosphoribosyltransferase. The Journal of Biological Chemistry, 6, 5932-5938.

Udvardy, A., Miskovics, A., Sipos, A. (2014) Antibacterial Aporphinoids – Progress and Perspectives Based on Structure-Activity Analysis, International Bulletin od Drug Research, 4, 1–34.

Van Vliet, A.H.M. (2010) Next generation sequencing of microbial transcriptomes: Challenges and opportunities. FEMS Microbiology Letters, 302:1-7.

Varghese, S., Wu, A., Park, S., Imlay, K.R.C., Imlay, J.A. (2007) Submicromolar hydrogen peroxide disrupts the ability of fur protein to control free-iron levels in Escherichia coli. Molecular Microbiology, 64, 822–830.

Völker, U., Hecker, M. (2005) From genomics via proteomics to cellular physiology of the Gram-positive model organism Bacillus subtilis. Cellular Microbiology, 7, 1077–1085.

Wang, Z., Gerstein, M., Snyder, M. (2009) RNA-Seq: a revolutionary tool for transcriptomics. Nature Reviews Genetics, 10, 57–63.

Wei, J., Liang, J., Shi, Q., Yuan, P., Meng, R., Tang, X., Yu, L., Guo, N. (2014) Genome-wide transcription analyses in Mycobacterium tuberculosis treated with lupulone. Brazilian Journal of Microbiology, 45, 333–341.

Wenzel, M., Bandow, J.E. (2011) Proteomic signatures in antibiotic research. Proteomics, 11, 3256–3268.

Wink, M. (2015) Modes of Action of Herbal Medicines and Plant Secondary

Metabolites. Medicines, 2, 251–286.

Wink, M., Schimmer, O. (2009) Molecular Modes of Action of Defensive Secondary Metabolites, Annual Plant Reviews: Functions and Biotechnology of Plant Secondary Metabolites, 39, 21-161.

Woolridge, D.P., Vazquez-Laslop, N., Markham, P.N., Chevalier, M.S., Gerner, E.W., Neyfakh, A.A. (1997) Efflux of the natural polyamine spermidine facilitated by the Bacillus subtilis multidrug transporter Blt. The Journal of Biological Chemistry, 272, 8864–8866.

Xiang, C.C., Chen, Y. (2000) cDNA microarray technology and its applications. Biotechnology Advances, 18, 35-46.

Yoshida, K.I., Ohki, Y.H., Murata, M., Kinehara, M., Matsuoka, H., Satomura, T., Ohki, R., Kumano, M., Yamane, K., Fujita, Y. (2004) Bacillus subtilis LmrA is a repressor of the lmrAB and yxaGH operons: Identification of its binding site and functional analysis of lmrB and yxaGH. Journal of Bacteriology, 186, 5640–5648.

You, M., Mahinda Wickramaratne, D.B., Silva, G.L., Chai, H., Chagwedera, T.E., Farnsworth, N.R., Cordell, G.A., Kinghorn, A.D., Pezzuto, J.M. (1995) (-)-Roemerine, an aporphine alkaloid from annona senegalensis that reverses the multidrug-resistance phenotype with cultured cells. Journal of Natural Products, 58, 598–604.

Zamboni, N., Mouncey, N., Hohmann, H.P., Sauer, U. (2003) Reducing maintenance metabolism by metabolic engineering of respiration improves riboflavin production by Bacillus subtilis. Metabolic Engineering, 5, 49–55.

Zhen, L., Jianhong, X. (2015) The application of the high throughput sequencing technology in the transposable elements. Yi Chuan Chen, 37, 885–898.

Zuber, P. (2009) Management of Oxidative Stress in *Bacillus*. Annual Reviews of Microbiology, 63, 575–597.

APPENDIX A. (-)-Roemerine alkaloid.

Roemerine: ^{1}H-NMR ($CDCl_3$, 500 MHz, δ)
2.45 ppm (3H, s, N-CH_3),
5.85-6.00 ppm (2H,dd, ―OCH_2O methylenes),
6.48 ppm (1H,s, C-3),
7.06-7.25 ppm (3H,m, C-8-9-10),
7.98 ppm (1H,d, C-11)

The identification of roemerine was carried out by comparing its ^{1}H-NMR spectral data and TLC Rf values with an authentic sample. ^{1}H-NMR spectra was recorded on a Varian Unity Inova 500 MHz spectrometer (Guinaudeau et al., 1975).

APPENDIX B. BSA calibration curve.

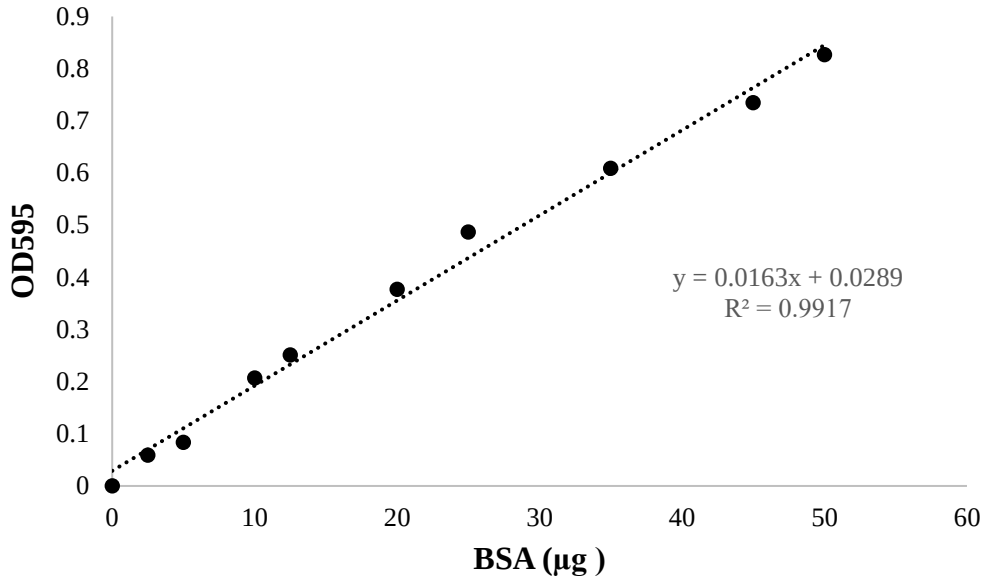

Figure A.1 BSA calibration curve for protein concentration determination using Bradford method.

APPENDIX C. Table of identified proteins.

Table A.1 Identified proteins with a fold change of < 1.5 under one-hour roemerine treatment.

Spot ID/SSP No	Gene Name	Protein Name	Best Protein Score	Sequence Coverage (%)	Experimental Protein Mass (kDa)/pI	Fold Change	Regulation
R14/5402	*mreB*	Rod shape-determining protein mreB	251	42	35.89/5.09	1.29	Up
R12/2410	*mdh*	Malate dehydrogenase	393	52	33.62/4.92	1.13	Up
R16/4503	*sucC*	Succinyl-CoA ligase [ADP-forming] subunit beta	184	33	41.35/5.04	1.06	Up
R15/2505	*hag*	Flagellin	403	55	32.61/4.97	1.30	Down

Table A.2 Identified proteins with a fold change of < 1.5 under one-hour boldine treatment.

Spot ID/SSP No	Gene Name	Protein Name	Best Protein Score	Sequence Coverage (%)	Experimental Protein Mass (kDa)/pI	Fold Change	Regulation
B3/6101	*yvyD*	Uncharacterized protein yvyD	241	46	21.97/5.36	1.18	Up
B11/9404	*yjlD*	NADH dehydrogenase-like protein yjlD	295	30	41.93/6.28	1.17	Up
B10/7301	*iolS*	Protein iolS	507	48	35.15/5.5	1.15	Up
B7/6306	*fbaA*	Probable fructose-bisphosphate aldolase	131	36	30.38/5.19	1.04	Up
A2/6306	*fbaA*	Probable fructose-bisphosphate aldolase	539	64	30.38/5.19	1.04	Up
B1/5102	*efp*	Elongation factor P	46	-	20.46/-	1.30	Down
B8/5308	*nadE*	NH(3)-dependent NAD(+) synthetase	511	51	30.38/5.07	1.20	Down
B6/9202	*cysK*	Cysteine synthase	377	68	32.79/5.64	1.03	Down
A4/-	*tig*	Trigger factor	378	53	47.46/4.42		
B18/-	*tig*	Trigger factor	363	51	47.46/4.42		

Table A.3 Identified proteins with a fold change of < 1.5 under one-hour bulbocapnine treatment.

Spot ID/SSP No	Gene Name	Protein Name	Best Protein Score	Sequence Coverage (%)	Experimental Protein Mass (kDa)/pI	Fold Change	Regulation
G7/3607	*tuf*	Elongation factor Tu	419	66	43.57/4.92	4.09	Up
F9/3605	*tuf*	Elongation factor Tu	237	52	43.57/4.92	2.99	Up
F4/1101	*tuf*	Elongation factor Tu	179	36	43.57/4.92	2.12	Down
G11/1906	*fusA*	Elongation factor G	51	17	76.57/4.8	2.35	Up
F11/1903	*fusA*	Elongation factor G	202	32	76.57/4.8	1.64	Down
F5/2105	*tuf*	Elongation factor Tu	270	31	43.57/4.92	1.24	Down
F12/2902	*ptsI*	Phosphoenolpyruvate-protein phosphotransferase	367	41	63.04/4.78		
F13/2904	*ptsI*	Phosphoenolpyruvate-protein phosphotransferase	253	32	63.04/4.78		
F14/2906	*ptsI*	Phosphoenolpyruvate-protein phosphotransferase	225	30	63.04/4.78		
G1/2002	*tpx*	Probable thiol peroxidase	218	82	18.20/4.89		
G2/8003	*tal*	Transaldolase	616	65	22.96/5.74		
G9/B11	*tig*	Trigger factor	134	36	47.46/4.42		
G10/B10	*tig*	Trigger factor	96	29	47.46/4.42		
G8/B8	*lysY*	Lysyl-tRNA synthetase	120	33	57.50/5.19		

Table A.3 Continued.

Spot ID/SSP No	Gene Name	Protein Name	Best Protein Score	Sequence Coverage (%)	Experimental Protein Mass (kDa)/pI	Fold Change	Regulation
F6/0204	*yorB*	SPBc2 prophage-derived uncharacterized protein yorB	26				
F7/0301	*dnaK*	Chaperone protein dnaK	37				
F3/0014	*rhaB*	Rhamnulokinase	24				
F1/0013	*sumT*	Uroporphyrinogen-III C-methyltransferase	25				

APPENDIX D. The 2-DE gel images of alkaloid treated cells.

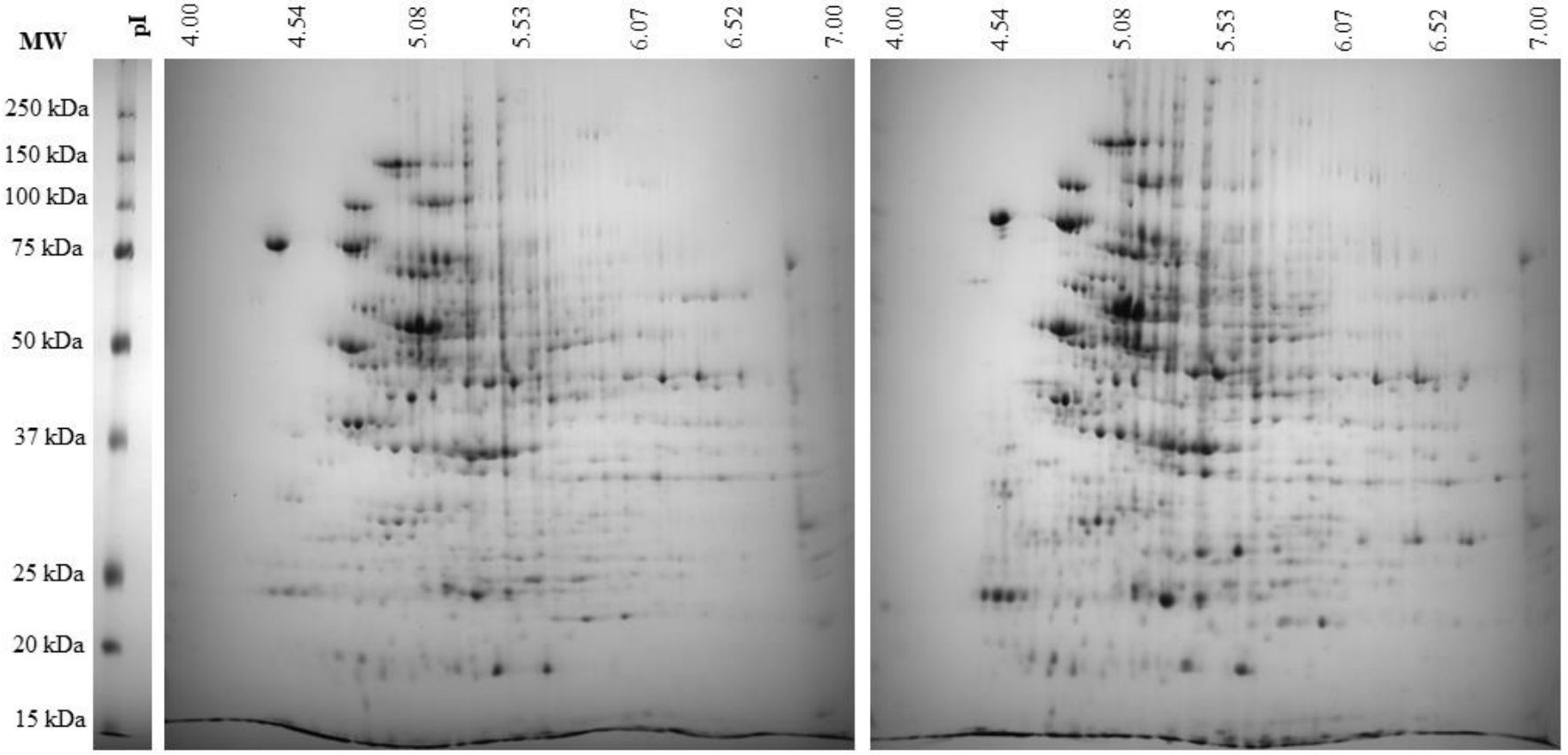

Figure A.2 The 2-DE gel images of proteins from biological replicates of control (left) and roemerine treated (right) cells.

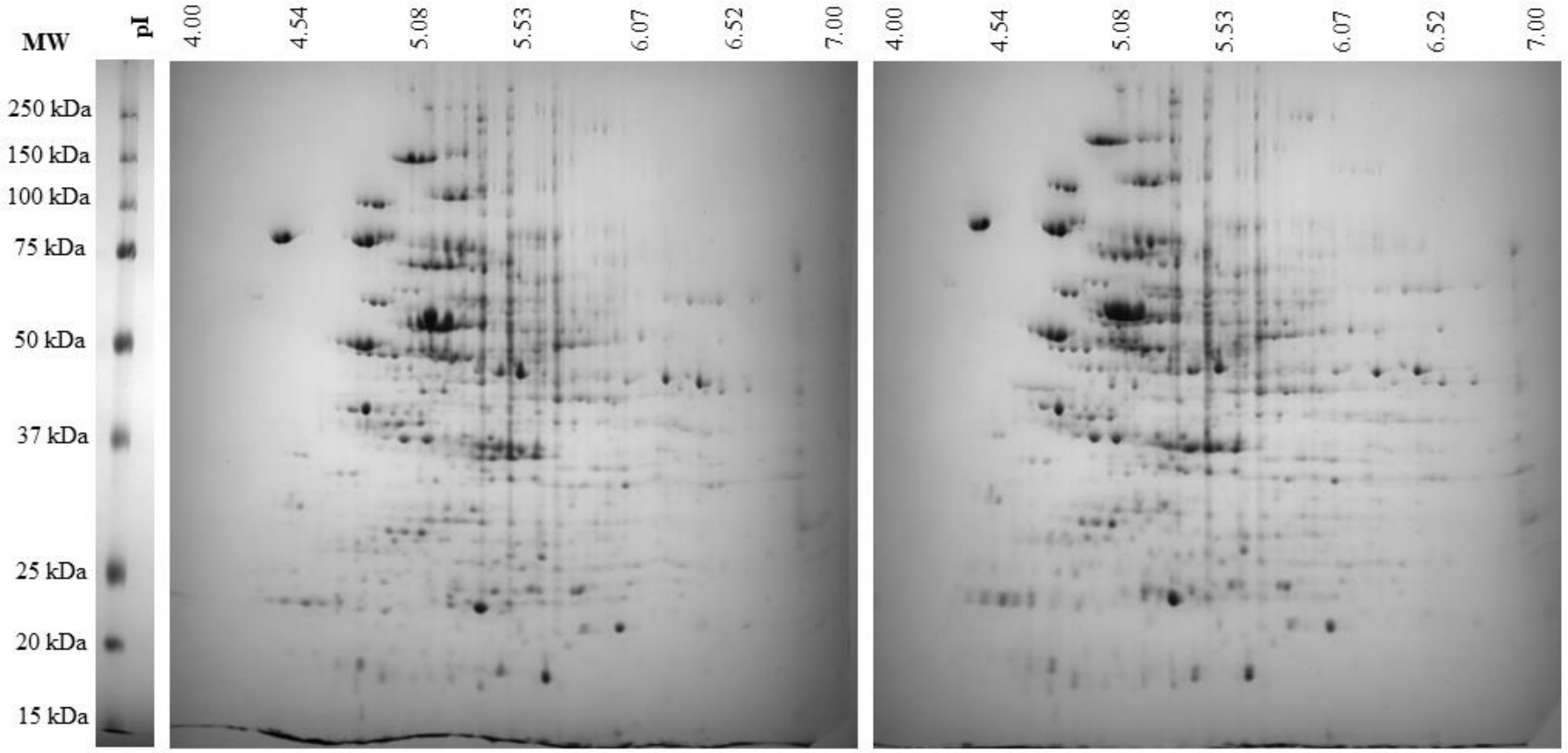

Figure A.3 The 2-DE gel images of proteins from biological replicates of control (left) and boldine treated (right) cells.

APPENDIX E. Differentially expressed genes.

Table A.4 Differentially expressed genes upon one-hour roemerine treatment.

Gene Name	DMSO Gene Level	Roemerine Gene Level	log2 Fold Change
iolH	572	22879	2.46
iolI	330	13074	2.46
iolJ	480	17944	2.45
liaH	128	7551	2.45
yfiY	90	3635	2.45
yhfQ	158	5583	2.45
iolG	731	21568	2.44
ybbB	54	2201	2.43
liaI	48	2876	2.43
fhuC	51	2464	2.43
feuB	69	2377	2.42
feuA	193	5290	2.42
iolF	720	18225	2.42
yrkO	189	5265	2.42
yusV	124	9597	2.41
yclN	327	7976	2.41
iolE	503	12151	2.41
ywjC	47	1338	2.40
mgsR	98	2398	2.40
yclQ	657	15212	2.40
ycgT	33	1085	2.40
iolD	977	22237	2.40
yclP	284	6603	2.39
fhuB	21	931	2.39
yfiZ	60	1379	2.39
iolB	262	5869	2.38
iolC	477	10211	2.38
nhaX	27	891	2.38
mmsA	760	15742	2.37
yfhA	45	1074	2.36
feuC	80	1786	2.36
yclO	309	6214	2.36
fhuG	58	1315	2.35
ybbA	42	908	2.34
opuBD	14	607	2.34
ywzA	33	664	2.32
efeU	89	1631	2.31
yrkN	124	2099	2.30
csbC	163	2477	2.30

Table A.4 Continued.

Gene Name	DMSO Gene Level	Roemerine Gene Level	log2 Fold Change
yhdN	64	1120	2.30
yfhK	74	1150	2.29
gsiB	22	404	2.28
ybyB	51	846	2.28
yfhC	647	9278	2.28
efeM	326	3171	2.26
yvkC	59	961	2.26
fhuD	49	8273	2.25
bmrU	11	291	2.25
yetG	89	15775	2.24
ggaA	154	1932	2.24
gspA	253	3468	2.24
opuBC	12	438	2.24
ybdZ	46	9884	2.23
ywjB	145	1872	2.23
ytaB	13	278	2.23
yusU	18	366	2.21
yflT	16	314	2.21
ydbN	32	3992	2.20
proJ	35	548	2.19
iolT	89	1104	2.17
ykgA	100	1199	2.15
ywiE	208	2175	2.14
ykuN	11	4345	2.11
yxeB	24	7521	2.10
ykzI	11	157	2.08
yrkP	30	374	2.06
ywtG	55	503	2.05
yyzH	4	91	2.05
yrkR	55	517	2.05
ywjA	341	2970	2.04
yutK	94	875	2.04
ohrB	17	208	2.04
yodA	34	324	2.01
yfmC	256	2054	2.00
ywmE	13	120	1.99
yrkQ	157	1368	1.98
dinB	230	1733	1.95
yqjM	1378	9081	1.90
guaC	293	1926	1.88
yqxL	11	113	1.87

Table A.4 Continued.

Gene Name	DMSO Gene Level	Roemerine Gene Level	log2 Fold Change
ycbP	45	302	1.85
iseA	108	648	1.84
ureB	66	356	1.80
yddE	21	174	1.80
yjbC	6889	38198	1.78
lmrA	57	358	1.78
dhaS	10798	58554	1.77
yqhB	22	158	1.77
opuE	103	537	1.77
exlX	126	740	1.74
yrkA	124	639	1.73
yetF	39	257	1.71
yumC	2790	13903	1.71
ydcQ	42	228	1.71
yojJ	1	41	1.71
yqaM	10	85	1.70
iolR	841	4001	1.70
ydjJ	6	56	1.69
yhbI	59	320	1.68
ydaG	238	1113	1.68
yhjD	9	61	1.68
paiA	82	410	1.67
bmr	500	2349	1.67
ycdF	23	131	1.67
dtpT	818	3771	1.66
araE	71	345	1.66
oppA	10212	46675	1.65
yoxC	20	112	1.64
yddB	42	203	1.64
ydaT	2	44	1.64
ureC	451	2026	1.63
sacV	40	212	1.62
yxbG	46	244	1.62
yocB	15	88	1.62
yjbE	71	355	1.62
ydcO	46	239	1.61
yodC	1970	8292	1.60
yorB	255	1075	1.59
ypuA	5206	21697	1.58
qodI	38	195	1.58
lmrB	217	917	1.57

Table A.4 Continued.

Gene Name	DMSO Gene Level	Roemerine Gene Level	log2 Fold Change
yncC	296	1219	1.57
glpD	271	1142	1.57
yppQ	308	1268	1.57
ydcR	49	207	1.56
msrA	220	902	1.56
rsbV	1112	3853	1.55
yuxJ	214	853	1.55
uvrA	5323	20682	1.53
ureA	67	264	1.53
yxjJ	28	96	1.52
yolD	1	45	1.52
ycgJ	84	339	1.52
ydzL	53	259	1.52
yhjN	663	2484	1.51
ybaK	14	65	1.50
yhcM	10	72	1.50
yrkH	7	39	1.48
yqaN	5	40	1.48
ysnF	23	115	1.48
argD	6	51	1.47
spxA	18410	66111	1.47
yhcA	448	1592	1.47
ydaC	13	66	1.47
yybF	190	679	1.47
yhbJ	186	728	1.46
ydcL	436	1515	1.46
yocK	40	152	1.46
bioYB	85	310	1.46
uxaC	105	384	1.46
yvzB	98	368	1.45
yddA	11	78	1.45
opuCC	12	70	1.44
yrkF	6	32	1.44
yjlB	29	123	1.44
ydaS	26	110	1.44
uvrB	2344	8100	1.43
cypB	1805	6173	1.43
uvrX	8	60	1.43
yvqJ	6	45	1.43
oppF	1247	4243	1.42
yesE	13	86	1.42

Table A.4 Continued.

Gene Name	DMSO Gene Level	Roemerine Gene Level	log2 Fold Change
yczO	10	56	1.41
yhaZ	447	1498	1.41
paiB	201	706	1.41
khtS	122	447	1.41
fadF	93	327	1.40
yneA	30	132	1.39
yvdR	72	285	1.39
ycgO	550	1764	1.38
yxeI	320	989	1.38
katA	2980	9627	1.38
yvgO	5	34	1.37
ydhK	44	140	1.37
khtT	73	251	1.37
opuCD	10	52	1.37
bltD	24	101	1.37
ysxD	191	602	1.37
yfkM	76	248	1.37
yqaK	10	68	1.36
padC	97	300	1.36
yclG	13	70	1.36
yhfH	0	15	1.35
tagC	88	283	1.34
ynfC	508	1605	1.34
yhcJ	410	1121	1.34
immA	307	960	1.34
rpmE2	60	197	1.34
argJ	13	59	1.33
spo0E	53	155	1.33
yjdA	363	1118	1.33
spoIIR	26	85	1.33
spoIVFA	23	83	1.33
yoqO	111	335	1.33
bcrC	2535	7556	1.33
yybC	49	166	1.33
csbD	2	14	1.32
yycD	1	23	1.32
proH	50	214	1.32
yddH	1	30	1.32
xkdA	28	117	1.32
yhaR	345	990	1.31
yflA	16	62	1.31

Table A.4 Continued.

Gene Name	DMSO Gene Level	Roemerine Gene Level	log2 Fold Change
ydcP	41	138	1.31
katE	91	266	1.30
yhfL	127	380	1.30
immR	300	900	1.30
yhaN	2345	6851	1.30
yjcS	98	292	1.30
lexA	2531	7250	1.29
fadR	471	1430	1.29
gmuD	124	368	1.29
yneB	81	284	1.27
ahpF	69660	196561	1.27
yxaH	109	323	1.27
yqaG	3	28	1.27
yhbD	23	81	1.27
iolS	6014	17208	1.27
htrA	5867	16444	1.27
ydiO	1574	4390	1.26
yyaN	18	56	1.25
ahpC	24674	67320	1.24
ytdP	18	65	1.24
yhcC	175	507	1.24
yyaT	95	253	1.24
yvdS	53	216	1.24
ydaD	11	45	1.24
rsbW	1245	3470	1.24
yddG	16	63	1.23
yerD	106	288	1.23
oppD	1164	3152	1.23
spbC	279	758	1.22
cwlD	32	103	1.22
minD	5576	14636	1.22
ywaE	90	250	1.21
yhaO	609	1591	1.21
rsbRD	67	190	1.21
ydcS	10	49	1.21
lysC	731	1880	1.19
yaaI	113	209	1.19
gmuG	98	264	1.19
yugJ	4334	11176	1.19
ywhK	33	97	1.19
yukJ	3012	7607	1.18

Table A.4 Continued.

Gene Name	DMSO Gene Level	Roemerine Gene Level	log2 Fold Change
csbA	119	291	1.18
yclH	27	64	1.18
rocA	334	846	1.17
aspA	714	1801	1.17
pupG	3762	9393	1.17
ysiB	865	2199	1.17
tyrZ	190	479	1.17
yugK	340	910	1.16
ykcB	47	130	1.16
yhaX	160	408	1.16
ydcF	3	26	1.15
cwlH	1	19	1.15
yisI	19	60	1.15
yonA	19	58	1.15
yomU	42	112	1.15
ydzJ	25	72	1.15
kinD	1756	4302	1.14
ywbO	436	1097	1.14
yocJ	838	2102	1.14
yesF	105	280	1.14
murB	2634	6323	1.13
yddI	5	24	1.13
yobU	4	19	1.13
etfA	1372	3336	1.13
plsC	787	1899	1.13
cypC	40	119	1.13
yetK	421	968	1.12
yvyD	56054	133338	1.12
yhaU	211	527	1.12
htrB	4159	9933	1.12
lcfA	1171	2903	1.11
nap	636	1503	1.11
ycxB	148	312	1.11
gntR	64	147	1.11
yhfK	4362	10198	1.11
ydiP	1901	4430	1.11
yvdQ	22	66	1.11
yqaJ	12	46	1.11
ypsB	3330	7627	1.11
mreC	6373	14777	1.10
sufD	15664	36740	1.10

Table A.4 Continued.

Gene Name	DMSO Gene Level	Roemerine Gene Level	log2 Fold Change
ythA	22	61	1.10
ykoX	214	548	1.10
yhcB	336	837	1.10
yuxL	877	2052	1.09
drm	3653	8479	1.09
ydaP	263	606	1.09
ykrL	1524	3516	1.09
yefB	69	140	1.09
ydaB	573	1323	1.08
dppD	6	20	1.08
acdA	126	301	1.08
etfB	874	2030	1.08
pgsC	82	175	1.07
bscR	225	544	1.07
xsa	94	222	1.07
sufB	23918	53503	1.07
gltT	5171	11678	1.07
yugS	42	110	1.06
yurZ	26	69	1.06
ywfA	13	43	1.06
yddD	11	51	1.06
ydfR	8	22	1.06
minC	4741	10810	1.06
ywaC	2004	4461	1.06
sacY	120	265	1.05
ygzD	96	232	1.05
sufS	13379	29719	1.05
perR	6357	13813	1.05
yjzE	59	155	1.05
ansA	358	798	1.04
mrpB	124	254	1.04
youA	47	96	1.04
ywaF	26	64	1.04
blt	68	157	1.04
yvgN	19044	41470	1.03
yetJ	1234	2634	1.03
ydeH	93	210	1.03
yrvD	301	617	1.02
divIC	3505	7705	1.02
pdhB	8299	17975	1.02
sufC	7960	17218	1.02

Table A.4 Continued.

Gene Name	DMSO Gene Level	Roemerine Gene Level	log2 Fold Change
opuCA	32	77	1.01
yebC	1279	2794	1.01
ydzE	40	99	1.01
ywaD	141	304	1.01
yqaL	17	68	1.01
ytnM	2	17	1.01
yrzT	97	203	1.00
pbpG	22	57	1.00
ctc	5761	11214	1.00
recA	6201	13128	1.00
*dhbF**	702	294142	0.50
*besA**	16	11108	0.46
*dhbE**	71	68929	0.44
*dhbC**	69	64373	0.44
*dhbB**	35	38168	0.44
*dhbA**	33	34385	0.43
*ykuO**	5	7025	0.41
*ykuP**	3	3634	0.40
*narH**	56875	47	-0.45
*narI**	44220	49	-0.47
*narJ**	27203	33	-0.49
yotB	18	2	-1.00
ftsE	1721	609	-1.00
pfkA	9098	3273	-1.00
yvrC	1814	586	-1.01
bioD	31	10	-1.01
yozV	108	34	-1.01
msmX	2486	839	-1.01
sul	1923	675	-1.01
yxzE	168	44	-1.01
xynC	303	95	-1.01
yncE	53	24	-1.02
yrhF	404	130	-1.02
yurH	50	13	-1.02
yqzF	1118	367	-1.02
yonS	420	131	-1.02
pucG	155	47	-1.02
yxiM	390	120	-1.03
yvrB	711	221	-1.03
pksD	545	168	-1.03
dapB	1376	469	-1.03

Table A.4 Continued.

Gene Name	DMSO Gene Level	Roemerine Gene Level	log2 Fold Change
ydjP	743	254	-1.03
ybzG	6144	2239	-1.03
aroE	9811	3417	-1.03
epsH	182	52	-1.04
yuaB	1695	543	-1.04
rbsC	5663	1849	-1.04
yoqM	837	273	-1.04
sdhC	4399	1476	-1.04
atpI	3961	1463	-1.05
ktrD	736	235	-1.05
yybB	463	144	-1.05
gudB	25717	8336	-1.06
yqjY	166	35	-1.06
lrpA	262	91	-1.06
hisZ	39	5	-1.06
yfkR	34	10	-1.06
ybfA	160	42	-1.06
yisQ	148	47	-1.06
proB	1057	333	-1.06
yqjI	38012	12168	-1.06
yjfA	21	2	-1.06
ald	31056	9933	-1.07
guaB	19121	6082	-1.07
tatAC	396	125	-1.08
cheR	525	173	-1.08
ybaR	706	218	-1.08
xynD	303	94	-1.08
ytmA	218	65	-1.08
rpmJ	2552	1038	-1.08
ytzI	1573	608	-1.08
ymzD	254	70	-1.09
yrhE	1441	458	-1.09
pksG	281	77	-1.10
pksC	999	305	-1.10
ywzB	420	121	-1.10
dacA	5840	1748	-1.11
yesJ	751	221	-1.11
yunG	147	45	-1.12
yvfH	7297	2191	-1.12
alaS	5576	1680	-1.12
ktrA	124	32	-1.13

Table A.4 Continued.

Gene Name	DMSO Gene Level	Roemerine Gene Level	log2 Fold Change
ysnE	46	13	-1.13
yraI	48	11	-1.13
yycS	42	7	-1.13
sigI	701	212	-1.13
yopN	188	56	-1.13
yfjC	435	120	-1.13
pabC	1005	328	-1.13
sipW	75	15	-1.14
bdbB	5355	1574	-1.14
pksS	2395	702	-1.15
albA	22913	6816	-1.16
yvgT	293	85	-1.16
yoaG	215	56	-1.16
purT	2880	834	-1.16
yqjZ	194	50	-1.16
ytzC	99	26	-1.16
cotA	59	10	-1.17
yoaD	58	15	-1.17
ybeC	14230	4076	-1.17
ybcF	30	3	-1.17
yxzJ	90	27	-1.18
yxiK	359	114	-1.18
ywlC	1083	317	-1.18
yxjI	460	131	-1.18
leuD	469	112	-1.19
sunA	15885	4411	-1.19
sspD	144	50	-1.19
yosT	162	41	-1.20
mleN	2335	661	-1.20
sboA	3194	964	-1.20
yojN	1554	440	-1.21
yjlA	558	143	-1.21
yndN	159	42	-1.21
yweA	1904	497	-1.23
ilvD	1473	382	-1.23
pbuG	1717	442	-1.24
mtlA	4641	1088	-1.24
trpA	2794	773	-1.25
dctP	946	236	-1.25
yolJ	15487	3974	-1.26
copB	38683	9915	-1.26

Table A.4 Continued.

Gene Name	DMSO Gene Level	Roemerine Gene Level	log2 Fold Change
licR	636	161	-1.27
csn	2414	605	-1.27
purB	3083	786	-1.27
yxzG	296	82	-1.28
cyeB	240	56	-1.28
tyrA	3836	965	-1.28
purE	602	132	-1.29
ylbM	447	112	-1.29
yukC	1024	254	-1.29
ykhA	1297	319	-1.30
bacC	503	133	-1.30
levD	255	55	-1.30
sat	391	92	-1.30
yutJ	5369	1298	-1.32
cydA	19655	4615	-1.32
hmp	554	124	-1.33
nin	374	85	-1.33
pel	2781	663	-1.33
yxjN	160	33	-1.35
yjhA	106	21	-1.35
hisC	5428	1300	-1.36
yvbY	12297	2809	-1.36
yxkI	1172	252	-1.36
dgcK	494	105	-1.36
purD	2197	507	-1.37
pyrG	11191	2521	-1.38
yhjA	2549	561	-1.39
ctrA	78	12	-1.39
levG	229	41	-1.40
purH	2590	556	-1.40
ywmC	51	6	-1.40
sunT	19171	4126	-1.41
yqxI	515	112	-1.41
bdbA	4227	875	-1.41
tasA	790	163	-1.41
hom	3322	713	-1.42
sacC	568	122	-1.42
yvrJ	49	13	-1.43
trpD	54	9	-1.44
purK	1942	402	-1.45
cysP	738	146	-1.45

Table A.4 Continued.

Gene Name	DMSO Gene Level	Roemerine Gene Level	log2 Fold Change
levE	227	40	-1.45
purF	3327	657	-1.47
thrB	3697	733	-1.48
yvfV	3994	746	-1.48
yvfW	13517	2669	-1.48
levF	276	52	-1.49
thrC	4526	894	-1.50
purL	4003	755	-1.51
gcvT	2981	554	-1.53
glcF	14098	2574	-1.54
albB	2773	546	-1.57
purN	915	136	-1.57
purM	1324	215	-1.58
yufN	48	2	-1.59
nucA	492	87	-1.60
nasE	2351	423	-1.60
albC	7273	1311	-1.60
cwlK	387	57	-1.61
gcvPA	3863	619	-1.62
purC	1152	200	-1.63
sumT	361	84	-1.63
yxaI	548	81	-1.64
albD	7847	1283	-1.64
leuC	1083	164	-1.65
cysC	216	28	-1.65
ilvB	1631	248	-1.65
splB	1008	160	-1.65
splA	170	22	-1.66
purQ	1051	162	-1.67
ywhL	291	37	-1.68
glcD	18688	2752	-1.70
ilvC	1591	232	-1.70
aroA	21156	3031	-1.72
albE	4272	621	-1.73
licC	1935	246	-1.77
cydB	7170	978	-1.79
ilvH	381	35	-1.80
licB	313	25	-1.81
gcvPB	4028	496	-1.81
albF	2107	256	-1.81
albG	861	95	-1.83

Table A.4 Continued.

Gene Name	DMSO Gene Level	Roemerine Gene Level	log2 Fold Change
fnr	22249	2396	-1.86
purS	457	66	-1.87
leuB	752	74	-1.95
licH	4528	419	-1.99
pyrP	2654	220	-2.03
zosA	12074	894	-2.09
mtlF	1660	87	-2.10
arfM	12737	32	-2.13
ycdC	2424	159	-2.17
licA	845	72	-2.17
narG	119396	324	-2.17
nasD	15587	948	-2.20
ydaO	4166	225	-2.23
yfnA	1432	72	-2.23
yrdP	3692	187	-2.23
narK	31958	126	-2.24
czcD	3070	140	-2.28
mtlD	6009	257	-2.30
ykwC	2893	113	-2.34
pyrE	7924	52	-2.34
pyrF	5853	41	-2.35
alsS	14666	98	-2.35
xpt	1120	33	-2.36
pbuX	2775	88	-2.37
alsD	9974	75	-2.38
pyrB	1131	21	-2.38
carB	16806	530	-2.39
pyrC	1893	36	-2.41
pyrD	5139	54	-2.42
pyrK	4512	92	-2.43
pyrAA	2957	57	-2.43
ywiC	7641	165	-2.44
cydC	9219	171	-2.45
cydD	10094	175	-2.45

*Manually curated genes

Table A. 5 Differentially expressed genes upon one-hour boldine treatment.

Gene Name	DMSO Gene Level	Boldine Gene Level	log2 Fold Change
yetG	89	654	1.30
dhbC	69	529	1.29
yxkC	1334	6727	1.26
feuA	193	1127	1.26
yfhA	45	319	1.19
ybdZ	46	432	1.15
yusV	124	569	1.12
rocD	728	2766	1.11
efeM	326	1033	1.09
besA	16	159	1.09
yokB	68	322	1.08
dhbE	71	360	1.06
dhbB	35	222	1.06
yjcM	1631	5476	1.05
yobJ	691	2414	1.05
yheJ	15	91	1.04
feuB	69	387	1.04
bdbB	5355	16958	1.02
yolJ	15487	49811	1.02
immR	300	1020	1.01
yhfQ	158	569	1.01
*dhbA**	33	133	0.83
*dhbF**	702	6667	0.32
*alsS**	14666	612	-0.23
*alsD**	9974	438	-0.24
*cydD**	10094	480	-0.24
*cydC**	9219	567	-0.26
*cydB**	7170	552	-0.27
*narI**	44220	3925	-0.29
*narJ**	27203	2728	-0.30
*mtlD**	6009	557	-0.30
*mtlF**	1660	190	-0.33
*narH**	56875	6352	-0.35
*lctP**	12707	2403	-0.37
*mtlA**	4641	757	-0.38
*narG**	119396	21637	-0.39
*narK**	31958	5921	-0.39
*cydA**	19655	8660	-0.75
ypbG	1148	366	-1.01
sacC	568	171	-1.03

Table A.5 Continued.

Gene Name	DMSO Gene Level	Boldine Gene Level	log2 Fold Change
ywaC	2004	641	-1.04
yrhE	1441	449	-1.05
rbsA	6635	2052	-1.08
licA	845	191	-1.09
fnr	22249	6362	-1.11
licC	1935	515	-1.12
licH	4528	1237	-1.15
rbsD	1600	500	-1.16
zosA	12074	2593	-1.27
ysbB	3057	629	-1.28

*Manually curated genes

Table A.6 Differentially expressed genes upon one-hour bulbocapnine treatment.

Gene Name	DMSO Gene Level	Bulbocapnine Gene Level	log2 Fold Change
*yfiY**	90	428	0.940245
*dhbB**	35	244	0.881706
*feuB**	69	367	0.827336
*dhbE**	71	291	0.792928
*feuC**	80	275	0.752534
*besA**	16	116	0.736612
*yfmC**	256	645	0.732898
*yfhA**	45	181	0.723144
*dhbA**	33	147	0.711493
*fhuD**	49	176	0.693335
*feuA**	193	1174	0.238435
*dhbF**	702	5190	0.221299
*dhbF**	702	5190	0.221299
*dhbC**	69	538	0.210554
*cydD**	10094	433	-0.1478
*cydC**	9219	476	-0.15586
*narI**	44220	3140	-0.17132
*cydB**	7170	627	-0.17745
*narJ**	27203	2361	-0.18509
*narH**	56875	5466	-0.22066
*narK**	31958	4506	-0.23692
*narG**	119396	19205	-0.24529
*alsS**	14666	2942	-0.25956
*lctP**	12707	3173	-0.2607
*alsD**	9974	2049	-0.26153
*fnr**	22249	4984	-0.26906
*arfM**	12737	3548	-0.28827

*Manually curated genes

CURRICULUM VITAE

Education

PhD 02/2013 – Cont. Marmara University, Department of Bioengineering,
Supervisor: Prof. Berna Sarıyar Akbulut
Thesis Title: 'Investigation of Aporphine Alkaloids for Their Antimicrobial Activities'

MSc 09/2010-12/2012 Ege University, Department of Bioengineering,
Supervisor: Prof. Nuri Azbar
Thesis Title: 'Assessment of 1,3-propanediol production by membrane supported bioreactor'

BSc 09/2006- 06/2010 Ege University, Department of Bioengineering
Supervisor: Assoc. Prof. Sayit Sargin
Thesis Title: 'Scale-Up Studies Of *Trichoderma Harzianum* Ege K38 Production as a Biocontrol Agent In Static And Solid State Culture'

Work Experiences

Research Assistant (2013-Cont.) Adana Science and Technology University, Department of Bioengineering

Research Assistant (2013-Cont.) Marmara University, Institute of Pure and Applied Sciences- ÖYP (Department of Bioengineering)

Projects

Evaluation of the alkaloids of the aporphine family as inhibitors of different efflux pumps using in vitro and in silico methods. Marmara University Scientific Research Project: FEN-B-120917-0534 (Researcher) 12/09/2017-Cont. (24 months).

Determination of the intracellular targets of different antimicrobial alkaloids using real time PCR and microarray technologies. Marmara University Scientific Research Project: FEN-A-050614-0238 (Researcher) Completed.

Systems Biology Approach for Integrative OMICs Data Analysis to Investigate the Action of AntimicrobialAgents (Researcher) TUBİTAK: MAG-113M052, Completed.

Investigation of the effect of the allosteric site of beta-lactamase for ligand recognition and binding (Researcher) TUBİTAK: MAG-113M533, Completed.

Publications

Altinisik Kaya FE, **Avci FG**, Sayar NA, Kazan D, Sayar A, Sariyar Akbulut B, 2018, What are the multi-omics mechanisms for adaptation by microorganisms to high alkalinity? A transcriptomic and proteomic study of a *Bacillus* strain with industrial potential. OMICS: A Journal of Integrative Biology, 22(11):717-732.

Avci FG, Sariyar Akbulut B, Ozkirimli E, 2018, Membrane active peptides and their biophysical characterization (Review). Biomolecules, 8(3):77.

Avci FG, Altinisik FE, Karacan I, Senturk Karagoz D, Ersahin S, Eren A, Sayar NA, Vardar Ulu D, Ozkirimli Olmez E, Sariyar Akbulut B, 2018, Targeting a hidden site on class A beta-lactamases. Journal of Molecular Graphics and Modelling, 84:125-133.

Avci FG, Sayar NA, Sariyar Akbulut B, 2018, An OMIC approach to elaborate the antibacterial mechanisms of different alkaloids. Phytochemistry, 149:123-131.

Ayyildiz D, Arga KY, **Avci FG**, Altinisik FE, Gurer C, Gulsoy G, Wozny K, Bruegger B, Mertoglu B, Kazan D, Sariyar-Akbulut B, 2016, Transcriptomic analysis displays the effect of (-)-roemerine on the motility and nutrient uptake in *Escherichia coli*. Current Genetics, 63(4):709-722.

Budeyri Gokgoz N*, **Avci FG***, Karaosmanoglu Yoneten K, Alaybeyoglu B, Ozkirimli Olmez E, Sayar NA, Kazan D, Sariyar Akbulut B, 2017, Response of *Escherichia coli* to prolonged berberine exposure. Microbial Drug Resistance, 23(5):531-544 (*Equal contribution).

Avci FG, Altinisik FE, Vardar Ulu D, Ozkirimli Olmez E, Sariyar Akbulut B, 2016, An evolutionarily conserved allosteric site modulates beta-lactamase activity. Journal of Enzyme Inhibition and Medicinal Chemistry, 31(S3):33-40.

Maervoet VET, De Maeseneire SL, **Avci FG**, Beauprez J, Soetaert WK, De Mey M, 2016, High yield 1,3-propanediol production by rational engineering of the 3-hydroxypropionaldehyde bottleneck in *Citrobacter werkmanii*. Microbial Cell Factories, 15:23.

Maervoet VET, De Maeseneire SL, **Avci FG**, Beauprez J, Soetaert WK, De Mey M, 2014, 1,3-propanediol production with *Citrobacter werkmanii* DSM17579: effect of a dhaD knock-out. Microbial Cell Factories, 13:70.

Avci FG, Huccetogullari D, Azbar N, 2014, The effect of cell recycling on the production of 1,3-propanediol by *Klebsiella pneumoniae*. Bioprocess and Biosystems Engineering, 37:513-519.

Presentations

Aksoy CS, **Avci FG**, Ugurel OM, Sayar NA, Sariyar-Akbulut B, 2018, Inhibition of berberine efflux by natural products to potentiate its activity in *Staphylococcus aureus* (Poster), EMBO Workshop: Bacterial Persistence and Antimicrobial Therapy, 10-14 June 2018, Ascona/Switzerland.

Sariyar-Akbulut B, Atas B, Aksoy S, **Avci FG**, Sayar AA, 2017, Evaluation of active natural products as bacterial efflux pump inhibitors (Poster), EpiChemBio (CM1406) and MuTaLig COST (CA15135) actions joint annual meeting, 22-24 September 2017, Porto/Portugal.

Avci FG, Guillerminet M, Orelle C, Jault JM, Sariyar Akbulut B, 2017, Roemerine: A new multidrug resistance pump inhibitor? (Poster), 7th Congress of European Microbiologists (FEMS), 9-13 July 2017, Valencia/Spain.

Avci FG, Velioglu C, Recber E, Unsal C, Gulsoy G, Sariyar-Akbulut B, 2016, Evaluation of Roemerine as a Multidrug Resistance Pump Inhibitor, 41st Federation of European Biochemical Societies (FEBS) Congress, 3-8 September 2016, Kusadasi/Turkey.

Ayyildiz, D, **Avci FG**, Arga KY, Sariyar-Akbulut B, 2016, (-)-Roemerine limits carbohydrate uptake which leads to alternative nutrients as acetyl-CoA sources (Oral), 41st Federation of European Biochemical Societies (FEBS) Congress, 3-8 September 2016, Kusadasi/Turkey.

Altinisik FE, **Avci FG**, Sariyar-Akbulut, B, Denizci AA, Kazan D, 2016, Understanding alkaliphilic adaptation of *B. marmarensis sp. nov*. (Poster), 41st Federation of European Biochemical Societies (FEBS) Congress, 3-8 September 2016, Kusadasi/Turkey.

Avci FG, Sariyar-Akbulut B, 2016, Evaluation the effect of plant-derived natural products on *Bacillus subtilis* 168 proteome (Poster), FEBS-IUBMB Workshop on Biointeractomics: from bimolecular interactions to networks, 17-20 MAy 2016, Seville/Spain.

Altinisik FE, **Avci FG**, Sariyar-Akbulut B, Denizci AA, Kazan D, 2016, Investigation of proteome profile of alkaliphilic *Bacillus marmarensis sp nov* under different pH conditions (Poster), FEBS-IUBMB Workshop on Biointeractomics: from bimolecular interactions to networks, 17-20 May 2016, Seville/Spain.

Ayyildiz D, **Avci FG**, Budeyri-Gokgoz N, Arga KY, Sayar NA, Kazan D, Wozny K, Bruegger B, Sariyar-Akbulut B, 2016, The plant derived alkaloid roemerine is involved in the modulation of motility in *Escherichia coli* (Poster), Biophysical Society 60th Annual Meeting, 27 February-2 March 2016, Los Angeles/USA.

Avci FG, Sariyar Akbulut, B, 2015, Effect of three aporphine alkaloids on *Bacillus subtilis* 168 (Poster), The 29th Annual Symposium of the Protein Society, 22-25 July 2015, Barcelona/Spain.

Altinisik FE, **Avci FG**, Sariyar Akbulut B, Ozkirimli Olmez E, Vardar Ulu D, Karacan İ, Senturk D, 2015, Mutations of a conserved tryptophan residue of the TEM-1 β-lactamase (Poster), The 29th Annual Symposium of the Protein Society, 22-25 July 2015, Barcelona/Spain.

Avci FG, Ozkirimli Olmez E, Sariyar Akbulut B, 2014, The importance of a conserved residue of the H10 helix in beta-lactamase (Poster), 16th European Congress on Biotechnology, 13-16 July 2014, Edinburgh/Scotland.

Avci FG, Ozkirimli Olmez E, Sariyar Akbulut B, 2013, Investigation of an Allosteric Site of R-TEM-1 beta-lactamase (Poster), 6th International Bioengineering Congress, 12-15 November 2013, Kusadasi/Turkey.

Gezgin Y, Sargın S, Eltem R, Vardar-Sukan F, Bakı B, **Avcı G**, İltüzer H, Satılmış S, 2010, Determination of Optimum Conditions for *Trichoderma* Micropropagules Production in Shake Flasks and Static Culture (Poster), 5th International Bioengineering Congress, 16-20 June 2010, İzmir/Turkey.

Seminars, Congresses, Workshops Attended

- International IFCC Course on Flow Cytometry, 20-22 June 2018, Istanbul/Turkey.
- From Network To Targets: Workshop on OMIC technologies and their applications, 7-9 June 2017, Istanbul/Turkey.
- X Annual Congress of the European Proteomics Association, 22-25 June 2016, Istanbul/Turkey
- Proteomics-Bioinformatics Workshop, 22-25 June 2016, Istanbul/Turkey.
- 1st German-Turkish Biogas Workshop, 19-20 October 2011, Izmir/ Turkey.
- Stem Cell Symposium, 16 March 2009, Izmir/Turkey.
- Engineering Days'09, 11-13 March 2009, Izmir/Turkey.
- The 4th National Bioengineering Congress, 15-18 October 2008, Izmir/Turkey.
- Environmental Conscious About Global Warming and Alternative Energy Sources Symposium, 01 April 2008, Izmir/Turkey.
- Nanobiotechnological Approaches Symposium, 07 March 2008, Izmir/Turkey.

Certificates

- Laboratory Research Experience Certificate, 2007, Izmir, Turkey.
- Flow Cytometry, 2018, Istanbul/Turkey.

Grants

- 2017-FEMS Research Grant (3 months) Université Claude Bernard Lyon 1 (CNRS), France
- 2012-ERASMUS Student Exchange Programme (3 months) - Universiteit Gent, Belgium